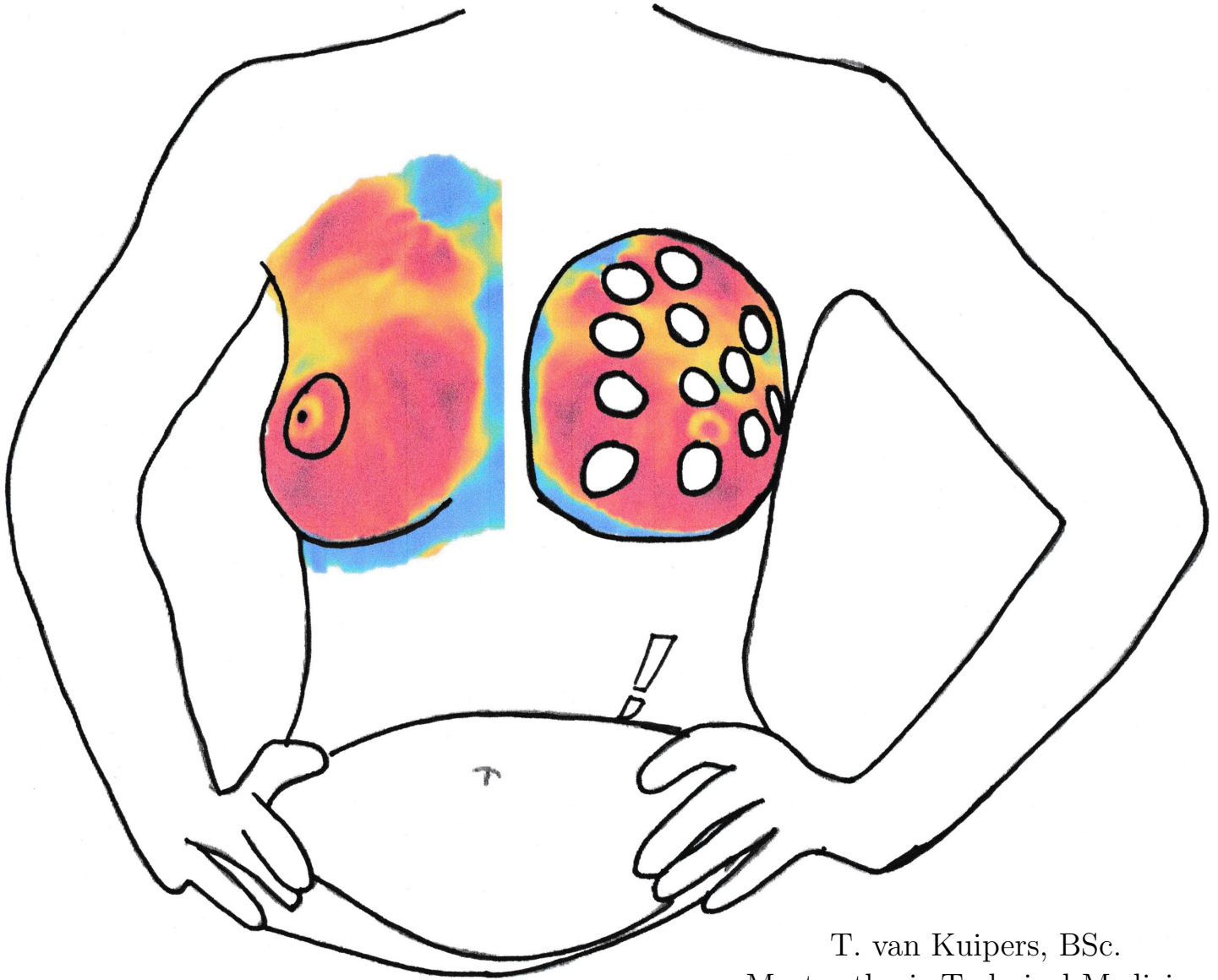


---

# Improvement of patient satisfaction after DIEP flap surgery by applying 3D techniques

---



T. van Kuipers, BSc.  
Master thesis Technical Medicine  
March, 2022

UNIVERSITY OF TWENTE. | **TECHMED CENTRE**

**Radboudumc**  
university medical center



Medisch Spectrum Twente  
een santeon ziekenhuis

  
**Borstkliniek Oost-Nederland**  
Topzorg voor uw levenskwaliteit



# IMPROVEMENT OF PATIENT SATISFACTION AFTER DIEP FLAP SURGERY BY APPLYING 3D TECHNIQUES

## **General information**

---

Thomas van Kuipers, BSc.

Technical Medicine at University of Twente, Techmed Centrum

Department of plastic surgery at MST, ZGT and RadboudUMC

## **Graduation committee**

---

Chairman & technical supervisor	Prof. dr. ir. R.M. Verdaasdonk
Medical supervisor	dr. H.A. Rakhorst
Process supervisor	Drs. P.A. van Katwijk
Technical Physician supervisor	dr. M.A. Koenrades
Technical Physician supervisor	dr. S. Hummelink
External member	ir. R.V. Schulte

## **Colloquium**

---

Date	9 March 2022
Time	16:00 Hour
Place	University of Twente



---

"Iets is alleen maar leuk omdat het een keer ophoudt, want als iets leuk is en het houdt niet meer op, is het op een gegeven moment niet meer leuk"

- *Youp van 't Hek* -

Thomas van Kuipers  
Master thesis  
2022  
Technical Medicine - Imaging and Intervention

University of Twente, Technical Medicine, Faculty of Science and Technology  
Medisch Spectrum Twente, Department of Plastic Surgery and 3D lab\*  
Ziekenhuisgroep Twente, Department of Plastic Surgery\*

\*In coöperation with the Department of Plastic Surgery Radboud UMC

UNIVERSITY  
OF TWENTE.

TECHMED  
CENTRE



Medisch Spectrum Twente  
een santeon ziekenhuis





# Preface

Na een jaar verpleegkunde gestudeerd te hebben in Amsterdam, begon ik in 2014 aan de Universiteit Twente met de studie Technische Geneeskunde. Met Technische Geneeskunde kon ik de uitdaging aangaan om zowel met mijn medische als technische interesse oplossingen te bedenken voor klinische problemen. Het was me al snel duidelijk dat vooral de beeldvorming en 3D technieken mij trokken.

In de master koos ik dan ook zonder twijfel voor de richting Imaging and Intervention. Het praktische gedeelte en de combinatie met klinische vakken trok mij heel erg tijdens de master. Om meer 3D ervaring te hebben koos ik als keuzevak 3D Computervision. Na mijn vierde stage in het MST bij het 3D lab en de plastische chirurgie die gedurende de eerste lockdown plaatsvond, kon ik hier ook mijn M3 klinische specialisatiestage gaan doen in het veld van de borstreconstructie bij borstkanker. Dit project focuste zich zoals u verderop zult lezen op het verbeteren van patiënt tevredenheid na de DIEP lap operatie met behulp van 3D technieken.

Ik keek erg uit om een jaar aan het project te zitten waar ik in maart 2020 een start mee heb gemaakt. Helaas gooide kort na de start Corona wederom roet in het eten, waardoor het de eerste maanden erg zoeken is geweest naar de richting voor onderzoek en meelopen in de kliniek beperkt mogelijk was. Uiteindelijk, na de lockdown, is het nog gelukt om van een aantal (gezonde) proefpersonen de borstmallen te analyseren. In deze thesis volgt het resultaat van een jaar werken met, bloed zweet en tranen. Mijn afstudeeropdracht heeft mij tot de conclusie gebracht dat 3D techniek meerwaarde heeft, 3D veelbelovend en automatiseerbaar is en bovendien goed wordt ontvangen door de patiënten zelf.

Mijn persoonlijke leertijd heeft me veel gebracht. Graag wil ik mijn begeleiders bedanken voor de begeleiding dit afgelopen jaar. Prof. R.M. Verdaasdonk voor het meedenken en zijn kritische blik op mijn onderzoek thesis. Hinne Rakhorst voor alle klinische ervaring die ik op heb kunnen doen, beantwoorden van vragen, mogelijkheid tot patiënten onderzoek en fijne gesprekken. Maaike voor het meedenken om een niet-WMO studie op te zetten, alle feedback het afgelopen jaar, waardoor ik steeds weer geprikkeld werd om een stapje verder te denken en kritisch naar mezelf te kijken. Ondanks door de Covid-19 pandemie hebben we elkaar helaas alleen maar online gezien, maar Stefan, ook jou wil ik bedanken voor het meedenken, vragen stellen en in contact brengen met diverse personen binnen het Radboudumc. Verder wil ik Paul, Nick, Koen en Douwe bedanken voor alle intervisies. Door het delen van ervaringen heb ik een persoonlijk groei doorgemaakt die ik meeneem in mijn persoonlijke en professionele leven. Als laatste wil ik graag mijn thesis opdragen aan mijn tante die nu op de wachtlijst staat voor een DIEP lap operatie; voor haar de enige reconstructie mogelijkheid na heftige chemokuren en radiotherapie. Ik hoop dat dit onderzoek zal bijdragen aan toekomstige onderzoeken, zorgt voor betere resultaten en vooral dat nog meer patiënten zoals zij tevreden kunnen zijn na een DIEP lap operatie.





# Abstract

## **Introduction:**

Breast cancer is the most common cancer in women worldwide. One in seven women in the Netherlands is diagnosed with breast cancer every year. Factors such as a higher survival rate and more knowledge about hereditary genes increase the demand for (autologous) breast reconstruction. Autologous reconstruction methods are preferred over silicone prosthesis. In most hospitals worldwide, the gold standard is the deep inferior epigastric perforator (DIEP) flap procedure. In this technique, the skin, perforators and subcutaneous fat are transplanted to shape a breast during a 5 - 8 hour operation. Approximately 20% of the DIEP flap patients undergo a secondary correction at the contralateral side to create symmetrical breasts. To improve patient satisfaction and clinical outcome, new techniques including 3D stereophotogrammetry (3D photography) and 3D printing are upcoming in surgical planning. This research aims to improve patient satisfaction by applying 3D techniques. Objectives were to validate the application of these techniques by validating the process from 3D photo to 3D print with breast phantoms and custom-made breast moulds on volunteers. For further validation of the breast moulds after DIEP flap and gaining more insight in breast symmetry, the possibilities to develop an objective breast symmetry algorithm were explored.

## **Method:**

Breast phantoms (four foam hemispheres and one female torso) were photographed on a Vectra XT system to validate the process from 3D photo to 3D print. Following the capture, the breasts were segmented and the 3D models were printed. Anatomical landmarks have been applied to measure landmark distances between each step in the process. In a clinical study, these landmarks and distance differences have been evaluated on human subjects (healthy volunteers and DIEP flap surgery patients). A distance error of 10 mm was considered acceptable for clinical application. Furthermore, it is described how an algorithm should work and what variables could be used to assess breast symmetry. To demonstrate this, clinical 3D photos of 25 patients were obtained and breast symmetry was scored by plastic surgeons and experienced observers.

## **Results:**

In the study with breast phantoms, the mean differences found were mostly  $< 3$  mm and  $< 1\%$ . The maximum mean deviation found was  $-3.4$  mm  $\pm 3.1$  mm ( $1.9\% \pm 1.7\%$ ) in the comparison between phantom and 3D print. The clinical study on volunteers showed a maximum mean deviation of  $2.0$  mm  $\pm 0.6$  mm ( $-1.3\% \pm 0.7\%$ ) in the lateral to medial distance. Most results showed difference of  $< 2$  mm and  $< 1.5\%$ . Before the developed can be used in clinic, it should be optimized in symmetry calculation. For optimizing the algorithm, a valid database as the gold standard should be developed to validate the algorithm. In the algorithm chapter, (new) analysis methods and parameters are described for further development. Further research should focus on further development of the algorithm, validation database

---

and application in the clinic.

**Discussion/Conclusion:**

Accurate 3D printed breast moulds can be fabricated from 3D photos with small errors found, mostly less than 2 mm. Further research should be performed to use the moulds as an intervention during DIEP flap surgery whether the use of a mould improves patients satisfaction. An objective algorithm should be used in such a study to calculate symmetry. This research provided the framework to develop such an algorithm.

**Keywords: DIEP flap, 3D photography, 3D print, Mould, Breast symmetry, Algorithm**

# Contents

<b>Preface</b>	<b>iii</b>
<b>Abstract</b>	<b>v</b>
<b>1 Introduction</b>	<b>3</b>
1.1 The DIEP flap procedure	4
1.2 Clinical problem	5
1.3 Aims	6
1.4 Outline of thesis	7
<b>2 Pre-clinical validation of the process from 3D photo to 3D print using a phantom model</b>	<b>9</b>
2.1 Introduction	9
2.2 Method	10
2.2.1 Experimental set-up	10
2.2.2 Data analysis	13
2.3 Results	13
2.4 Discussion	15
2.4.1 Limitations	16
2.4.2 Future	17
2.5 Conclusion	17
<b>3 Clinical validation study to 3D printed breast moulds on volunteers</b>	<b>19</b>
3.1 Introduction	19
3.2 Methods and materials	20
3.2.1 Study population	20
3.2.2 Study design	21
3.2.3 Image acquisition (Step 1 and 2)	22
3.2.4 3D modelling (Step 3)	22
3.2.5 3D printing (Step 4)	22
3.2.6 Taking 3D breast mould photo (step 5)	23
3.2.7 Data analysis (Step 6 and 7)	23
3.3 Results	23
3.4 Discussion	24
3.4.1 Limitations	27
3.4.2 Future	27
3.5 Conclusion	28
<b>4 Develop an objective breast symmetry validation method</b>	<b>29</b>
4.1 Patient satisfaction on symmetry and 3D moulds	29
4.2 Method	30
4.2.1 Programming language software	30
4.2.2 Landmark definition/selection & ROI segmentation	31
4.2.3 Define variables to be used	32
4.2.4 Analysis method to compare symmetry of breasts	35
4.2.5 Build up observer database	36
4.3 Validation of an algorithm	36
4.3.1 The variables	36
4.3.2 Observer database	38
4.3.3 Comparison breast symmetry algorithm vs observers	39
4.4 Discussion and future developments	40
4.4.1 Algorithm	40
4.4.2 Variables	41
4.4.3 Testing	41
4.4.4 Breast contour analysis	41
4.5 Conclusion	43
<b>5 Future perspectives</b>	<b>45</b>
5.1 Implementation of 3D printed moulds in the clinic	45
5.2 Future research	47
<b>6 Conclusion</b>	<b>51</b>
<b>Appendix</b>	<b>63</b>



# Chapter 1

## Introduction

Nowadays, breast cancer is the most common type of cancer in women worldwide with more than two million new cases every year.[64, 83] In the Netherlands, one in seven women is diagnosed with breast cancer in their lifetime which comes down to around 17,000 new patients per year.[1, 2] The number of patients diagnosed with breast cancer has doubled since 1989. According to the Dutch Comprehensive Cancer Organisation (IKNL) 20% of the patients is younger than 50 years, 59% is between the ages of 50 and 74 years and 21% is older than 75 years.[29] In 2020, there were 139,871 patients who had been diagnosed with breast cancer in the last ten years and recovered or were still undergoing treatment. Besides these high numbers of breast cancer cases, also the survival rate has improved in the last decades to more than 80%.[67, 82] In the Netherlands, the five-year survival rate increased from 42,000 women in 1999 to 67,000 women in 2019.[46] More than one-third of female breast cancer patients is needed to undergo a mastectomy or lumpectomy.[24] Additionally, today's education about self-screening and breast cancer-, and the discovery of the genes such as BRCA1 and BRCA2 contributed to a higher demand for (preventive) mastectomies to neutralize the additional risk for breast cancer. As a result, the demand for breast reconstructions has increased.[54]

Breast reconstruction is mostly performed at patients requests. The main reasons are related to psychological, social and/ or sexual issues, often in combination with unsatisfactory aesthetics.[4, 18, 20, 25, 92, 96, 100] Ideally, breast reconstruction aims to restore a naturally shaped breast, for which, several techniques were developed in the past century.[54] The least invasive option is an external prosthesis wearing in a bra. A disadvantage is that women experience discomfort in size, shape and during activities such as swimming and running.[3, 33, 34, 65] More invasive is to insert a silicone prosthesis in a pocket under the breast skin or pectoral muscle. Due to increasing groups of women on social media who complaining about symptoms related to breast implant illness [26], and sharing information about a small risk of 1 to 3% to develop breast implant-associated anaplastic large cell lymphoma (BIA-ALCL) [9], the interest in a third option, autologous reconstruction, has increased. Also for some patients who requested breast reconstruction, DIEP flap surgery is the only possibility. Outcomes such as a more nat-

ural shape, longevity and fewer revisions have added to the popularity of autologous breast reconstruction.[44, 68, 100]

Several tissue perfused flaps were introduced in the past century for autologous breast reconstruction.[19, 61] In the seventies, the most popular was the transverse rectus abdominal musculocutaneous (TRAM) flap.[75] The drawback of this flap is that the transfer of a part of the abdominal muscle causes loss of function and abdominal wall weakness.[53, 69] The solution was introduced in 1994 by Robert J. Allen and Penny Treece [5] who developed the deep inferior epigastric perforator (DIEP) flap procedure. With preserving the abdominal muscle, only transfer adipose and skin tissue is transferred to the thorax where the anastomosis to the abdominal and thoracic vessels is made with a microscope. A time consuming (5 - 8 hours) and skilled work. Besides the microscope, specialized tools to suture and connect the vessels are used to guarantee the flap of blood supply.[38, 49]

## 1.1 The DIEP flap procedure

An extended description of the DIEP flap procedure can be found in appendix A. In short, the DIEP flap procedure has become the gold standard for breast reconstruction in most hospitals around the world.[18, 20] During the DIEP flap procedure, abdominal skin and fat are transferred to the chest wall with blood vessels for blood supply (Figure 1.1). The skin and subcutaneous fat of the lower abdomen is adequate tissue for breast reconstruction because it gives a soft and natural shaped reconstruction. The harvest perforators are the branches of the external iliac artery, the deep inferior epigastric arteries. Re-attaching of the small abdominal vessels to the mammary vessels is started with a microscope. Until the blood supply is restored, the abdominal flap is isolated from blood, called the ischemia time. A longer ischemia time is related to a higher complication rate. Major complications are total flap loss, partial flap loss and compromised flap, but these complications do not occur often. A recent study performed at Ziekenhuisgroep Twente (ZGT) to the complications in unilateral and bilateral DIEP flap surgeries found a complication rate of 7.4% in the unilateral group and 6.7% in the bilateral group between 2017 and 2019.[47] This is a large decrease in comparison with the rates between 2013 and 2017 with 16.7% for unilateral and 26.7% for the bilateral group.[47] In the total interval from 2013 to 2019, only 1.2% of the patient flap loss occurred and in 5.3% a compromised flap was seen.[47] 12.9% of the patients needed reoperation in the theatre.[47] Also, a longer surgery time is related to more complications.[96] The surgery time should be reduced to decrease the number of complications.

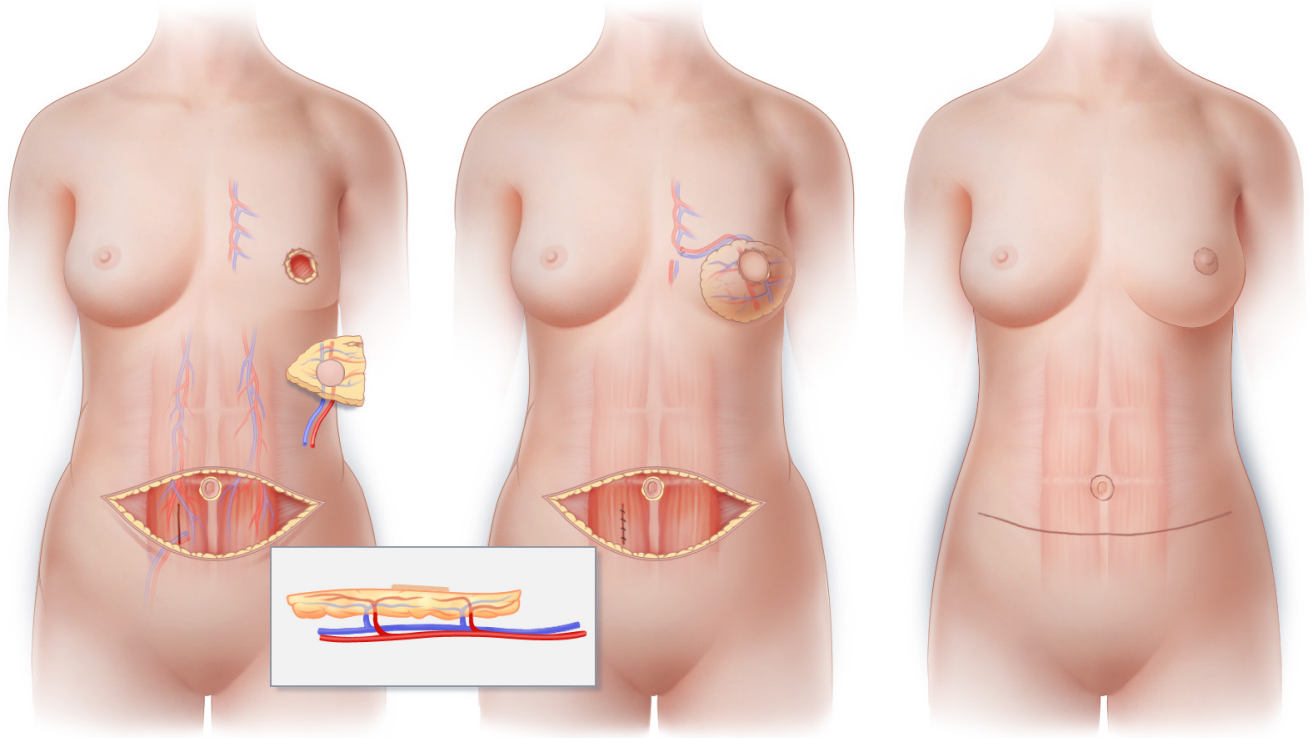


Figure 1.1: Schematic overview of the DIEP flap breast reconstruction. The perforator vessels, abdominal skin and fat are dissected from the abdominal rectus muscle. This free flap is transferred to the chest. The perforators are anastomosed to the internal arteria mammary. Depicted from <https://tprsg.com/restorative-techniques/perforator-flap-reconstruction/flap-procedures/diep-flap>

## 1.2 Clinical problem

Despite the full dedication of the plastic surgeons to create the best result possible, there are still women unsatisfied with symmetry after surgery. Although the satisfaction rate after DIEP is higher than in implant reconstruction, more than 50% of the patients undergo a(n) (aesthetic) second surgery.[47, 85] Approximately 20% of the DIEP flap patients undergo a secondary correction at the contralateral side to create symmetrical breasts. (H.A. Rakhorst, personal communication, 6 January 2022).

To prevent secondary corrections, the aim of the reconstruction is to obtain symmetrical breasts. Technical innovations, such as 3D, planning aim at improving the result of breast reconstruction by making pre-operative decisions possible and by applying the technology during surgery. Hence, 3D printed anatomical breast moulds segmented out of pre-operative captured 3D photos can be used for shaping the abdominal flap to a reconstructed breast and obtaining breast symmetry.

Hummelink et al.[45] described the application of a mould in a sterile sleeve during surgery in 6 patients (3 unilateral and 3 bilateral). However, due to insufficient donor site or reduction at the contralateral side, the final

results showed deviations in breast volume (167 - 284 cc) in mainly the unilateral reconstructions. Therefore, to apply a mould, the patients have to be satisfied with their unaffected breast and contain enough abdominal donor fat.[45]

In two studies performed at the Osaka university[86, 87], breast moulds were used in unilateral DIEP flap surgery patients. They noticed that the breast moulds resulted in a slightly larger reconstructed breast because the mould is obtained from a skin surface 3D photo, while a DIEP flap is inserted in a subcutaneous pocket. But 5-10% reduction of postoperative swelling still results in symmetrical breasts. The use of 3D printed moulds could reduce operation time and support inexperienced surgeons to obtain symmetrical breasts.[87] Furthermore, it is a simple, fast and low-cost innovation. But most importantly, the use of a mould in patient-specific 3D planning should improve the symmetric result in volume and shape after DIEP flap surgery and therefore patient satisfaction.[6, 86]

Although these studies mentioned that breast moulds can contribute to obtaining symmetric breasts, they have not dealt with the validation of breast moulds obtained from 3D photography. This raised the question if it is possible to obtain a breast mould having the same size and form as the contralateral breast to make it fit correctly. The added value of using breast moulds to obtain symmetric breasts and improve patient satisfaction after DIEP flap surgery has to be further investigated. Several factors influence womens satisfaction such as shape, volume, treatment trajectory and nipple complex.[30, 58, 76] Thus, to do reliable research on the effect of breast moulds on symmetry and patient satisfaction after DIEP flap surgery, an objective method is required to quantify breast symmetry to patient satisfaction. Additionally, this method should eventually be used for the symmetry analysis in an RCT to objectively analyse if a mould can improve the symmetry after the DIEP flap.

### 1.3 Aims

The main aim of this research is to improve patient satisfaction after DIEP flap reconstruction by application of 3D techniques. The techniques that will be explored in this thesis are 3D stereophotogrammetry (3D photography), 3D printing and 3D symmetry analysis methods. Therefore, the following objectives are set out to achieve this main aim:

1. **Validate the process from 3D photo to 3D print using breast phantoms by measuring anatomical landmark distances (chapter 2)**
2. **Validate the size of 3D printed breast moulds segmented from 3D photos by measuring anatomical landmark distances on healthy volunteers and patients undergoing DIEP flap surgery (chapter 3)**
3. **Explore the possibilities to develop an objective grading method for breast symmetry to quantify patient satisfaction (chapter 4)**



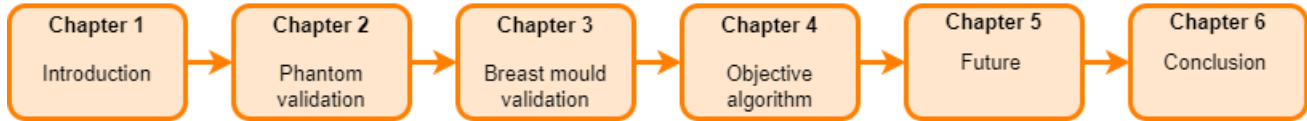


Figure 1.2: Overview of the thesis chapters

## 1.4 Outline of thesis

The outline of this thesis is as follows and displayed in Figure 1.2. After this introduction, chapter 2 will follow with a validation study, to assess the accuracy of the process from a 3D photo to a 3D printed mould by measuring anatomical landmark distances using phantoms. Chapter 3 describes a validation study with volunteers for the validation of 3D printed breast moulds. In chapter 4, the possibilities of developing an objective breast symmetry algorithm are explored. Chapter 5 discusses future perspectives for using the 3D printed moulds in the clinic and what is further needed for implementation. Also, the added value of using an algorithm for clinical use and handheld imaging devices are discussed. In chapter 6 an overall conclusion of this thesis is described.



## Chapter 2

# Pre-clinical validation of the process from 3D photo to 3D print using a phantom model

### 2.1 Introduction

3D techniques have made their entrance in plastic surgery for analysing surgical planning and outcomes. Modern 3D photo imaging systems are non-invasive, fast and frequently used in preoperative imaging for cosmetic breast enlargement. In several previous studies, volume was used to evaluate breast symmetry instead of the less complex (landmark) distance measurements.[56, 60, 62, 97] Several studies investigated the accuracy of 0.15 mm  $\pm$ 0.15 (Vectra), 0.21 mm and 0.25 mm  $\pm$ 0.157 (3dMD) of 3D photography with landmark distances on the face.[28, 63, 94] Maximum deviations described of face landmark distances by Guo et al.[37] are in the order of a maximum of 3% (Vectra M3, a comparable system to the Vectra XT) which claimed that 3D photography is a highly reliable tool for 3D surgery planning in plastic surgery for aesthetic and reconstructive purposes.[37]

As 3D photography has shown its value, the accuracy of 3D prints obtained from 3D imaging modalities is questioned. 3D printed models from segmented CT images have proven their added value and accuracy. In a study[10], three test objects (cube and two cylinders) were scanned with a CT scanner, 3D printed and the dimensions of the test objects and 3D prints were measured with a calliper. A high accuracy was demonstrated with a mean absolute difference of 0.23 mm (*Test object* – 3D copy) and relative mean difference of 0.55% ( $\frac{\text{Test object} - 3D \text{ copy}}{3D \text{ copy}} \times 100$ ).[10] A review study demonstrated a mean difference of 0.20 mm (0.95%) for FDM printing.[17] Although CT proves to be an accurate method for developing 3D printed models and for locating the perforators in DIEP flap patients, 3D photography is the preferred method for obtaining 3D printed breast moulds. 3D photography is free of radiation,

enables the patient to stand instead of lie and has a fast capture time.[39, 93]

The mentioned studies demonstrated that 3D photography and 3D printing are accurate and reliable techniques to use in clinical setting. However, in literature there is a lack of studies using 3D photography and 3D printing in one validation process. Also, there is no definition of clinically acceptable variability in linear measurements of the breast. So, in this study, the accuracy of the process from 3D photo to 3D print is validated in this study. So this study aims at validating the accuracy of the process from 3D photo to 3D print

## 2.2 Method

### 2.2.1 Experimental set-up

The procedure from 3D photo to print consists of four steps which were numbered with Arabic numbers from 1 to 4. Below a description of the tasks is explained for each step. The Roman numbers I to V, stand for the comparisons between the different steps that were analysed in the result section. Figure 2.2 and Figure 2.3 show these steps and comparisons schematically:

#### 1. Simulation of breast and clinical landmarks - Physical ruler measurement

A female torso and four foam hemispheres of different sizes attached to a male torso were used to validate the process from 3D photo to print. Based on clinical use and other studies[40, 99], the following anatomical landmarks (Figure 2.1) were reconstructed on the mannequins were the Jugular Notch (JN), Midclavicular (MC), Lateral (L), Medial (M) breast point, Nipple (N) and inframammary fold (IMF). The distances between the landmarks (landmark distances) were measured as contoured lines across the surface. Figure 2.1 shows these distances between the landmarks, namely JN - N (green), MC - N (Blue), L - M (red), MC - IMF (orange), N - IMF (pink).

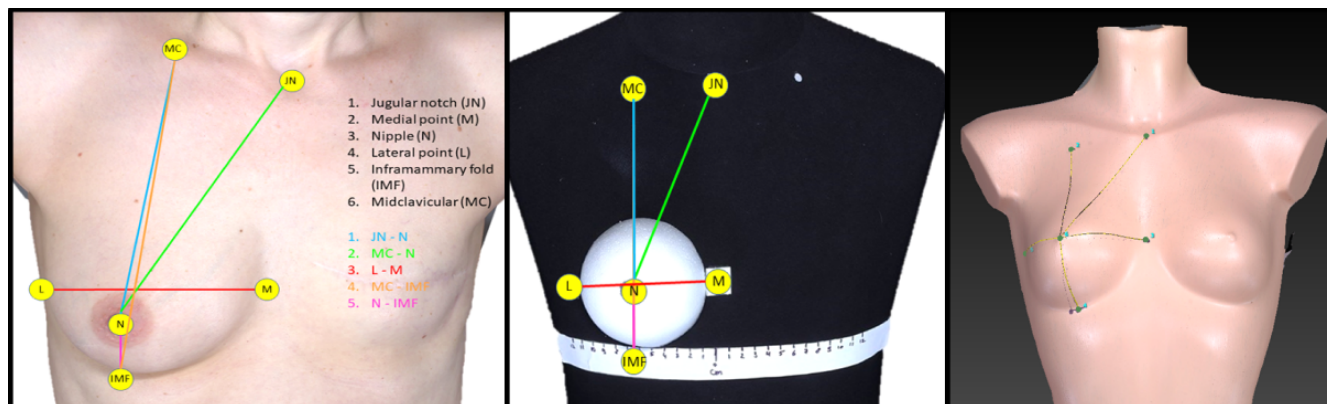


Figure 2.1: List of the landmark distances measured in this study. In the left Figure, the landmarks on a real patient. In the middle, the landmarks reconstructed on the male torso. In the right photo the female torso that is used.

## 2. Taking a 3D photo with Vectra XT system - Digital measurement

3D photos were taken of the torsos with a Vectra XT system (Canfield sci, New Jersey, USA) resulting in four photos with foam hemispheres on the male torso and one photo of the female torso. The Landmark distances were digitally measured in the Vectra XT software.

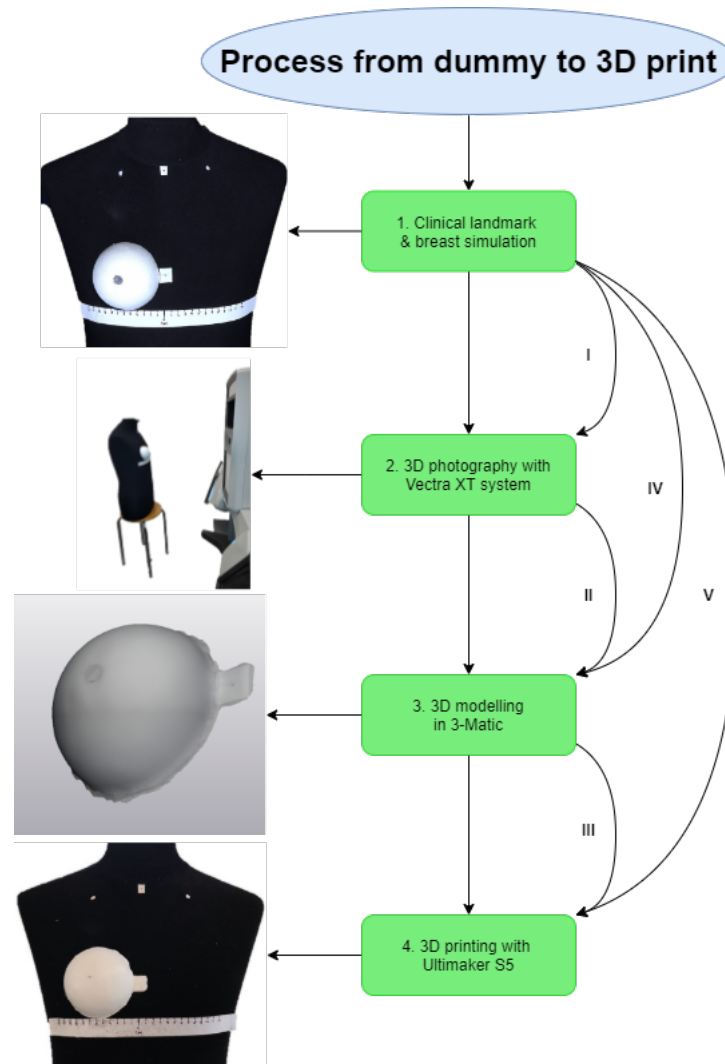


Figure 2.2: Schematic display of the process from a taken 3D photo to obtain a 3D printed model. In step 1, the clinical landmarks were simulated and the foam hemispheres were attached to simulate the breast. In step 2, the 3D photo is taken with the Vectra XT. In step 3, the 3D photo is segmented to a 3D model, and this 3D model was printed in step 4 and re-attached to the mannequin to simulate a breast. The numbers I, II, III, IV and V are the comparisons that were performed in the analysis.

## 3. 3D modelling in 3-Matic - Digital measurement

After taking the photos, the files were exported as .OBJ files and the foam hemispheres and the female torso were segmented in 3-Matic (Materialise, Leuven, Belgium). Segmentation was performed by subtracting a picture

without the hemispheres from a picture that did contain the hemispheres. The segmentation on the female dummy was performed by cutting the breast boundary digitally.

#### 4. 3D printing with Ultimaker and simulation breast with 3D print - Physical ruler measurement

The created files were printed with an Ultimaker S5 (Ultimaker B.V., Utrecht, Netherlands). The print code was generated using Ultimakers Cura 3D print software. Polylactic Acid (PLA), a thermoplastic polyester, was used for the 3D printed models. One of the two extruders was used in the printing process. The printer settings were standardized: extruder temperature 205°C, building board 60°C, chamber temperature 25°C, layer height 0.2 mm and 10% support infill. The 3D models were printed in a ratio of 1:1.

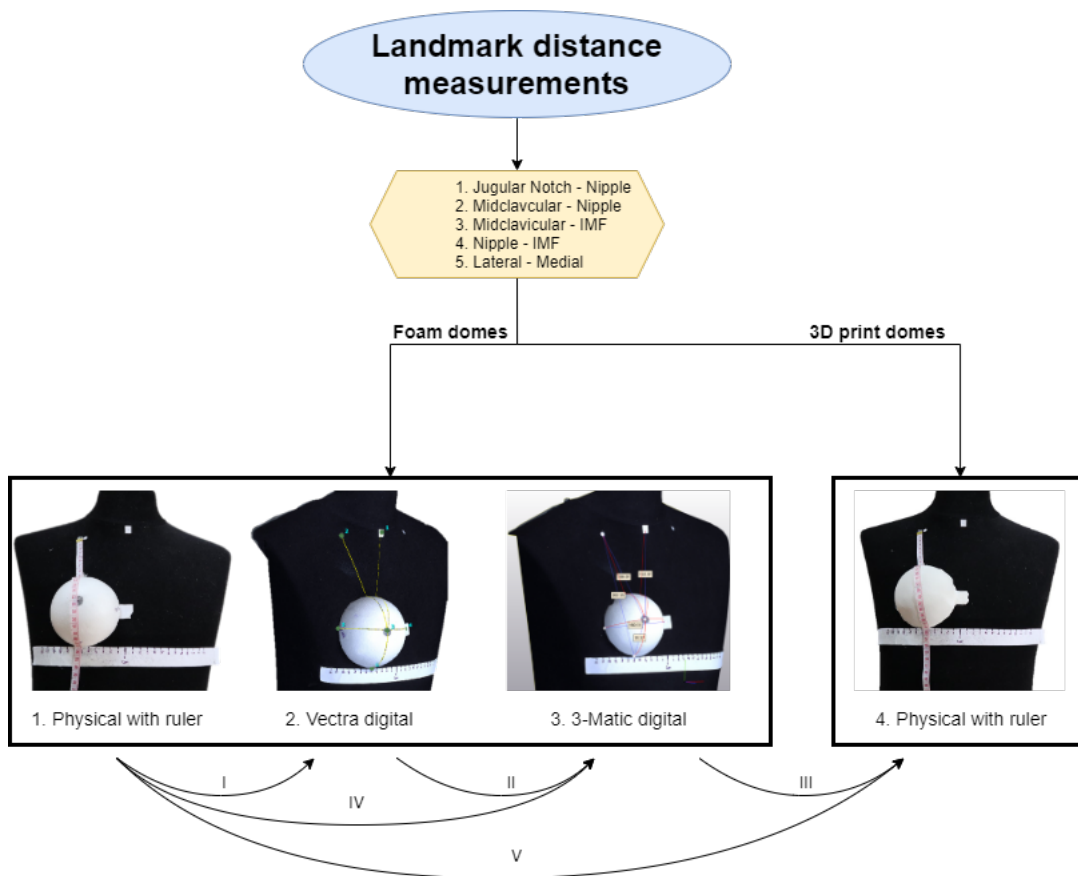


Figure 2.3: This flowchart displays the measured landmark distances (1. Jugular notch - Nipple, 2. Mid-clavicular - Nipple, 3. Midclavicular - IMF, 4. Nipple - IMF and 5 Lateral to Medial, Figure 2.1 displays these landmarks in detail). Steps 1, 2, 3 are the four measurement moments and were performed during the corresponding number in Figure 2.2. Also, the numbers I, II, III, IV and V are the same comparisons as in Figure 2.2.

After printing, the 3D printed models were relocated on the torsos and a 3D photo was taken. The five clinical landmark distances were measured four times in each step 1 to 4. The distances were measured in millimetres once, to mimic a physical exam:

- (a) Physical on the foam hemisphere
- (b) Digital in the Canfield software
- (c) Digital in 3-Matic
- (d) Physical on the 3D printed models.

### 2.2.2 Data analysis

Descriptive statistics were applied between the different measurement steps (comparison I-V) in the process from 3D image to 3D print. The first physical measurements on the female torso and foam hemispheres (attached to the male torso) were considered as the reference (step 1: Clinical landmarks & breast simulation - Physical ruler measurement). The other three steps were compared with these first step (comparison I, IV and V). Furthermore, the two digital measurements were compared reciprocally (comparison II). And last, the measurement between 3-Matic and 3D print was compared (comparison III). The mean deviations and standard deviations (SD) were displayed in two tables represented in mm and percentages per comparison (I-V) and landmark distance. The results were calculated in Microsoft Excel 365 (Microsoft, Washington, USA).

## 2.3 Results

For most landmark distance measurements, the mean differences between comparisons I-V was mostly < 3 mm (Table 2.1). In Table 2.2, the mean differences calculated in percentages were displayed and there can be observed that all percentages are mostly less than 1%. The maximum deviation in comparison V was  $-3.4 \text{ mm} \pm 3.1$  with corresponding percentages of  $1.9\% \pm 1.7$ . In the other comparisons (I - IV), the maximum deviations were respectively  $-1.2 \text{ mm} \pm 0.7$  ( $0.6\% \pm 0.4\%$ ) in I, in II  $-0.1 \text{ mm} \pm 0.1$  ( $1.0\% \pm 0.5\%$ ), III  $-2.2 \text{ mm} \pm 3.1$  ( $1.2\% \pm 1.7$ ) and in IV  $-1.2 \pm 0.7$  ( $0.6\% \pm 0.3$ ). Figure 2.4 showed the median, minimum and maximum deviation per step. In four of the five cases, the maximum deviation occurred in the MC - N distance, except for comparison II. The largest deviations were observed in comparisons III and V containing the physical measurements. The landmark distances showed similar results in the observed comparisons. Therefore, digital measurements seemed to prove more accurate than physical ruler measurements.

Table 2.1: Descriptive statistics for the comparisons of the process from 3D photo to 3D print in mm. Most mean deviations were < 3 mm. The maximum deviation found is -3.4 mm  $\pm$  3.1 mm in the phantom - 3D print distance (V).

Distance (number of samples)	Compared steps					
	Phantom - Vectra (I) Mean (mm)    SD (mm)	Vectra - 3-matic (II) Mean (mm)    SD (mm)	3-Matic - 3D print (III) Mean (mm)    SD (mm)	Phantom - 3-Matic (IV) Mean (mm)    SD (mm)	Phantom - 3D print (V) Mean (mm)    SD (mm)	
J - N (5)	-0.2    0.9	0.0    0.6	-1.4    2.0	-0.2    0.9	-1.6    2.1	
N - IMF (5)	0.00    0.6	-0.8    0.4	0.8    0.4	-0.8    0.7	0.0    0.8	
M - N (5)	-1.2    0.7	0.0    0.6	-2.2    3.1	-1.2    0.7	-3.4    3.1	
M - IMF (5)	-0.6    0.4	-0.6    0.9	-1.8    1.7	-1.2    0.7	-3.0    1.8	
L - M (5)	0.00    1.2	-0.4    1.1	-0.6    0.4	-0.4    0.9	-1.0    1.1	

Table 2.2: Descriptive statistics for the comparisons of the process from 3D photo to 3D print in percentages. The mean difference between the measurements were all less than 2%. The maximum deviation found is 1.9%  $\pm$  1.7% in the phantom 3D print distance (V).

Distance (number of samples)	Compared steps					
	Phantom - Vectra (I) Mean (%)    SD (%)	Vectra - 3-matic (II) Mean (%)    SD (%)	3-Matic - 3D print (III) Mean (%)    SD (%)	Phantom - 3-Matic (IV) Mean (%)    SD (%)	Phantom - 3D print (V) Mean (%)    SD (%)	
J - N (5)	0.1    0.4	0.2    0.3	0.8    1.1	0.3    0.4	1.1    1.0	
N - IMF (5)	-0.1    0.6	1.0    0.5	-1.2    0.7	0.9    0.7	-0.3    0.7	
M - N (5)	0.6    0.4	0.0    0.2	1.2    1.7	0.6    0.3	1.9    1.7	
M - IMF (5)	0.2    0.2	0.2    0.2	0.8    0.8	0.5    0.3	0.6    0.3	
L - M (5)	-0.1    0.5	0.3    0.15	0.4    0.3	0.2    0.4	0.6    0.2	



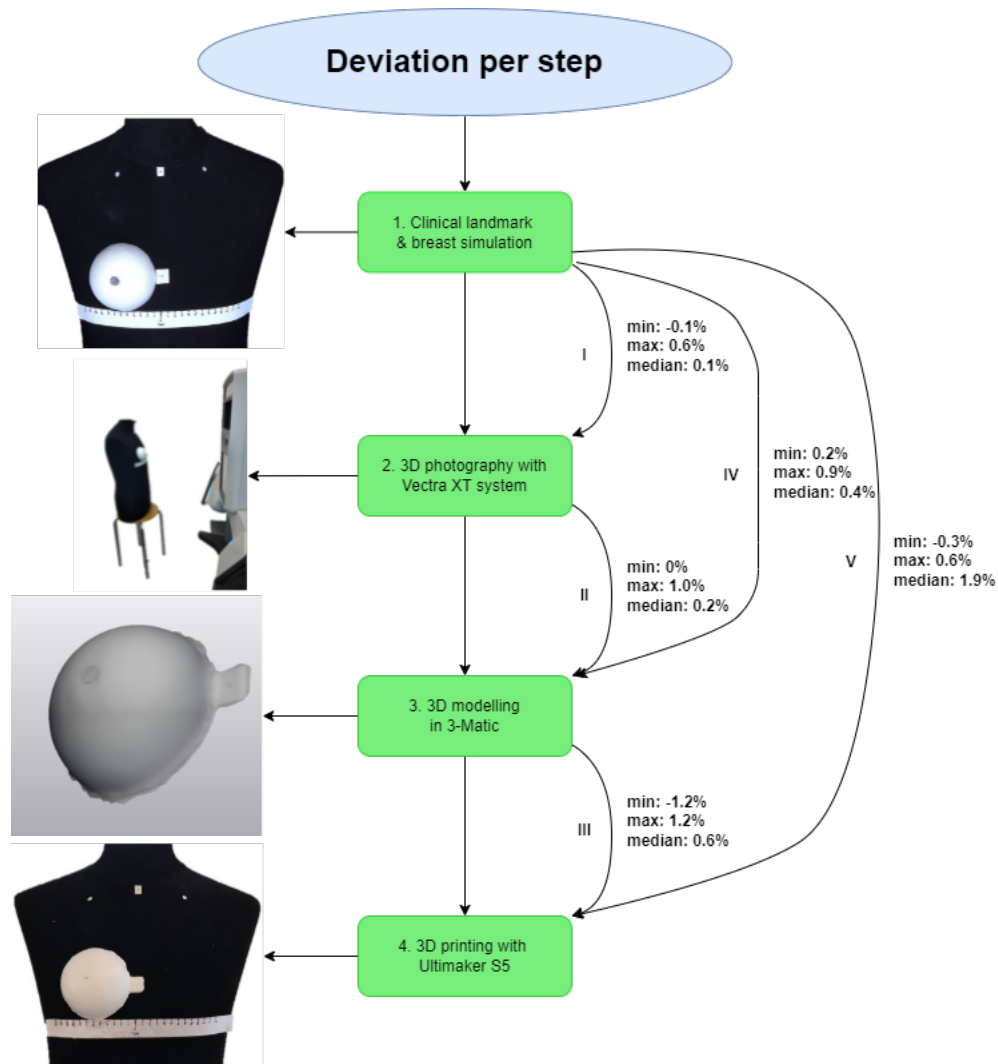


Figure 2.4: The median, minimum and maximum deviation per step.

## 2.4 Discussion

In this study, the process to fabricate 3D printed models from 3D photos using breast phantoms was validated. The mean difference between the landmark distances, comparisons I-V, were analysed in mm and percentages. Most of the deviations (21 out of 25) found in this study were between the 0 and 2 mm. Only three measurements were > 2 mm. Two of these mean deviations found were -3.4 mm (1.9%)  $\pm$ 3.1 ( $\pm$ 1.7%) and -3.0 mm (0.6%)  $\pm$ 0.6 mm (0.3%) in comparison V (Phantom - 3D model) in the MC - N distance. The third mean deviation > 2 mm occurred in comparison III and was in the order of -2.2 (1.2%)  $\pm$ 3.1 mm (1.7%). Remarkable is that in the comparisons with the 3D print (III and V), higher deviations could be observed compared to the other comparisons (I, II, IV) (Figure 2.4). Due to the accuracy of the Ultimaker S5 (layer resolution of 0.2 mm), it is plausible that the deviations were a result of the segmentation process and replacing of the 3D models on the male torso. The deviations in the comparisons without

the 3D model (I, II, IV) could be attributed to human measurement error. Similar results were shown by the study of Catherwood et al.[16] (a mean difference of 1.36 mm with a maximum and minimum of respectively 3.15 mm and 0.02 mm.)[16] They used a Di3D (Di3D.com, Glasgow, UK) photography system for the validation study, which is comparable to the Vectra XT system. This study indicates that accurate 3D prints can be developed from 3D photos.

The researched process to develop 3D printed models from 3D photos is accurate according to the results. Therefore, 3D photography, segmentation of the 3D photo and 3D prints can be applied to develop breast moulds. The comparisons with the physical and digital measurements (III and V) showed the largest deviations. Therefore, in future research, it is advised to use digital measurements only. This way of measuring the landmark distances is preferred because during with physical measurements soft tissue can be pushed moved leading to extra mm in the distances.

In order to validate the process of using 3D photos making 3D prints of human shapes, it is important to reduce the number of variables. The reason is that using a rigid object provided a better methodology compared to human subjects for testing the performance of the devices and process. Therefore, a torso was chosen over female patients. This step leads to more reliable validation data of the process. The data were highly homogenous showing reliability of the camera setup, image processing and subsequent measurements. These results are quite promising for the next step, comparing actual patient data. Shape and size of patients breasts differ which can causing more difficult image acquisition for bigger breasts. Therefore, the results can not be extrapolated.

Also, the precise measurement tools contributed accurate results with a scale of 1 mm of the surgical ruler and 0.001 mm of the digital programs. For the human eye, the measured results will be similar. The achieved accuracy of the digital programs justifies using the measurements on 3D printed breast moulds. Regardless, the clinical relevance of such precise engineering accuracy is quite sufficient.

### **2.4.1 Limitations**

The study also has its limitations. A small sample size ( $n = 5$ ) per landmark distance was used. Considering the results, the study using breast phantoms will be sufficient. Extra samples would only lead to more data of the same accurate results. Another limitation is that the distance measurements were performed once by the researcher in this study. Therefore, the intra- and interobserver variability was not calculated and the exact measurement deviation caused by the researcher is unknown. It is plausible that deviations of 1-2 mm can be attributed to a human error and be therefore considered an intra-observer variability. This would be then an acceptable consistent deviation to the results.

### **2.4.2 Future**

The next step in the development of 3D printed breast moulds is to validate breast moulds on human subjects. Challenges to overcome in this clinical validation will be the segmentation of different breast sizes, shapes and ptosis grades. Only measuring the landmark distances digitally will solve the problem of soft tissue deformation.

## **2.5 Conclusion**

In this study, a validation study was performed on the process from 3D photo to 3D print using breast phantoms. The maximum mean deviation found was  $-3.4 \text{ mm} \pm 3.1$  with corresponding percentages of  $1.9\% \pm 1.7\%$ , but most of the results were  $< 3 \text{ mm}$  and  $1\%$ . In conclusion, this suggests that 3D prints can be developed accurately from 3D photos for the application of breast moulds. However, further research in a clinical study is needed to validate 3D printed breast moulds on participants



## Chapter 3

# Clinical validation study to 3D printed breast moulds on volunteers

### 3.1 Introduction

This study is the continuation of the study in chapter 2 in a clinical setting. The results were accurate with a maximum mean deviation of -3.4 mm between digital and physical measurements. Most measurements were < 3 mm. Because the used rigid torsos were non-representative for the human body, the influence of human variables (body shape, (soft) tissue, ptosis, cup size) on developing accurate breast moulds are still unexplained.

Previous studies in the Netherlands (Radboud) and Japan (Osaka University) investigated the application of 3D printed breast moulds for DIEP flap surgery in the clinic. The breast moulds were obtained from 3D photos and used during DIEP flap surgery.[45, 86] However, a validation of the moulds is missing in these studies. Therefore, a relation of the results with the use of a breast mould can not be concluded and it could depend on the insight of the plastic surgeon or suitable chosen patients. Thus, before these moulds can be applied in MST and ZGT during DIEP flap surgery, 3D printed moulds have to be validated to ensure the size of the moulds fit the breast. According to Lee et al.[56], who investigated the differences of breast landmark distances between digital and physical measurements on females, found most differences < 10 mm. Nevertheless, this study measured only landmark distances on bodies instead of fabricating and validating 3D printed moulds. However, due to the results of chapter 2 and the results of Lee et al. it is expected that in the current study the differences between the landmark distances will be < 10 mm. Therefore, this study aims to validate the size of 3D printed breast moulds segmented from 3D photos by measuring digitally landmark distances on female volunteers.

## 3.2 Methods and materials

### 3.2.1 Study population

A total of 10 participants (16 healthy breasts) were enrolled in this prospective study. Four pre-operative DIEP flap patients (3 unilateral and 1 bilateral) were included while the other six participants were healthy volunteers (1 unilateral and 5 bilateral). The average age of the group was 32.2 years  $\pm$  11.8 (range, 22 - 56 years) and BMI 22.6  $\pm$  2.6 (range, 20.0 - 25.4). The cup sizes in the group were A (2), C (3), D (2) and E (3). Written informed consent was obtained from each volunteer. There were no exclusion criteria, except that the participants should be 18+ and have no piercings in the breast region due to the risk of reflection disorders.

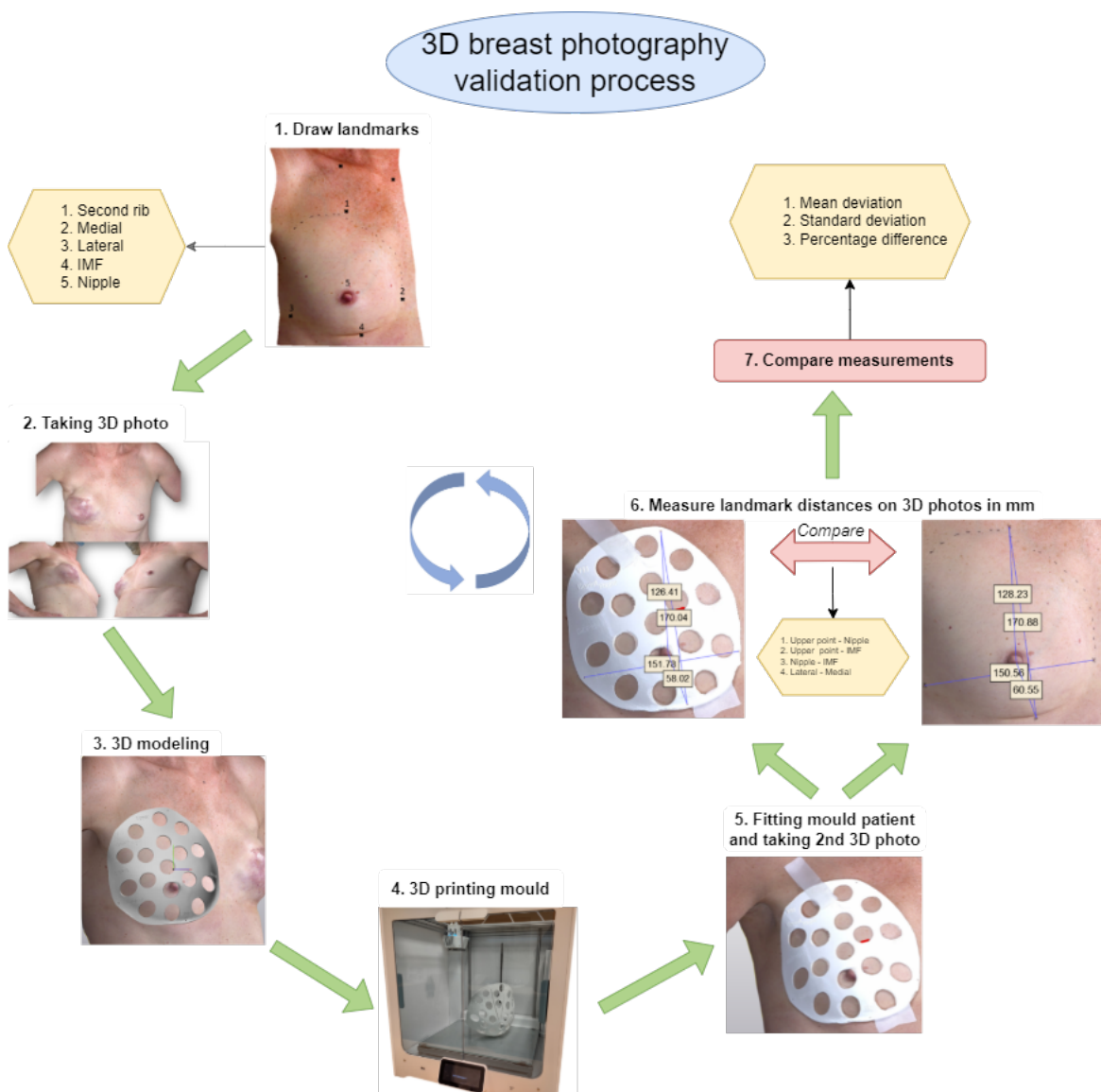


Figure 3.1: Flowchart of the validation process of a 3D printed mould segmented from a 3D photo. The four straight-line distances that were measured: **1.** 2nd rib - Nipple, **2.** 2nd rib - IMF, **3.** Nipple - IMF and **4.** Lateral - Medial.

### 3.2.2 Study design

In Figure 3.1, a schematic overview of the setup for this clinical validation study is shown. Each subject underwent seven steps for the execution to validate the breast moulds size:

1. Drawing landmarks
2. Taking a 3D photo
3. 3D modelling
4. 3D printing
5. Fitting the mould on the breast and taking second 3D photo
6. Measuring landmark distances on the landmark photo and mould photo
7. Analysing measurements



Figure 3.2: The used landmarks for the measurements

In comparison with the validation study performed in chapter 2, the landmark distances and measurement method slightly differed. In the present study, the jugular notch and midclavicular landmark were substituted by a landmark on the second rib. This created the possibility to incorporate the landmarks into the mould's surface. Also, straight-line measurements were performed instead of contour lines. Contour lines generate longer distances due to the holes in the moulds design which induce notches in the picture. The final four clinical landmark distances are the second rib - nipple, nipple - IMF, lateral - medial and second rib - IMF. They were measured digitally in 3-Matic on the participant's breast(s) and on a 3D photo with a custom-made mould on the breast(s). In figure 3.2, the used landmarks were displayed.

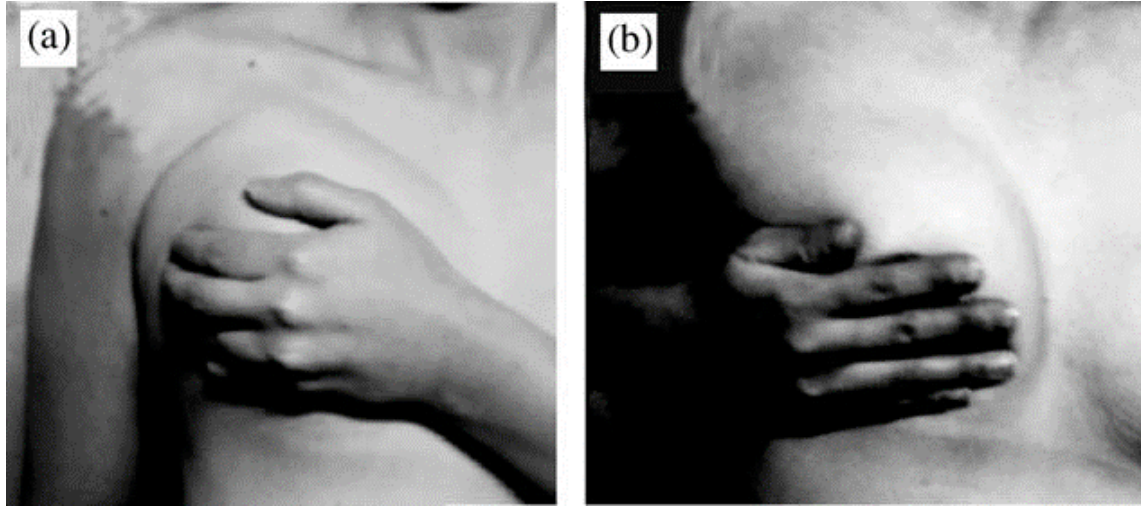


Figure 3.3: Folding line method used to determine the breast boundaries for designing the mould with a) cranial pushing and b) medial pushing

### 3.2.3 Image acquisition (Step 1 and 2)

1. The ten participants were scanned using a Vectra XT system (Canfield Sci, New Jersey, USA) according to a 3D photography protocol (Appendix D.1). Before drawing the landmarks a blank image was taken, after that, the landmarks were added at the height of the second rib, medial, lateral and on the lowest point of the breast. To determine the boundaries of the mould, the folding line method (Figure 3.3) was applied, and the breast boundaries were drawn on the body[55].

2. A second photo was taken of the breasts with boundaries and landmarks. The participant was asked to stand in front of the cameras with the hands positioned at the hips for reproducible images. In this position, the breast photo was captured. The 3D pictures were saved in the Vectra XT supplied software and exported as an Object (OBJ) file. This is a file format to store a 3D object with colour information. The colour was used for the visualization of the landmarks.

### 3.2.4 3D modelling (Step 3)

3. 3-Matic version 15.0 (x64) (Materialise, Leuven, Belgium) was used for the segmentation of the 3D photos. The 3D photo was edited by drawing a curve along the determined breast boundary on the photo. By removing the superfluous surface, the segmented breast remained for further development of the breast mould. Now, the segmented breast was further edited through a design protocol to create a breast mould (Appendix D.2). Finally, the mould was exported to STL for 3D printing.

### 3.2.5 3D printing (Step 4)

4. An Ultimaker S5 (Ultimaker B.V., Geldermalsen, The Netherlands) 3D printer in the 3D lab MST was used for 3D printing the breast moulds. The print code was generated using Ultimakers Cura 3D print software. Polylactic Acid (PLA) filament was used for printing the breast moulds, a thermoplastic polyester. It solidified after one of the



Table 3.1: Descriptive statistics for the comparison between a 3D breast photo and a 3D mould photo. The mean values and SD of the four landmark distances are calculated and are less than 10 mm.

Distance (number of samples)	Difference between 3D breast photo and 3D printed breast mould			
	Distance		Percentage	
	Mean (mm)	SD (mm)	Mean (%)	SD (%)
U - N (16)	0.4	1.9	-0.2	2.6
N - IMF (16)	-0.8	1.0	1.3	3.0
L - M (16)	2.0	0.6	-1.3	0.7
U - IMF (16)	1.8	0.7	-1.0	0.7

extruders ejected the filament on the building platform. The following process settings were standardized: extruder temperature 205 °C, building board 60 °C, room temperature the same as the ambient temperature, layer height print 0.2 mm, infill 100%, no use of support infills, maximum overhang without support 60°C (90°C no support and 0°C support everywhere). The 3D breast moulds were printed in a ratio of 1:1.

### 3.2.6 Taking 3D breast mould photo (step 5)

5. The participants were asked to visit the hospital a second time for fitting the breast mould and be photographed with the mould on the breast. Through the holes of the mould was observed if the breast fitted the mould and no air was observed between the skin and mould.

### 3.2.7 Data analysis (Step 6 and 7)

6. The straight-line distances between the landmarks were measured in 3-Matic. The healthy volunteers and DIEP flap patients were considered as one group because only the healthy breasts of the volunteers were used for the development of the moulds.

7. The relative mean differences and standard deviations (SD) were displayed in a table in mm and percentages. The differences were calculated by subtracting the measurements of the 3D breast photo from the 3D mould photo. The mean values and standard deviation in mm and percentages were determined in Microsoft Excel 365 with the built-in function for these parameters. Negative mm values can be interpreted as an overestimation of the mould, while an overestimation is positive for the percentage results. A Bland-Altman plot was used to detect outliers in the measurements.

## 3.3 Results

The relative mean differences between the 3D breast photo and 3D breast mould photo are displayed in table 3.1 in mm and percentages. A mean maximum difference of 2.0 mm  $\pm$  0.6 (-1.3%  $\pm$  0.7) is shown in the lateral to medial (L - M) distance. Only in the N - IMF distance, an overestimation of the mould is found of -0.8 mm (1.3%).

Due to space constraints, Bland-Altman plots were not included for all the distances, but as an example, Figure 3.4 depicts the Bland-Altman plot for the U - N distance. The red displayed dot is considered as an outlier because this value exceeded the 10 mm limit.

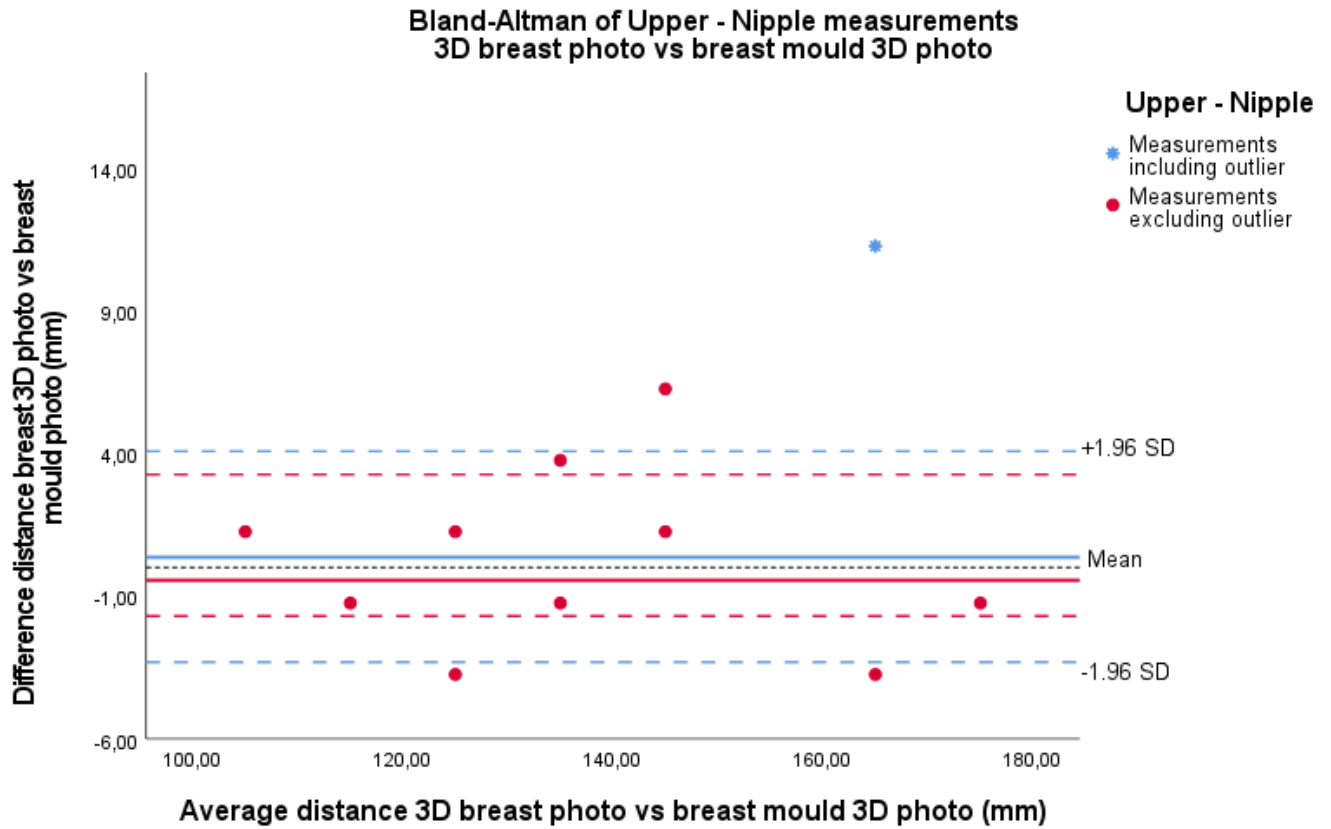


Figure 3.4: Bland-Altman plot of the upper nipple distance including the outlier. The blue (dotted) lines are the results of the mean and limits of agreement including the outlier. The red (dotted) lines excluding the outlier. The black dotted line is the zero line. The influence of the outlier is that the mean shifts from a positive value of 0.4 mm to -0.5 mm or in words from a small overestimation to a small underestimation.

### 3.4 Discussion

In this study, the size of 3D printed breast moulds segmented from 3D photos was validated on volunteers with landmark distance measurements. Straight-line distances were digitally measured on 3D photos of female breasts with and without a 3D printed breast mould. The differences between the landmark distances were analysed between the 3D breast photo and the 3D breast mould photo. The results were considered as accurate if below the 10 mm.

The maximum mean deviation found was  $2.0 \text{ mm} \pm 0.6 \text{ mm}$  ( $-1.3\% \pm 0.7\%$ ) in the L - M distance. This deviation was calculated by negative and positive distances, so this deviation suggests a small underestimation of the moulds sizes (distances breast minus distances mould). Underestimations are also observed in the U - N (0.4 mm) and U - IMF (1.8 mm) distances instead of small overestimation (-0.8 mm) in the N - IMF distance. The underestimations could be explained by the shrink of PLA when it is cooling down in the printer. The density of PLA changes due to crystallization with the transition from liquid to solid-state, resulting in shrinking material. The amount of shrink is dependent on temperature difference and environment humidity and can be 2.6% for general PLA according to

Ultimaker[7], which is 2-3 of mm for the current study. However, the heated building plate led to less temperature difference at the bottom of the printer. Therefore, more on top of the printer, an increased temperature difference can lead to more shrink of the material. The underestimated distances were printed more on top than the N - IMF which can probably be induced by this effect. A cover on top of the Ultimaker printer can keep the temperature more constantly in the building room.

The found deviations fell within the limit of 10 mm, thus the moulds are considered accurate for clinical application. Comparing with Lee et al.[56] who analyse digital and physical breast landmark distance measurements, they also found that most differences were less than 10 mm. They concluded that their results were sufficient to use in preoperative planning and postoperative evaluation of the breast.[56]

Most of the studies focused on developing and/or validating an accurate method for volume determination.[62, 73, 97–100] Wesselius et al.[97] validated the Vectra software for volume measurements and found a deviation of  $\pm 5$  per cent for a breast volume calculation.[97] The current study showed more promising results for accurate breast measurements with the landmark distances comparing the percentages ( $< 2\%$  for the current study). For the current study, the study of Menezes et al.[27] is probably more important. In this study, the hardware of the Vectra system was validated and found that random errors were always lower than 1 mm for digital measurements. So, they concluded the Vectra system as an accurate system for plastic and aesthetical surgery[27] although it could contribute to an extra millimetre in the distance measurements.

Comparing the 3D breast photo with the digital mould model and the 3D breast mould photo, the position of the nipple in the mould is displaced. In the left image in Figure 3.5, the nipple is seen through one of the holes in the mould, while in the photo with mould, the surface of the mould covers the nipple. This suggests that the mould can cause a displacement of the nipple and/or the shape of the breast. Therefore, it is important to position the mould correct on the breast. Landmarks can help with the positioning, for example with arrows on the mould that should be pointed to the landmark as the jugular notch and midclavicular.

A displacement of the maximum mean difference is observed from 0.4 to -0.5 mm shifting from underestimation to overestimation of the mould. Thus, the replacement of the mould on the breast can cause deformation of the breast and thus of the flap during surgery. Therefore, the measurement is included in the results to calculate the maximum mean difference. Despite the displacement, the maximum mean difference remains accurate enough for application in the clinic which is below the supposed limit of 10 mm. The outlier is included in the results to indicate the impact of the wrong positioning.

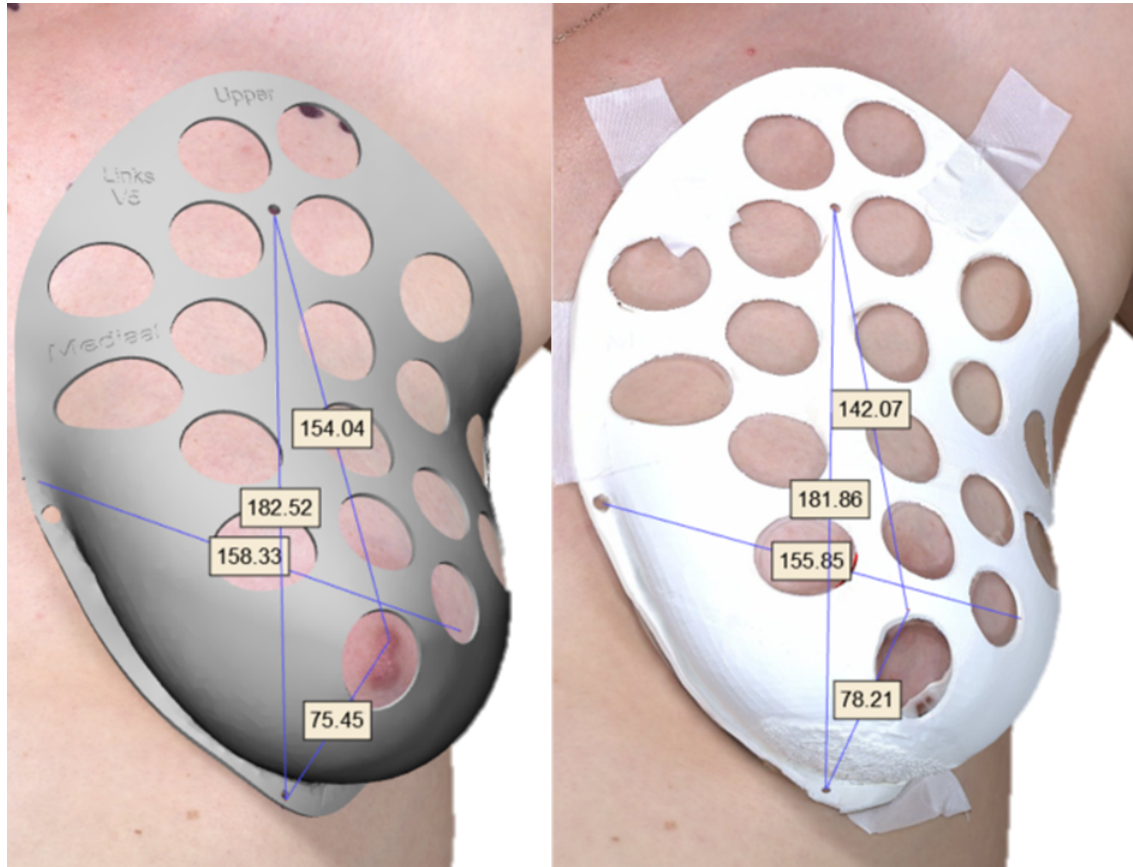


Figure 3.5: The origination of the outlier. Left, the 3D breast photo is displayed with the designed mould in 3-Matic as overlay on the breast. At the right, the 3D mould photo. Comparing the photos, a nipple displacement of 12 mm can be observed.

One outlier exceeded the limit of 10 mm (12 mm) in the U - N distance in volunteer 5. Figure 3.5 shows the breast in question with the landmark distances. In Figure 3.4 the influence of the outlier on the maximum mean difference is displayed in a Bland-Altman plot. The red (dotted) lines and point show the data excluding the outlier, the blue including the outlier. Interestingly, the distance N - IMF shows a deviation of 3 mm. One would be expected that the deviation was in the order of the deviation of the outlier distance U - N of 12 mm because these distances are in line with each other. This can be explained by a rotation of the nipple causing a translation. The breast surface is located in an XYZ coordinate system with the nipple as a coordinate on this surface. If the upper landmark is point (U), IMF (I) and nipple (N), a triangle UIN could be imagined. Because the U - N distance showed the largest deviation and the other distances showed similar values in this triangle, the conclusion is that the translocation of the nipple was caused by a rotation induced by positioning the mould.

### 3.4.1 Limitations

A limitation of the study is caused by the use of tape to fix the mould on the breast and the difference in positioning of the volunteers between the first and second photo. The most ideal situation is to use tape or adhesive material inside the mould on the boundary to fix the mould on the body. However, this could be unpleasant for the patient due to the amount of tape on the skin. Further, the volunteers could assume another position in rotation, and lean forward or backwards. Perhaps, these factors have influenced the landmarks in the mould photo causing it harder to find the middle of the landmarks leading to a possible deviation of 2 mm.

This caused deviations in the photo for example in the small landmark holes. Therefore, the landmarks were harder to recognize, because it was more visible as a small stripe instead of a circle. As result, the middle of landmarks had to be estimated, which could mean an error of 2 mm.

Another limitation of the study and the researched discipline is the lack of an acceptable defined limit for differences between landmark distances in literature.[80] Therefore, this study agrees with a limit of 10 mm landmark distance difference between breast and digital breast mould to define it as clinically accurate.

### 3.4.2 Future

The healthy volunteer group showed different characteristics compared to DIEP flap patients. The mean age of the volunteers was 32.2 ( $\pm 11.8$ ) years while in other studies the average age of DIEP flap patients lies between 47.5 and 51 years[8, 41]. Also, the BMI of the study group was lower than in a DIEP flap group,  $22.6 \pm 2.6$  (study group) vs around  $27 \pm 3.8$  (DIEP patients) [8]. Menopausal women produce less oestrogen leading to more body fat. This could explain why the BMI is higher in the DIEP flap group, in addition that DIEP flap patients need additional fat for enough flap volume. A higher BMI is associated with ptosis breasts[22, 43]. More ptosis and body fat can make it difficult to draw the landmarks and breast boundary accurately and hence the 3D modelling of the mould. Therefore, the influence of different human variables on developing moulds could be investigated.

Despite the moulds fitting the breasts perfectly, the folding line method to determine the breast boundaries cause an upper boundary almost touching the clavícula. Therefore, the folding line pressure method used to determine the breast boundaries is not suitable for all patients. Further research should be performed on which variables can influence this method, for example, breast ptosis. Also, a comparison between the boundaries of the folding line method and plastic surgeons pre-clinical drawn boundaries can be made to validate the design of the mould. The plastic surgeon can fill in a questionnaire answering specific questions about the moulds design such as fitting and size. Only moulds of healthy breasts were developed, validation of mirrored moulds on the contralateral side could be the next step.

The accuracy of developing breast moulds is demonstrated in this study by measuring landmark distances on a 3D breast photo and a 3D breast photo including the mould. Further research should investigate the moulds during

DIEP flap surgery as an intervention. A breast mould may contribute to symmetric breasts and patient satisfaction after a DIEP flap procedure. Patient satisfaction is dependent on factors such as symmetry. Treatment trajectory and can be scored by questionnaires such as the BREAST-Q. An objective method should be developed to gain more insight into the number of patients who are satisfied with the symmetry and do not request a secondary correction. Therefore, the development of such a method has to be explored and validated with clinical data. This could be, for example, observers score a database of for example 25 breast 3D photos on symmetry from zero (poor symmetry) to one (perfect symmetry). The same 3D photos are then segmented to the left and right breast surface and loaded into the algorithm that calculated the symmetry between them. The observer symmetry outcomes should be considered as the gold standard. The results of the algorithm will be compared to these outcomes and similar results will suggest a correct working algorithm. After this development, a clinical study with patients can be performed to compare patient satisfaction and symmetry. For example, a 3D photo is taken of a patient pre-operatively. The patient fills in the BREAST-Q questionnaire and Harris score (questionnaires about patient satisfaction). After the DIEP flap reconstruction, the patient will perform the same procedure two times, 2 weeks and 3 months after the operation. The breasts (left and right) can be segmented from the 3D photos, loaded into the algorithm and symmetry determined.

### **3.5 Conclusion**

A validation study was performed to validate the size of 3D printed breast moulds by measuring landmark distances on female volunteers segmented from 3D photos. The maximum mean deviation between landmark distance measurements found was  $2.0 \text{ mm} \pm 0.6 \text{ mm}$  ( $-1.3\% \pm 0.7\%$ ) which suggest a small underestimation of the breast moulds dimensions. Most of the mean results were  $< 2 \text{ mm}$ . The results fell within the limits of 10 mm resulting in an accurate outcome for clinical measurements. Thus breast moulds can be fabricated accurately for a healthy breast. However, the effect on patient satisfaction and breast symmetry has to be further investigated in DIEP flap surgery patients using a breast mould during DIEP flap surgery.

## Chapter 4

# Develop an objective breast symmetry validation method

A large diversity of studies and methods is used to measure patient satisfaction. The results of these studies differ and are difficult to compare.[30, 58, 76, 101] In the previous chapters, validation studies of the process from 3D photo to 3D printed models and the size of breast moulds were performed. These studies showed the possibility to create accurate breast moulds. These moulds can be used in a future study to further optimize symmetry after DIEP flap surgery and thereby increase patient satisfaction.

In order to interpret the symmetric result of breast reconstruction, developing an objective method is recommended to determine this surgery outcome. In this chapter, a first proposition to implement an algorithm to validate breast symmetry is described, including its validation. Finally, future development of the algorithm is proposed.

### 4.1 Patient satisfaction on symmetry and 3D moulds

Several studies have investigated the patients' satisfaction after DIEP flap surgery.[25, 88] Despite the full dedication of plastic surgeons to create the best result possible, there are still women unsatisfied with the symmetry after surgery.[Personal communication, H.A. Rakhorst, September 18th 2021]

Most of the studies on patients' symmetry experience focus on the volume of breasts.[14, 20, 101] Although some studies mention that volume measurements can be used for analysing breast symmetry [101], others show large deviations.[23] Therefore, there is no golden standard for objectively determining the symmetry and therefore predicting patient satisfaction.

Up until now, 2D photos have been used in various developed software to compare breast symmetry.[52] But the upcoming 3D photography enables the development of other methods using different and more variables instead of volume and 2D photos. Catanuto et al.[14] mentioned variables such as anatomical landmark distances, surface area,

angles, curvature and IMF shape for characterising the breast. From all variables, curvature was the most innovative result of this study which they used in a later study to describe the breast shape. It may become the new gold standard in the pre- and postoperative evaluation of surgical results.[15] Two other studies[57, 102] used curvature for detecting the breast boundaries, specifically the IMF.

The use of 3D photos can contribute to the surgical results and it has facilitated the computation of morphologic measures such as volume, ptosis and symmetry. This can be important for pre-operative planning and postoperative assessment of outcomes in breast reconstruction.[14, 15, 57, 102]

To determine if moulds provide better symmetry and patient satisfaction after DIEP flap surgery, an objective method is needed. In this chapter, the development of an objective algorithm for calculating breast symmetry is explored.

## 4.2 Method

The development of an objective validation method and related variables to determine breast symmetry from 3D photos is complex and several prerequisites need to be fulfilled. This paragraph discussed the following prerequisites:

1. Programming language software
2. Landmark definition/ selection ROI segmentation
3. Define variables to be used
4. Analysis method to compare the symmetry of breasts
5. Build up a validation database

### 4.2.1 Programming language software

For this study, MATLAB (MathWorks, Natick, USA) was chosen (Appendix C) because it can fulfil the required functionality of developing an algorithm and a lot of pre-existing scripts on the topic are available. Other languages (C++ and Python) are more complicated, but could perhaps also accomplish the required functionality.



### 4.2.2 Landmark definition/ selection & ROI segmentation

The 3D photo is segmented to the left and right breast before loading these 3D breast surfaces into the algorithm. 3-Matic (Materialise, Leuven, Belgium) was used to find landmarks, crop the surface and fill open vertices. 3-Matic was used for obtaining the breasts ROI because this software filled up open vertices created by cropping the 3D surface. The chosen landmarks were based on clinical use and obtaining only breasts surface (ROI). This led to the following landmarks (Figure 4.1):

1. Umbilicus
2. Jugular notch
3. Sternum point (2 cm under Jugular notch)
4. Lowest breast point (1 cm under IMF of the most ptotic breast)
5. Lateral breast point
6. Upper chest wall point



Figure 4.1: landmarks used to determine the ROI breast surface.

A summary of the creation of the ROI based on these landmarks is described in this section (Appendix D.3) contains the complete protocol). By selecting the landmarks and creating planes between these landmarks, the surface can be cropped to obtain the ROI. The following planes were created:

1. Midline plane plane through landmarks 1 and 3
2. Chest wall plane plane through landmarks 3 and 6
3. Abdominal plane plane through landmark 4 perpendiculars on plane 1
4. Lateral plane Through the lateral breast points, 5.

The superfluous parts were removed resulting in the ROI used for building up the database.

### 4.2.3 Define variables to be used

In this section, an explanation of the Gaussian curvature and surface area used in the MATLAB script is described for 3 surfaces.

#### Gaussian curvature

First, the curvature is explained by a simple 2D oscillating curve  $C$  with three points in the  $XY$ -plane  $K$ ,  $L$  and  $M$  (Figure 4.2). The curvature of these points can be calculated by the inverse radius ( $R$ ) of a unique circle through this point given by equation  $\kappa = \frac{1}{R} \text{ cm}^{-1}$ . It can be concluded that the larger the radius the smaller the curvature and vice versa.

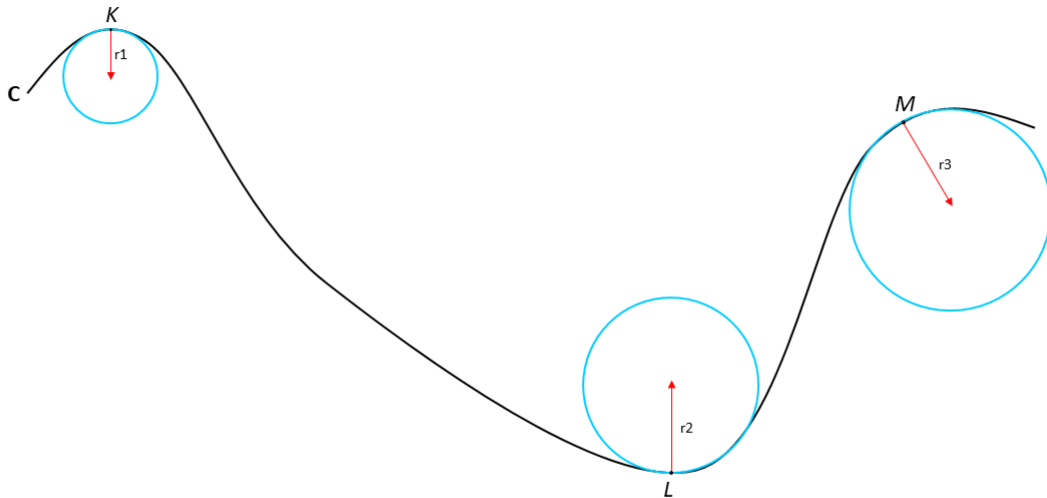


Figure 4.2: Image of the curvature in 2D. A curve with three points  $K$ ,  $L$  and  $M$ . On these points is a circle determined with corresponding radius of that point. The curvature can be calculated by the inverse radius.

For 3D surfaces, every coordinate has multiple curvatures, one in every direction. The principal curvatures are the values for the minimum and maximum bending (curvature) on a coordinate. The principal curvatures are indicated by  $\kappa_1$  and  $\kappa_2$  and are perpendicular to each other. Let  $M$  be a smooth surface in  $\mathbb{R}^3$  with a point  $\mathbf{P}$  as in Figure 4.3.  $\vec{N} = (0,0,1)$  is the unit normal vector to  $M$  at  $\mathbf{P}$ .  $\vec{T}$  is the unit vector in  $T_pM$ ,  $\vec{T} = (\vec{T}_1, \vec{T}_2, 0)$ . The parametrized curve  $\mathbf{c}$  is given by slicing  $M$  through the plane spanned by  $\vec{N}$  and  $\vec{T}$  ( $\mathbf{c}(t) = (\vec{T}_1t, \vec{T}_2t, f(\vec{T}_1t, \vec{T}_2t))$ ). By calculating the partial second derivatives of the original function  $\mathbf{f}$ , a Hessian 2x2 matrix can be obtained. From the Hessian, the eigenvalues,  $\lambda_1$  and  $\lambda_2$ , can be calculated. These are equal to the principal curvatures used for curvature analysis.[59]

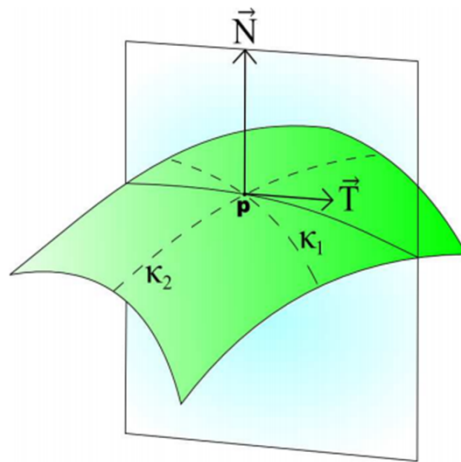


Figure 4.3: Surface  $M$  with normal vector  $\vec{N}$  and unit tangent vector  $\vec{T}$  of point  $p$ . The principal curvature are  $\kappa_1$  and  $\kappa_2$  determined from the vectors. The principal curvatures are the eigenvalues of point  $\mathbf{P}$ . [59]

Different curvatures can be derived from the principal curvatures. In this algorithm, the Gaussian curvature was used, because it is a scale-dependent curvature. This means that equal shapes of different sizes will result in another outcome. This is important in the case of breast symmetry because equal shape and size are needed for symmetrical breasts and thus patient satisfaction. The Gaussian curvature ( $G$ ) is calculated by the product of the principal components  $\kappa_1$  and  $\kappa_2$ , thus  $G = \kappa_1\kappa_2$  with unity  $\text{cm}^{-2}$ . The used curvature analysis in the algorithm is developed by Ben Shabat[77]. In Figure 4.4 an example of Gaussian curvature analysis is displayed of patients 3D photo This image shows a 25 year old patient with BRCA gene who requested preventive mastectomy and DIEP flap breast reconstruction.

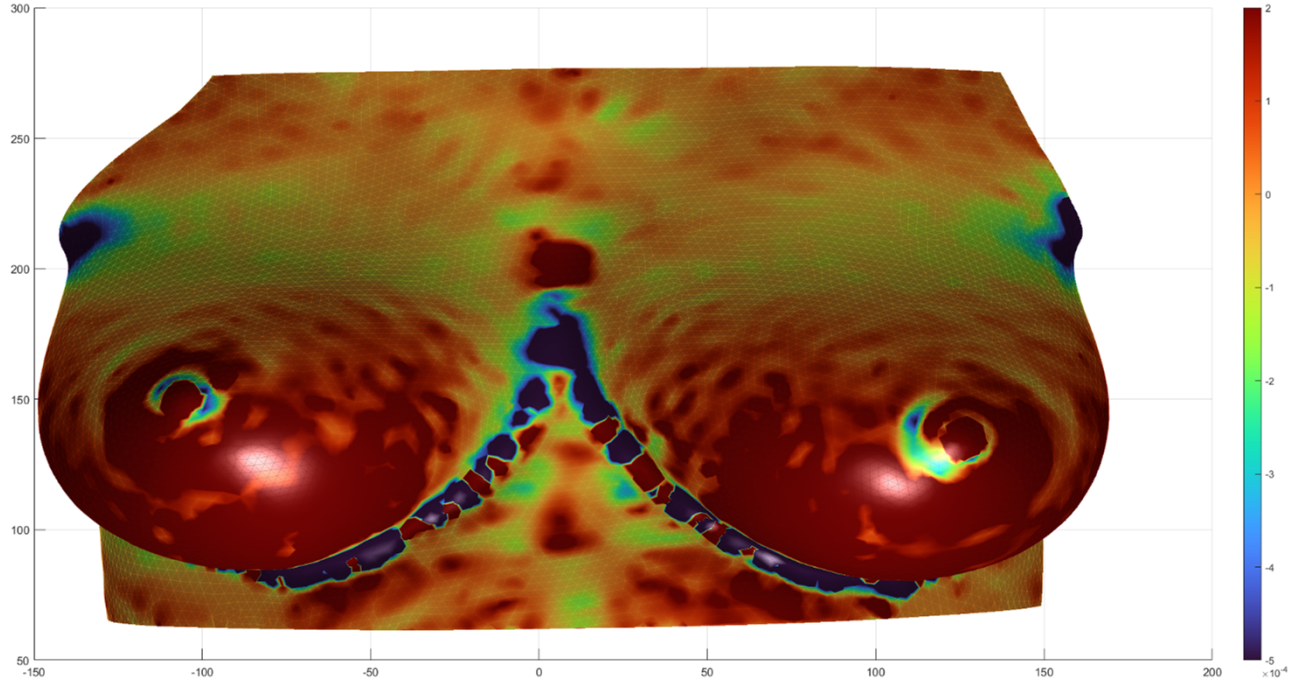


Figure 4.4: Example of 3D photo with Gaussian curvature analysis. Red indicates a convex curvature value while blue a concave curvature value. This image shows a 25 year old patient with BRCA gene who requested preventive mastectomy and DIEP flap breast reconstruction.

### Surface area

The calculation of a surface area with unit  $\text{cm}^2$  is dependent on the shape of a surface. The algorithm calculated the surface area from the faces (triangles) of a 3D photo with vectors illustrated in Figure 4.5. Let vector  $a$  and  $b$  two edges of a face. The cross-product of  $a$  and  $b$  ( $a \times b$ ) results in a vector  $c$ , the orthogonal of  $a$  and  $b$ . The magnitude of vector  $c$  can be calculated by

$$M = \sqrt{(C_x^2 + C_y^2 + C_z^2)} \quad (4.1)$$

and is equal to the surface area of a parallelogram created by  $a$  and  $b$ . Because the parallelogram is a quadrangle and the faces triangles, multiply  $M$  by  $\frac{1}{2}$  results in the correct surface area of the face. The sum of all the calculated triangle areas results in the total surface area of the 3D surface. The entire surface equation is  $\frac{1}{2} \sum M$ .

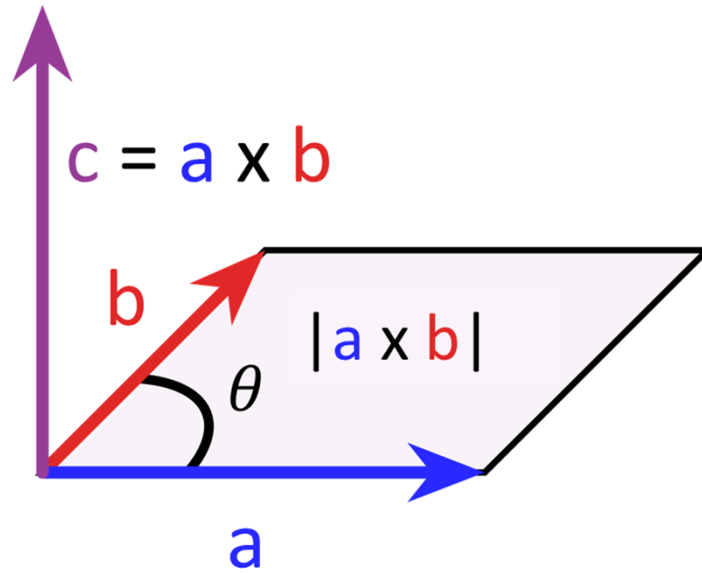


Figure 4.5: The cross product of vector a and b results in vector c. The length of c is calculated by the magnitude M and is the surface of the parallelogram created by a and b.

#### 4.2.4 Analysis method to compare symmetry of breasts

To compare symmetry between the left and right breast, an interpretable grading scale is required to compare the symmetry between the left and right breast for curvature and surface area. Furthermore, this outcome should be comparable with the outcome of clinical data. For example, similar to the Breast-Q (score between 1 - 100) or observers (1 - 10). In this algorithm, several equations were attempted to calculate symmetry for the curvature and surface area in a straightforward way, such as the equation  $c = \frac{a}{a+b}$ . The following equations for Gaussian curvature symmetry and surface area symmetry were used:

$$Curvaturesymmetry = \frac{MeanGaussianleft}{MeanGaussianleft + Meangaussianright} \quad (4.2)$$

And

$$Surfaceareasymmetry = \frac{Surfacearealeft}{Surfacearealeft + Surfacearearight} \quad (4.3)$$

Both equations resulted in a score between zero and one, with zero poor symmetry and one perfect symmetry. The total symmetry is calculated by summing the curvature symmetry and surface area and divided by two.

$$Totalsymmetry = \frac{Curvaturesymmetry + Surfaceareasymmetr}{2} \quad (4.4)$$

Also, this outcome is between zero and one, with zero poor symmetry and one perfect symmetry.

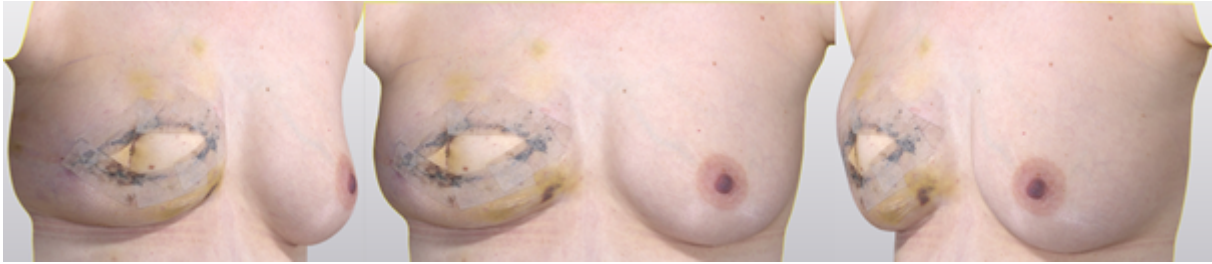


Figure 4.6: Example of a photo that was used in the questionnaire send to the (non)-expert observers to score breast symmetry

#### 4.2.5 Build up observer database

In order to validate the algorithm, clinical data is needed. 25 pre- and postoperative 3D breast photos of DIEP flap surgery patients were edited to develop a database. Three planes (frontal and two lateral) were obtained from these photos and merged (Figure 4.6). These merged photos were uploaded to Qualtrics (Qualtrics, Seattle, USA) and sent to (non-)experts for symmetry scoring. The observers analysed the photos on vertical, horizontal and projection symmetry.

### 4.3 Validation of an algorithm

The algorithm was validated on three aspects to ensure its correct functionality and results. These aspects are:

1. The variables
2. Observer database
3. Comparison algorithm results vs observers outcomes

#### 4.3.1 The variables

The algorithm outcome is validated with outcomes of Excel with ten digital created spheres in 3-Matic with different radii in a range from 1 to 512 cm. They were compared with the equations for Gaussian curvature ( $G = \kappa_1 \kappa_2$ ) and spherical surface ( $A = 4\pi r^2$ ) implemented in Excel. This validation is visualized in Figure 4.7 (curvature) and Figure 4.8 (surface area). The green line (algorithm calculation) and the red line (Excel outcome) fits in both images, indicating that the algorithm of MATLAB and Excel calculated the same results.

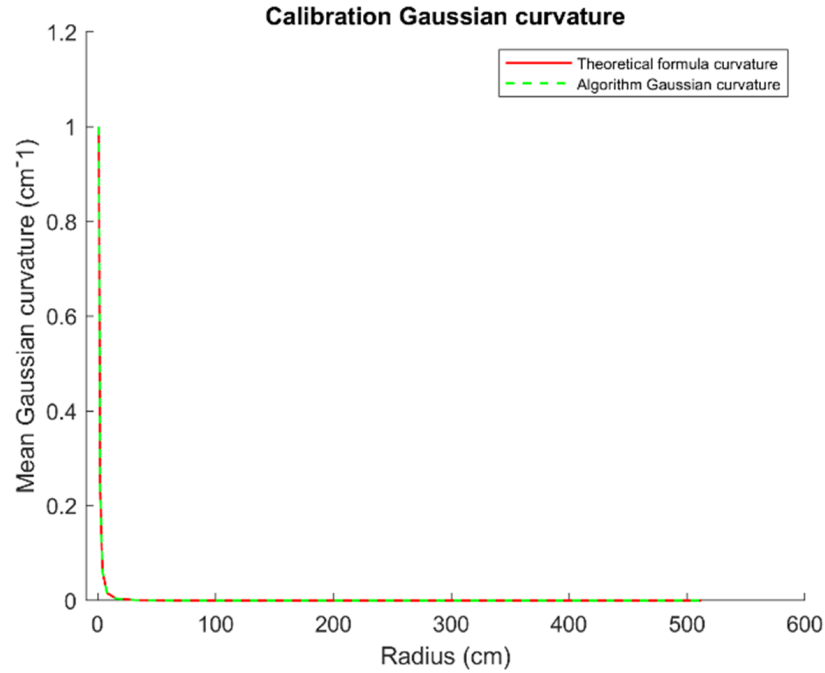


Figure 4.7: Graph to show that the outcome of the algorithm is equal to the Excels outcome for the Gaussian curvature, because both lines fit. The red line is the theoretical equation calculated in Excel and green the outcome of the algorithm.

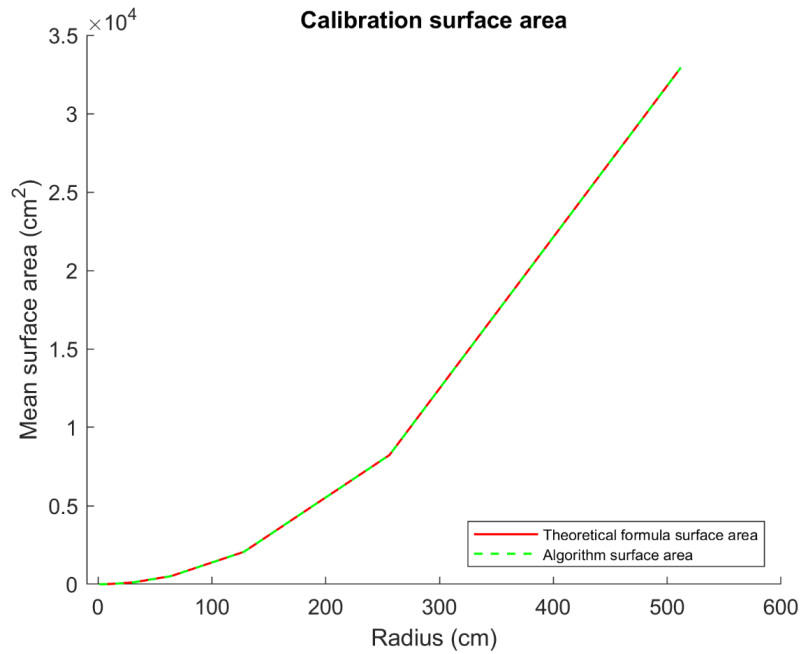


Figure 4.8: Graph to show that the outcome of the algorithm is equal to the Excels outcome for the surface area, because both lines fit. The red line is the theoretical equation calculated in Excel and green the outcome of the algorithm

### 4.3.2 Observer database

To perform a reliable comparison between the algorithm and observers, agreement between the observers is required. The intraclass correlation coefficient (ICC) and kappa are often used methods to prove an agreement between observers. SPSS (IBM, New York, USA) was used in this study to determine the ICC and kappa of the observer database. An ICC of 0.84 was shown, which demonstrates an almost perfect correlation between the observers. The kappa values vary from 0.49 to 0.70 which suggests a moderate to substantial correlation. According to epidemiology, these kappa values are usual outcomes for clinical diagnostics.[12] The kappa value is corrected for coincidence and is, therefore, lower than the ICC.

In Figure 4.9 the observer results were displayed in individual results, mean value and SD. Most agreement between the observers is in the poor symmetry cases (0.1 - 0.2) and good symmetry (0.9 - 1). Most disagreement between the observers is observed in the cases between the 0.2 and 0.8. This suggests that generally symmetry is subjective, except if breasts are of good or poor symmetry. Using observer data for algorithm validation, in an ideal situation, total agreement between the observers is required. However, an algorithm of  $\pm 0.1$  point between the different observers is a more realistic range that should be sufficient for validation.

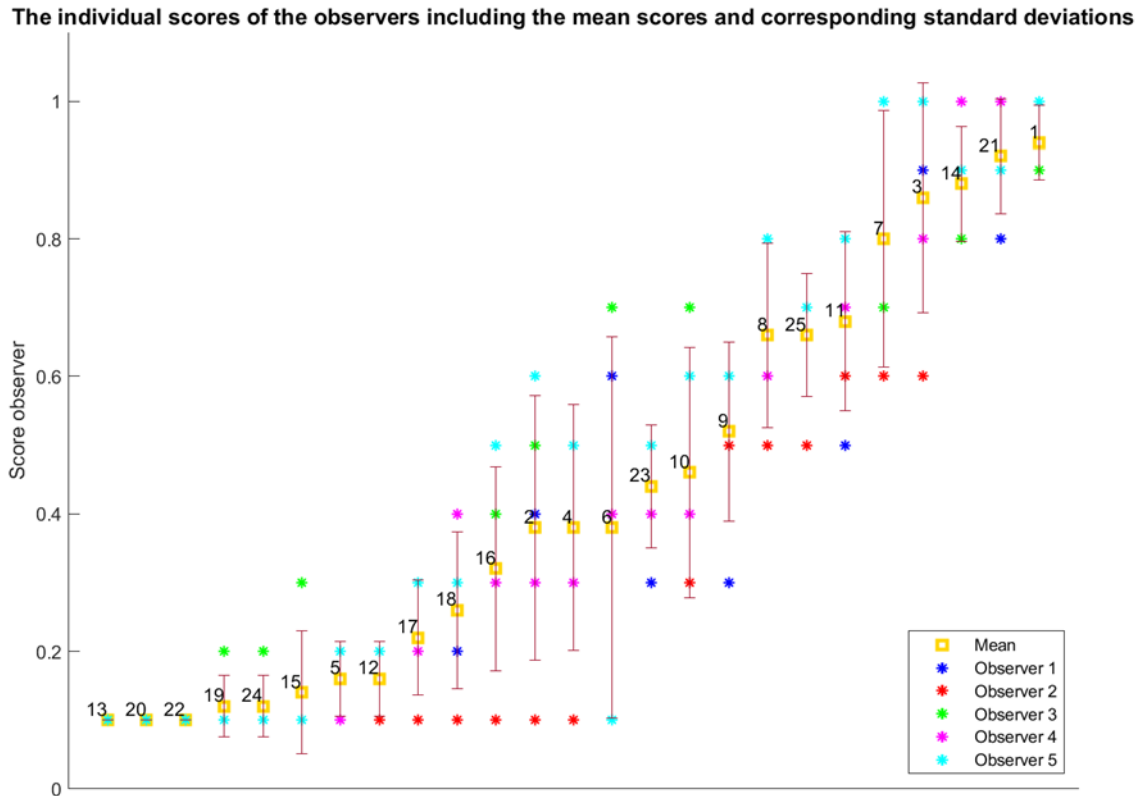


Figure 4.9: Five observers responded on the 25 breast symmetry cases. The results are displayed in this graph together with the individual scores, mean and standard deviation. The mean score is in ascending order.



### 4.3.3 Comparison breast symmetry algorithm vs observers

Three comparisons were performed between the algorithm and observers and displayed in Figure 4.10:

1. Mean observer outcome (yellow) vs surface area algorithm (blue) Top
2. Mean observer outcome (yellow) vs curvature symmetry algorithm (red) Middle
3. Mean observer outcome (yellow) vs total symmetry algorithm (green) (Curvature score + Surface area score) - Bottom

The observer outcome was considered the gold standard in the comparisons to the algorithm surface area (Top), Gaussian curvature (Middle) and total algorithm outcome (Bottom). The surface area outcome structurally showed high symmetry outcome. Therefore, an overestimation could be observed in most cases, except that for the cases which were considered good symmetry by the observers. However, for an accurate reproducible variable, a maximum deviation of  $\pm 0.1$  between the observers and the surface area algorithm is required to apply this variable as a symmetry outcome measurement. The Gaussian curvature and total symmetry of the algorithm show random outcomes in comparison with the observer outcome. Therefore, the variables will currently suffice to use in symmetry analysis. Optimisation should improve the calculation to a maximum deviation between the algorithm and observers for a reliable comparison.

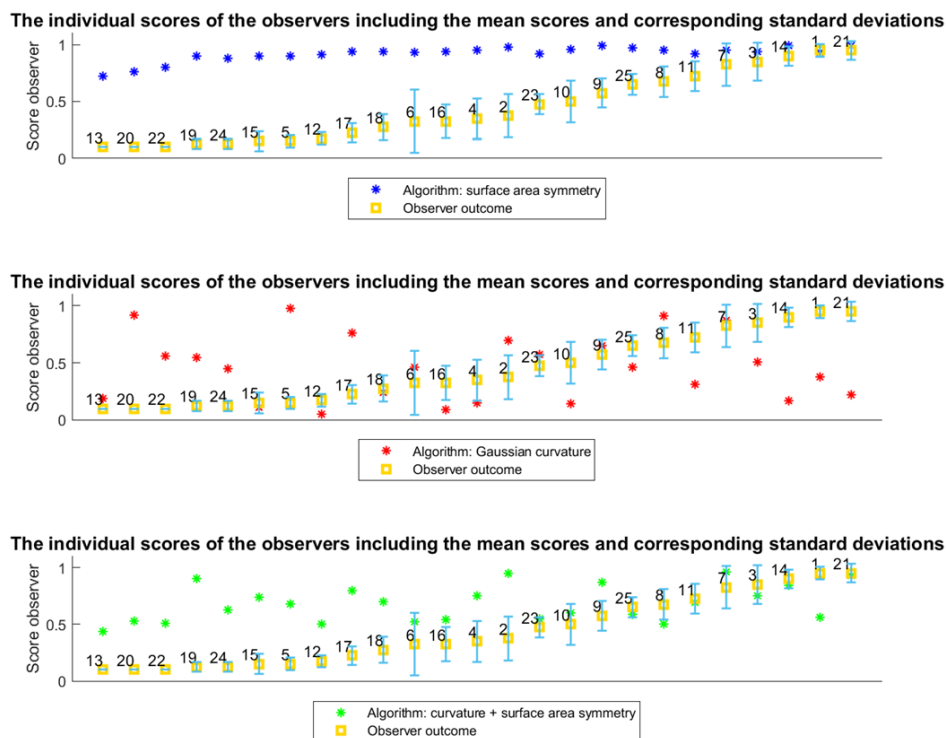


Figure 4.10: Outcome of the algorithm compared with the mean observer outcome. In the top, the mean observers vs the surface area of the algorithm is displayed. In the middle, the Gaussian curvature vs the mean observer outcome is displayed and in the bottom graph the total symmetry summed by the Gaussian curvature and surface area compared with the observer outcome symmetry is showed.

## 4.4 Discussion and future developments

The current development is the start for further development and detailing of the variables and the algorithm for use in the clinic. Before the algorithm can be implemented in the clinic several optimizations can be implemented. First, the ROI segmentation procedure takes time and is difficult and needs to be optimized to make it faster and easier. Second, the detection of the breast boundary can be optimized for the exact detection in the algorithm, for example with curvature. This will contribute to a more reliable breast area determination. Both factors will add to a reliable symmetry analysis.

The surface area outcomes showed a high symmetry between the breasts in each case. This suggested that the surface area is unsuitable for use in this symmetry analysis. It will always leads to an overestimation of the symmetry factor. The calculation of the curvature can be developed by dividing the breast into quadrants and other symmetry statistic analyses. It is advised to discuss methods for this analysis with an expert.

### 4.4.1 Algorithm

The root means squared (RMS) distance and Hausdorff distance (dH) are reflection symmetry analyses along the midline. In the first method, RMS, the left or right breast is reflected onto the other and a grid is applied on one of the breasts. The perpendicular distance from the vertices to the other breast is calculated. Zero distance between the breasts indicates the same symmetry. A limitation of RMS is the dependency of the reflection. Poor matching of the surface can result in a considerable deviation, while the breasts can resemble each other.[72]

The Hausdorff distance dH calculates the minimum distance between the vertices of two datasets X and Y (left and right breast in this case). The two datasets have to be superimposed on top of each other causing them to be approximately in the same plane. The vertices of X will match with the vertices of Y and calculate the minimum distance between the vertices. The largest distance between a vertex of X and Y is the Hausdorff distance. It is advised to use the mean distances of a few vertices to reduce the influence of a potential outlier in the database. This increases the sampling time but improves the result.[81]

Ray Casting can avoid this problem of sampling. Similar to Hausdorff, two meshes X and Y were superimposed on top of each other causing them to be approximately in the same plane. A set of rays along the z-axis were cast through the meshes. The rays intersect both meshes at different points. The distance between the intersection points of the same ray between X and Y is determined. The total distance of the rays is divided by the number of rays to calculate the symmetry deviation. Comparison between Ray Casting and Hausdorff distance is a 2% better accuracy of the Hausdorff distance with 97% according to Stephenson et al using a different scanned object such as a fake head.[81]

### 4.4.2 Variables

Despite the decent values of the ICC and kappa, the deviation between observers and algorithm is 0.6 in some cases (bad to tolerable symmetry). This subjective large difference shows exactly the motivation for the development of an objective algorithm. The principal curvatures ( $\kappa_1$  and  $\kappa_2$ ) can also be used for other curvatures, such as the (4.5) shape index (S) and (4.6) curvedness (C).

$$S = \frac{2}{\pi} * \arctan\left(\frac{\kappa_1 + \kappa_2}{\kappa_1 - \kappa_2}\right) \text{with } (\kappa_1 \geq \kappa_2) \quad (4.5)$$

and

$$C = \sqrt{\frac{\kappa_1^2 + \kappa_2^2}{2}} \quad (4.6)$$

The S contains the shape information, while C contains the size information. The product of SC (SC classification) merged the most valuable information of both in one equation. Also, the SC can replace the Gaussian curvature, because of its fair sensitivity to surface changes, independent for principal orientation, less influenced by image noise and is invariant to geometric transformations.[13, 51]

### 4.4.3 Testing

Patient satisfaction is often based on different aspects in comparison to how plastic surgeons rate success such as treatment trajectory and decreased satisfaction of their breasts.[23] Therefore, the algorithm should be validated also with patient data for better clinically relevant outcomes.

The factor calculation may be improved because the current equation can lead to a negative symmetry result. Despite variations tried with absolute values, thresholds and orientating the left and right breast in the same direction, no solution was established.

The observer database shows different outcomes in several cases judging the breast symmetry (Figure 4.9). This indicates and proves that breast symmetry is subjective and therefore the need for an objective method. Further, the observer outcome was considered as the gold standard compared with the algorithm outcome. However, due to the differences in outcome, this method can be judged as invalid and subjective. In short, a comparison between the observer outcome with the algorithm is comparing two invalid methods. Therefore, another reliable and valid method should be investigated before a judgement can be pronounced about the algorithm's working. A solution could be to develop a database with a comparison between left and right breast with clinical contour line distances.

### 4.4.4 Breast contour analysis

Another, more simple approach to describe the breast shape could be with a few breast contour lines, for example, the contour of the IMF, midclavicular to IMF and lateral to medial. Analysis such as in Figure 4.11 can be performed. It is

possible to describe the contour as a polynomial, for this contour line:

$$f(x) = a_1 * e^{-\left(\frac{x-b_1}{c_1}\right)^2} + a_2 * e^{-\left(\frac{x-b_2}{c_2}\right)^2} + a_3 * e^{-\left(\frac{x-b_3}{c_3}\right)^2} + a_4 * e^{-\left(\frac{x-b_4}{c_4}\right)^2} + \dots \quad (4.7)$$

However, investigation to describe the segments of the contour can make it more specific. In the example of Figure 4.11 the breast is separated into three segments:

1. Upper breast - start nipple
2. Nipple
3. End nipple - IMF

Mathematical estimations of these segments lead to a linear approach for segment 1, a parabolic for segment 2 and an exponential approach for segment 3. This thought is the first exploration for this approach. Further research can investigate the feasibility of this approach is the number of segments per contour, the best mathematical approach, how to apply it for analysing breast symmetry and to implement it in an algorithm for software development.

Widespread possibilities for 3D analysis and variables are available for developing an objective algorithm. Therefore, it is hopeful that this can be realized in short term. In this chapter, the first development of an objective algorithm is described, but should be further developed for use in the clinic.

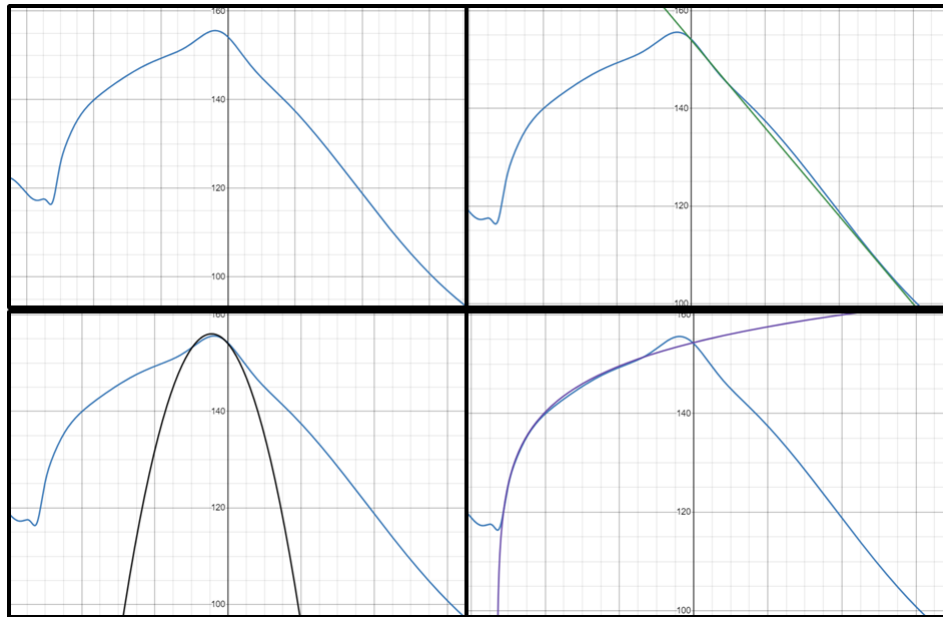


Figure 4.11: Example of the mathematical approach of breast contour segments, top left the original contour, right top the linear approach of the upper breast to start nipple, left below the nipple as a parabolic equation and right below the end nipple to IMF as an exponential equation.

## 4.5 Conclusion

In conclusion, the first step is taken to develop an objective algorithm. A valid database as the gold standard should be developed to validate the algorithm. In this chapter, (new) analysis methods and variables are described for further development. Also, with a database, visualizations were displayed as an example for other researchers. Further research should focus on further development of the algorithm, validation database and application in the clinic.



# Chapter 5

## Future perspectives

In this chapter, a potential clinical application of implementing a 3D printed mould, handheld cameras and the use of symmetry calculating software has been outlined. Secondly, thoughts about future research has been described.

### 5.1 Implementation of 3D printed moulds in the clinic

Most results of the clinical distance measurements showed less than 10 mm deviation between the 3D breast photos with or without a mould. With these results, the step to implement moulds during breast reconstruction surgery can definitely be taken. The moulds used for breast reconstruction and research in MST and ZGT are created by technical medicine interns. The next step will be to extend the clinical workflow for a better implementation of the 3D printed breast moulds. An implementation workflow (from 3D photo of the patient to use in the operation room) for sterile breast moulds is developed in the Radboudumc[71]. Protocols such as the 3D photography protocol and mould design protocol were developed in cooperation with ZGT, MST and Radboudumc. Due to different software systems, printing companies and other workflows in the clinic, direct implementation of the Radbouds workflow is not possible, but the protocols may be a good starting point to develop an implementation workflow specifically for ZGT and MST to use breast moulds during DIEP flap surgery.

Breast moulds could also be used for more practical applications, such as supporting inexperienced plastic surgeons during DIEP flaps as training and, hence, accelerating the learning curve. Also, the use of breast moulds in less skilled flaps, such as the LICAP, LAP or TUG flap can support the plastic surgeon during breast reconstruction.[42, 75][Personal communication H.A. Rakhorst, October 1st 2021] The potential use of breast moulds is for primary breast reconstruction to save women from secondary corrections. The use of a mould in unilateral patients who are satisfied with their unaffected breast and have sufficient abdominal volume is most obvious because there is a reference breast to design a mirrored mould. However, in bilateral reconstructions, moulds could be obtained for women who have still their breasts before mastectomy is performed, for example in

a BRCA case. Therefore, a requirement for the moulds design is that it is created from the original breast(s) of a patient.

More requirements for the breast mould are invented by a technical medicine student who interviewed six plastic surgeons for her clinical internship. The result of this inventory was a stiff, transparent, circle pattern sterile mould with anatomical landmarks and a thorax border.[89] Therefore, the decision to use a (sterile) mould during DIEP flap should be made after using both types of moulds and taking into account the costs of the two methods.

Distinguishing between a sterile mould and a non-sterile mould should be based on cost-effectiveness and skilfulness during surgery. The non-sterile moulds were put in a sterile sleeve which might impede the surgeon during surgery. The outcome could be evaluated by a questionnaire from the experience in the operating room using the (non-) sterile mould. A sterile mould of PA12 Nylon, printed by a company is estimated at 274 euros for a C cup, while an in-house non-sterile printed PLA mould is estimated at 94 euros. A sterile BioMed Clear Resin mould is estimated at 166 euros. Total costs of the moulds were estimated at 513.04 for the PA12 Nylon sterile mould, € 382.36 for the BioMed Clear Resin sterile mould and € 295,24 for a non-sterile PLA mould. A DIEP flap surgery costs 17,000 euros in the Netherlands[70], including outpatient clinic visits and hospitalization days after the surgery. This means a mould of 513.04 euros has an impact of 3% on the budget, a non-sterile mould 1.7%. Using a non-sterile in-house printed mould is a low-threshold and cheaper technique to use in DIEP flap surgery. In a master thesis[48] estimated that a PLA non-sterile 3D breast mould is most cost-effective for application during DIEP flap surgery with incremental costs of € -786.79 and an ICER of € -4,325.85. Thus, it is worthwhile to investigate the estimated cost-effectiveness in a study. Such as in an RCT with the mould as an intervention during DIEP flap including the costs of the used camera system.[48]

The used 3D photography system in this thesis was the Canfield Vectra XT system. This robust immovable system operates very well for the application of designing a mould. However, the group of plastic surgeons work in different locations causing patients for DIEP flap to visit another location than the hospital with the Vectra XT system. Even though, the health professionals aim to cluster patients visits to prevent extra visits and travelling for the patient. A solution to this problem could be using handheld scanners such as the Artec Eva (Artec, Luxembourg). Even, the iPhone X (Apple Inc., Cupertino, California, USA) has the potential to be implemented in the clinic for capturing 3D breast photos. These devices are small, cheaper and the specifications are impressive compared to expensive systems such as the Vectra XT. In a previous master thesis by Sharma et al.[79], they compared three devices (iPhone X, Vectra XT and Artec Eva) on several specifications. With the lower costs of 600 euros for the iPhone and € 13,700 for the Artec, the specifications of these scanners were not inferior to the 40,000 euros that the Vectra XT system costs. The resolution of the iPhone and Artec is 0.5 mm which is more than two times better than Vectra (1.2 mm). Furthermore, the iPhone can capture and process photos in real-time. The Vectra XT and Artec have capture and



processing time, which is for the Vectra XT system more than a minute in processing time and for the Artec 2 million points per second, but it is unclear how fast this is in seconds for capturing a female thorax.[79] These handheld scanners can open up new opportunities in the clinic. The devices can be easily transferred between hospitals or chambers of the outpatient clinic allowing health professionals flexibility to perform the scan. This could be a solution for the three hospital locations in Twente. Handheld scanners make it possible to take 3D photos with the same device at all three different hospital locations. Also, patients can have all their appointments at one location. Another advantage could be that 3D photos can be checked faster for deformities leading to a shorter undressed time for the patient if the photo is useable. Therefore, further research into implementing these scanners in the clinic is recommended.

Since May 26, 2021, the European legislation for medical devices has been changed (MDR 2017/ 745), by which the medical software in chapter 4 is classified as class IIa. As a result, certification is now needed and for using the software in the clinic and clinical study has to be performed before using it. According to the MDR, the non-sterile mould can be classified as class Is, because it is packed in a sterile sleeve during surgery. A sterile mould would be classified as class IIa, but is dependent on the intended use. Both moulds should be therefore verified by a notified body. Internal fabricated medical devices have to fulfil the safety and performance requirements described in appendix I of the MDR[36]. On the website of the Dutch Government is a list with requirements if fulfilled; other requirements of the MDR might be ignored.[31] Manufacturers of medical devices are allowed to use different quality management systems, but advised and most common is the international certified NEN-EN-ISO 13485 standard.

Last but not least, the technical physician (TM) may play a major role in the application of using a mould during DIEP flap. Having the clinical responsibility (BIG registration) and knowledge, the technical physician is able to explain information about the DIEP procedure, perform a clinical follow-up and take 3D photos on the outpatient clinic. Consequently, plastic surgeons will be able to focus on more complex cases. The patients benefit is that one visit will be sufficient to discuss (further) treatment, a physical exam and taking additional (3D) photos. Furthermore, the TM can take responsibility for designing the mould, organise printing it at the 3Dlab or 3D printing company and regulate that the mould will be delivered at the sterilization department or operating theatre. During the surgery, the TM can assist the surgeon in using the mould.

## 5.2 Future research

Future research such as a randomized control trial (RCT) using a mould during DIEP flap surgery as an intervention is recommended. In Figure 5.1, a mould was used to estimate the volume and of the abdominal flap to reconstruct the breast. The results of this RCT can show the added value of using a mould in patient satisfaction after surgery, a reduction of surgery time and the effect on the number of secondary surgeries. This thesis illustrates the development



Figure 5.1: Using a mould during DIEP flap surgery for estimating the volume and shape of the abdominal flap

and application of 3D techniques in breast reconstruction surgery for optimizing and analysing breast symmetry. To collect evidence if moulds improve the symmetrical result, patient satisfaction and reduce surgery time, further research will be needed.

Gaining insight into the satisfaction of women related to a symmetry grade is investigated in an ongoing study at the department of plastic surgery of ZGT/ MST/ 3D lab MST. This is needed to develop a common method to score the symmetry between breasts related to patient satisfaction. This method could be used later to determine if a mould can contribute to better symmetry and patient satisfaction. Furthermore, an algorithm can be applied for the symmetry analysis in the RCT to objectively analyse if a mould can improve the symmetry after the DIEP flap.

Although, the developed algorithm needs to be further developed, using such an algorithm for symmetry determination could be added and used in the clinic. In chapter 4, the results are discussed and several future directions and applications are suggested, such as shape index, curvedness and Hausdorff distance. The algorithm can be deployed

for patient education. Disagreement between plastic surgeons and patients after DIEP flap can occur about the symmetrical result[21, 95]. Plastic surgeons can be more critical than the patient, but in other cases, patients are more critical and claim that a correction has to be performed, although the result will not improve.[95] With an objective and fast algorithm that determines the breast symmetry correct, the patient can be informed about the symmetry in comparison to other women in this category. It can support the plastic surgeon to convince the patient that another correction will not contribute to an improvement of symmetry. Further, a prediction model can be investigated to show how much symmetry can increase with a correction surgery.

The focus of this study was on the validation of 3D printed moulds on healthy breasts and exploring a 3D symmetry analysis of 3D photos. However, several other researches in DIEP flap such as in sensory innervation, fluorescent techniques for blood supply in the flap, augmented reality and 3D bioprinting have been conducted. Improve pre- and postoperatively DIEP flap surgery with multiple techniques can contribute to higher successful DIEP flap reconstructions, faster recovery, lower costs and higher patient satisfaction.



# Chapter 6

## Conclusion

The overall goal of this project is to improve patient satisfaction after DIEP flap surgery with the application of 3D techniques. Three objectives were set out to achieve this main aim:

1. 1. Validate the process from 3D photo to 3D print using breast phantoms by measuring anatomical landmark distances (chapter 2)
2. 1. Validate the size of 3D printed breast moulds segmented from 3D photos by measuring anatomical landmark distances on healthy volunteers and patients undergoing DIEP flap surgery (chapter 3)
3. 3. Explore the possibilities to develop an objective grading method for breast symmetry to quantify patient satisfaction (chapter 4)

In chapter 2, For most landmark distance measurements, the mean differences between comparisons I-V were mostly  $< 3$  mm and  $< 1\%$ . The maximum mean deviation was  $-3.4$  mm  $\pm 3.1$  ( $1.9\% \pm 1.7\%$ ) in comparison V (from breast phantom to 3D print) in the MC N distance. The smallest deviations were found in the comparison between Vectra and 3-Matic. The next step was to investigate 3D printed breast moulds on volunteers.

The maximum mean deviation found in the clinical study on volunteers was  $2.0$  mm  $\pm 0.6$  mm ( $-1.3\% \pm 0.7\%$ ). Most results were  $< 2$  mm and  $< 1.5\%$ . These results are accurate because they fell within the limit of 10 mm deviation. Nevertheless, the outlier of 13 mm shows that correct positioning of the mould should be taken into account to prevent dislocation of the breast. In conclusion, 3D printed breast moulds can be obtained accurately for the same breast and can be used for 3D DIEP flap surgery planning. The next step is to use a mirrored mould as an intervention during unilateral DIEP flap surgery and monitor the clinical outcome in patient satisfaction and symmetry in further research. To determine the symmetry objectively instead of subjective patient outcomes, an algorithm may provide a solution.

In the last study of this thesis the possibilities to develop an objective algorithm were explored. A first proposition to implement an algorithm to validate breast symmetry was performed, including validation of the prerequisites showing with data. Finally, future development of the algorithm is proposed. In further research other parameters, a

correct symmetry factor and validation with a second dataset (for example patient or larger expert database) should be investigated to develop the algorithm for clinical reproducibility. Also, the observer database turned out to be subjective, thus for algorithm validation, first an objective database should be developed.

In the clinic, a definitive workflow for using breast moulds has to be developed for continuity. The Technical Physician (TM) can play an important role in using breast moulds in the clinic. With clinical responsibility (BIG registration) and knowledge, the TM can have conversations with patients, perform the procedure to develop the mould and assist the plastic surgeon in the operating room. Further research, for example, an RCT, should focus on using a breast mould during DIEP flap surgery as an intervention. Clinical outcomes such as reducing costs- and surgery time, symmetrical breasts and patient satisfaction can show the added value of a breast mould, but should be first investigated.

# Bibliography

- [1] Nederlands Kankerregistratie (NKR). cijfers over kanker.
- [2] Cijfers over borstkanker, 2020.
- [3] A. A and S. Appavu. External Breast Prosthesis for Post Mastectomy Women. *Asian Journal of Nursing Education and Research*, 11(03):427–430, 2021.
- [4] C. R. Albornoz, P. B. Bach, B. J. Mehrara, J. J. Disa, A. L. Pusic, C. M. McCarthy, P. G. Cordeiro, and E. Matros. A paradigm shift in U.S. Breast reconstruction: Increasing implant rates. *Plastic and Reconstructive Surgery*, 131(1):15–23, 2013.
- [5] R. J. Allen and P. Treece. Deep inferior epigastric perforator flap for breast reconstruction. *Annals of Plastic Surgery*, 32(1):32–38, 1994.
- [6] M. Barone, A. Cogliandro, M. Signoretti, and P. Persichetti. Analysis of Symmetry Stability Following Implant-Based Breast Reconstruction and Contralateral Management in 582 Patients with Long-Term Outcomes. *Aesthetic Plastic Surgery*, 42(4):936–940, 2018.
- [7] M. Bergsma. Onderzoek naar de mogelijkheden van FDM 3D printen met zaagsel ten behoeve van interieur-bouw. 2015.
- [8] J. Beugels, L. T. Hoekstra, S. M. Tuinder, E. M. Heuts, R. R. van der Hulst, and A. A. Piatkowski. Complications in unilateral versus bilateral deep inferior epigastric artery perforator flap breast reconstructions: A multicentre study. *Journal of Plastic, Reconstructive and Aesthetic Surgery*, 69(9):1291–1298, 2016.
- [9] M. d. Boer, M. Mureau, R. v. d. Hulst, J. D. Boer, D. D. Jong, and H. Rakhorst. ACHTERGRONDINFORMATIE EN FREQUENTLY ASKED QUESTIONS BIJ BIA-ALCL ( BORST IMPLANTAAT GEASSOCIEERD. *Nederlandse vereniging voor Plastische Chirurgie*, 2016.
- [10] C. Bortolotto, E. Eshja, C. Peroni, M. A. Orlandi, N. Bizzotto, and P. Poggi. 3D Printing of CT Dataset: Validation of an Open Source and Consumer-Available Workflow. *Journal of Digital Imaging*, 29(1):14–21, 2016.
- [11] M. Botsch, L. Kobbelt, M. Pauly, P. Alliez, and L. Bruno. *Polygon mesh processing*. Natick, 2010.
- [12] P. d. L. Bouter, d. i. M. v. Dongen, and P. d. i. G. Zielhuis. *Epidemiologisch onderzoek*. Houten, 6th edition, 2010.

- [13] H. Cantzler and R. B. Fisher. Comparison of HK and SC curvature description methods. *Proceedings of International Conference on 3-D Digital Imaging and Modeling, 3DIM*, 2001-Janua(February 2001):285–291, 2001.
- [14] G. Catanuto, A. Spano, A. Pennati, E. Riggio, G. M. Farinella, G. Impoco, S. Spoto, G. Gallo, and M. B. Nava. Experimental methodology for digital breast shape analysis and objective surgical outcome evaluation. *Journal of Plastic, Reconstructive and Aesthetic Surgery*, 61(3):314–318, 2008.
- [15] G. Catanuto, W. Taher, N. Rocco, F. Catalano, D. Allegra, F. L. M. Milotta, F. Stanco, G. Gallo, and M. B. Nava. Breast Shape Analysis with Curvature Estimates and Principal Component Analysis for Cosmetic and Reconstructive Breast Surgery, 2019.
- [16] T. Catherwood, E. McCaughan, E. Greer, R. A. Spence, S. A. McIntosh, and R. J. Winder. Validation of a passive stereophotogrammetry system for imaging of the breast: A geometric analysis. *Medical Engineering and Physics*, 33(8):900–905, 2011.
- [17] M. P. Chae, R. D. Chung, J. A. Smith, D. J. Hunter-Smith, and W. M. Rozen. The accuracy of clinical 3D printing in reconstructive surgery: literature review and in vivo validation study. *Gland Surgery*, 10(7):2293–2303, 2021.
- [18] M. P. Chae, W. M. Rozen, N. G. Patel, D. J. Hunter-Smith, and V. Ramakrishnan. Enhancing breast projection in autologous reconstruction using the St Andrew’s coning technique and 3D volumetric analysis. *Gland Surgery*, 6(6):706–714, 2017.
- [19] M. C. Champaneria, W. W. Wong, M. E. Hill, and S. C. Gupta. The evolution of breast reconstruction: A historical perspective. *World Journal of Surgery*, 36(4):730–742, 2012.
- [20] K. Chen, C. J. Feng, H. Ma, F. Y. Hsiao, L. M. Tseng, Y. F. Tsai, Y. S. Lin, L. Y. Huang, W. C. Yu, and C. K. Perng. Preoperative breast volume evaluation of one-stage immediate breast reconstruction using three-dimensional surface imaging and a printed mold. *Journal of the Chinese Medical Association*, 82(9):732–739, 2019.
- [21] M. Cohen, B. Evanoff, L. T. George, and K. E. Brandt. A subjective rating scale for evaluating the appearance outcome of autologous breast reconstruction. *Plastic and Reconstructive Surgery*, 116(2):440–449, 2005.
- [22] C. E. Coltman, J. R. Steele, and D. E. McGhee. Effects of age and body mass index on breast characteristics: a cluster analysis. *Ergonomics*, 61(9):1232–1245, 2018.
- [23] R. O. Craft, S. Colakoglu, M. S. Curtis, J. H. Yueh, B. S. Lee, A. M. Tobias, and B. T. Lee. Patient satisfaction in unilateral and bilateral breast reconstruction. *Plastic and Reconstructive Surgery*, 127(4):1417–1424, 2011.



- [24] L. Cui, P. Fan, C. Qiu, and Y. Hong. Single institution analysis of incidence and risk factors for post-mastectomy pain syndrome. *Scientific Reports*, 8(1):1–6, 2018.
- [25] T. H. Damen, R. Timman, E. H. Kunst, J. P. Gopie, P. J. Bresser, C. Seynaeve, M. B. Menke-Pluijmers, M. A. Mureau, S. O. Hofer, and A. Tibben. High satisfaction rates in women after DIEP flap breast reconstruction. *Journal of Plastic, Reconstructive and Aesthetic Surgery*, 63(1):93–100, 2010.
- [26] R. Danciu, C. Marina, V. Ardeleanu, R. Marin, R. Scăunau, and L. Răducu. Breast implant illness: a step forward in understanding this complex entity and the impact of social media. *Journal of Mind and Medical Sciences*, 6(2):351–355, 2019.
- [27] M. De Menezes, R. Rosati, V. F. Ferrario, and C. Sforza. Accuracy and reproducibility of a 3-dimensional stereophotogrammetric imaging system. *Journal of Oral and Maxillofacial Surgery*, 68(9):2129–2135, 2010.
- [28] F. Dindarolu, P. Kutlu, G. S. Duran, S. Görgülü, and E. Aslan. Accuracy and reliability of 3D stereophotogrammetry: A comparison to direct anthropometry and 2D photogrammetry. *Angle Orthodontist*, 86(3):487–494, 2016.
- [29] A. Eijkelboom, M. Luyendijk, M. v. Maaren, L. d. Munck, K. Schreuder, S. Siesling, and J. Verloop. Borstkanker in Nederland, 2021.
- [30] Y. Eltahir, L. L. Werners, M. M. Dreise, I. A. Van Emmichoven, P. M. Werker, and G. H. De Bock. Which breast is the best? Successful autologous or alloplastic breast reconstruction: Patient-reported quality-of-life outcomes. *Plastic and Reconstructive Surgery*, 135(1):43–50, 2015.
- [31] European Union. Verordeningen, 2017.
- [32] D. Fan, Y. Li, X. Wang, T. Zhu, Q. Wang, H. Cai, W. Li, Y. Tian, and Z. Liu. Progressive 3D Printing Technology and Its Application in Medical Materials. *Frontiers in Pharmacology*, 11(March):1–12, 2020.
- [33] M. I. Fitch, A. McAndrew, A. Harris, J. Anderson, T. Kubon, and J. McClennen. Perspectives of women about external breast prostheses. *Canadian oncology nursing journal = Revue canadienne de nursing oncologique*, 22(3):162–174, 2012.
- [34] P. Gallagher, A. Buckmaster, S. O’Carroll, G. Kiernan, and J. Geraghty. Experiences in the provision, fitting and supply of external breast prostheses: Findings from a national survey. *European Journal of Cancer Care*, 18(6):556–568, 2009.
- [35] J. Geng. Structured-light 3D surface imaging: a tutorial. *Advances in Optics and Photonics*, 3(2):128, 2011.

- [36] D. Government. Wetgeving Medische Hulpmiddelen, 2021.
- [37] Y. Guo, A. C. Rokohl, F. Schaub, X. Hou, J. Liu, Y. Ruan, R. Jia, K. R. Koch, and L. M. Heindl. Reliability of periocular anthropometry using three-dimensional digital stereophotogrammetry. *Graefe's Archive for Clinical and Experimental Ophthalmology*, 257(11):2517–2531, 2019.
- [38] M. Hamdi and A. Rebecca. The Deep Inferior Epigastric Artery Perforator Flap (DIEAP) in Breast Reconstruction. *Seminars in Plastic Surgery*, 20(2):095–102, 2006.
- [39] M. Hameeteman, A. C. Verhulst, T. J. Maal, and D. J. Ulrich. An analysis of pose in 3D stereophotogrammetry of the breast. *Journal of Plastic, Reconstructive and Aesthetic Surgery*, 69(12):1609–1613, 2016.
- [40] H. Henseler, B. S. Khambay, A. Bowman, J. Smith, J. Paul Siebert, S. Oehler, X. Ju, A. Ayoub, and A. K. Ray. Investigation into accuracy and reproducibility of a 3D breast imaging system using multiple stereo cameras. *Journal of Plastic, Reconstructive and Aesthetic Surgery*, 64(5):577–582, 2011.
- [41] N. S. Hillberg, J. Beugels, S. M. van Kuijk, R. R. van der Hulst, and S. M. Tuinder. Increase of major complications with a longer ischemia time in breast reconstruction with a free deep inferior epigastric perforator (DIEP) flap. *European Journal of Plastic Surgery*, 43(2):133–138, 2020.
- [42] C. Holm, M. Mayr, E. Höfter, and M. Ninkovic. Perfusion zones of the DIEP flap revisited: A clinical study. *Plastic and Reconstructive Surgery*, 117(1):37–43, 2006.
- [43] N. S. Huang, C. L. Quan, M. Mo, J. J. Chen, B. L. Yang, X. Huang, and J. Wu. A prospective study of breast anthropomorphic measurements, volume & ptosis in 605 Asian patients with breast cancer or benign breast disease. *PLoS ONE*, 12(2):1–10, 2017.
- [44] S. Hummelink, Y. L. Hoogeveen, L. J. Schultze Kool, and D. J. Ulrich. A New and Innovative Method of Preoperatively Planning and Projecting Vascular Anatomy in DIEP Flap Breast Reconstruction: A Randomized Controlled Trial. *Plastic and reconstructive surgery*, 143(6):1151e–1158e, 2019.
- [45] S. Hummelink, A. C. Verhulst, T. J. Maal, and D. J. Ulrich. Applications and limitations of using patient-specific 3D printed molds in autologous breast reconstruction. *European Journal of Plastic Surgery*, 41(5):571–576, 2018.
- [46] M. Integraal. MT integraal.
- [47] J. E. D. Jacobs, N. Beudeker, C. A. Bargon, S. Siesling, N. H. Brouwer, O. T. Zöphel, U. Schmidbauer, Y. C. M. M. Smulders, J. G. Wijbenga, and H. A. Rakhorst. Lean DIEP flap surgery : saving time and reducing complications. *European Journal of Plastic Surgery*, (0123456789), 2021.

- [48] Jelle Jonker. A cost-effectiveness analysis of a breast reconstruction method combined with a 3D printed mold compared to a conventional breast reconstruction without a 3D printed mold for unilateral reconstructions. Technical Report August, 2021.
- [49] J.M. van Steveninck-Barends. Borstreconstructie volgens de DIEPflap methode. *WSC NIEUWS*, 30(1):4–8, 2014.
- [50] S. Kholgh Eshkalak, E. Rezvani Ghomi, Y. Dai, D. Choudhury, and S. Ramakrishna. The role of three-dimensional printing in healthcare and medicine. *Materials and Design*, 194:108940, 2020.
- [51] J. J. Koenderink and A. J. van Doorn. Surface shape and curvature scales. *Image and Vision Computing*, 10(8):557–564, 1992.
- [52] W. Krois, A. K. Romar, T. Wild, P. Dubsky, R. Exner, P. Panhofer, R. Jakesz, M. Gnant, and F. Fitzal. Objective breast symmetry analysis with the breast analyzing tool (BAT): improved tool for clinical trials. *Breast Cancer Research and Treatment*, 164(2):421–427, 2017.
- [53] S. S. Kroll, G. P. Reece, M. J. Miller, G. L. Robb, H. N. Langstein, C. E. Butler, and D. W. Chang. Comparison of cost for DIEP and free TRAM flap breast reconstructions. *Plastic and Reconstructive Surgery*, 107(6):1413–1416, 2001.
- [54] R. Lakhtakia. A brief history of breast cancer: Part I: Surgical domination reinvented. *Sultan Qaboos University Medical Journal*, 14(2):166–169, 2014.
- [55] H. Y. Lee, K. Hong, and E. A. Kim. Measurement protocol of women’s nude breasts using a 3D scanning technique. *Applied Ergonomics*, 35(4):353–359, 2004.
- [56] J. Lee, M. Kawale, F. A. Merchant, J. Weston, M. C. Fingeret, D. Ladewig, G. P. Reece, M. A. Crosby, E. K. Beahm, and M. K. Markey. Validation of stereophotogrammetry of the human torso. *Breast Cancer: Basic and Clinical Research*, 5(1):15–25, 2011.
- [57] D. Li, A. Cheong, G. P. Reece, M. A. Crosby, M. C. Fingeret, and F. A. Merchant. Computation of breast ptosis from 3D surface scans of the female torso. *Computers in Biology and Medicine*, 78:18–28, 2016.
- [58] Y. N. Liang and B. Xu. Factors influencing utilization and satisfaction with external breast prosthesis in patients with mastectomy: A systematic review. *International Journal of Nursing Sciences*, 2(2):218–224, 2015.
- [59] J. Liu, F. Sadre-Marandi, S. Tavener, and C. Chen. Curvature Concentrations on the HIV-1 Capsid. *Computational and Mathematical Biophysics*, 3(1):43–53, 2015.

- [60] A. Losken, I. Fishman, D. D. Denson, H. R. Moyer, and G. W. Carlson. An objective evaluation of breast symmetry and shape differences using 3-dimensional images. *Annals of Plastic Surgery*, 55(6):571–575, 2005.
- [61] A. Losken and M. J. Jurkiewicz. History of breast reconstruction. *Breast Disease*, 16(2):3–9, 2002.
- [62] A. Losken, H. Seify, D. D. Denson, A. A. Paredes, and G. W. Carlson. Validating three-dimensional imaging of the breast. *Annals of Plastic Surgery*, 54(5):471–476, 2005.
- [63] T. J. Maal, L. M. Verhamme, B. Van Loon, J. M. Plooiij, F. A. Rangel, A. Kho, E. M. Bronkhorst, and S. J. Bergé. Variation of the face in rest using 3D stereophotogrammetry. *International Journal of Oral and Maxillofacial Surgery*, 40(11):1252–1257, 2011.
- [64] C. Mattiuzzi and G. Lippi. Current cancer epidemiology. *Journal of Epidemiology and Global Health*, 9(4):217–222, 2019.
- [65] D. E. McGhee, K. L. Mikilewicz, and J. R. Steele. Effect of external breast prosthesis mass on bra strap loading and discomfort in women with a unilateral mastectomy. *Clinical Biomechanics*, 73(May 2019):86–91, 2020.
- [66] A. Mishra and V. Srivastava. Biomaterials and 3D printing techniques used in the medical field. *Journal of Medical Engineering and Technology*, 45(4):290–302, 2021.
- [67] Z. Momenimovahed and H. Salehiniya. Epidemiological characteristics of and risk factors for breast cancer in the world. *Breast Cancer: Targets and Therapy*, 11:151–164, 2019.
- [68] L. R. Mundy, L. H. Rosenberger, C. N. Rushing, D. Atisha, A. L. Pusic, S. T. Hollenbeck, T. Hyslop, E. S. Hwang, K. Tomita, K. Yano, M. Taminato, M. Nomori, K. Hosokawa, C. Healy, R. J. Allen, E. Bastiaannet, G. J. Liefers, A. J. De Craen, P. J. Kuppen, W. Van De Water, J. E. Portielje, L. G. Van Der Geest, M. L. Janssen-Heijnen, O. M. Dekkers, C. J. Van De Velde, R. G. Westendorp, K. L. Moore, A. F. Dalley, and A. M. Agur. The evolution of perforator flap breast reconstruction: Twenty years after the first DIEP flap. *Plastic and reconstructive surgery*, 5(3):801–807, 2014.
- [69] M. Y. Nahabedian, T. Tsangaris, and B. Momen. Breast reconstruction with the DIEP flap or the muscle-sparing (MS-2) free TRAM flap: Is there a difference? *Plastic and Reconstructive Surgery*, 115(2):436–444, 2005.
- [70] NZA. Microchirurgische vrije lap reconstructie, 2021.
- [71] A. Ooms. IMPLEMENTATION OF STERILIZED 3D-PRINTED BREAST MOLDS FOR AUTOLOGOUS BREAST RECONSTRUCTIONS. Technical report, 2021.

- [72] R. L. OConnell, R. Di Micco, K. Khabra, L. Wolf, N. deSouza, N. Roche, P. A. Barry, A. M. Kirby, and J. E. Rusby. The potential role of three-dimensional surface imaging as a tool to evaluate aesthetic outcome after Breast Conserving Therapy (BCT). *Breast Cancer Research and Treatment*, 164(2):385–393, 2017.
- [73] R. L. OConnell, K. Khabra, J. C. Bamber, N. deSouza, F. Meybodi, P. A. Barry, and J. E. Rusby. Validation of the Vectra XT three-dimensional imaging system for measuring breast volume and symmetry following oncological reconstruction. *Breast Cancer Research and Treatment*, 171(2):391–398, 2018.
- [74] M. Pagac, J. Hajnys, Q. P. Ma, L. Jancar, J. Jansa, P. Stefek, and J. Mesicek. A review of vat photopolymerization technology: Materials, applications, challenges, and future trends of 3d printing. *Polymers*, 13(4):1–20, 2021.
- [75] W. M. Rozen, A. K. Rajkomar, N. S. Anavekar, and M. W. Ashton. Post-mastectomy breast reconstruction: A history in evolution. *Clinical Breast Cancer*, 9(3):145–154, 2009.
- [76] J. A. Schwitzer, H. C. Miller, A. L. Pusic, E. Matros, B. J. Mehrara, C. M. McCarthy, P. A. Lennox, N. Van Laeken, and J. J. Disa. Satisfaction following unilateral breast reconstruction: A comparison of pedicled TRAM and free abdominal flaps. *Plastic and Reconstructive Surgery - Global Open*, 3(8):1–8, 2015.
- [77] I. B. Shabat. GetCurvatures computes the curvature tensor and the principal curvatures at each vertex of a mesh given in a face vertex data structure, 2014.
- [78] A. Shamata and T. Thompson. Documentation and analysis of traumatic injuries in clinical forensic medicine involving structured light three-dimensional surface scanning versus photography. *Journal of Forensic and Legal Medicine*, 58(April):93–100, 2018.
- [79] S. Sharma. *Implementation of 3D technologies for quantification and improvement of clinical diagnostics*. PhD thesis, 2020.
- [80] K. Steen, K. V. Isaac, B. D. Murphy, B. Beber, and M. Brown. Three-Dimensional Imaging and Breast Measurements: How Predictable Are We? *Aesthetic Surgery Journal*, 38(6):616–622, 2018.
- [81] M. Stephenson, A. Clark, and R. Green. Novel methods for reflective symmetry detection in scanned 3D models. *International Conference Image and Vision Computing New Zealand*, 2016-Novem(September 2018), 2016.
- [82] Y. S. Sun, Z. Zhao, Z. N. Yang, F. Xu, H. J. Lu, Z. Y. Zhu, W. Shi, J. Jiang, P. P. Yao, and H. P. Zhu. Risk factors and preventions of breast cancer. *International Journal of Biological Sciences*, 13(11):1387–1397, 2017.
- [83] Z. Q. Tao, A. Shi, C. Lu, T. Song, Z. Zhang, and J. Zhao. Breast Cancer: Epidemiology and Etiology. *Cell Biochemistry and Biophysics*, 72(2):333–338, 2015.

- [84] C. M. Thakar, S. S. Parkhe, A. Jain, K. Phasinam, G. Murugesan, and R. J. M. Ventayen. 3d Printing: Basic principals and applications. *Materials Today: Proceedings*, (xxxx), 2021.
- [85] A. Thorarinsson, V. Fröjd, L. Kölby, R. Lewin, N. Molinder, J. Lundberg, A. Elander, and H. Mark. A retrospective review of the incidence of various complications in different delayed breast reconstruction methods. *Journal of Plastic Surgery and Hand Surgery*, 50(1):25–34, 2016.
- [86] K. Tomita, K. Yano, Y. Hata, A. Nishibayashi, and K. Hosokawa. DIEP flap breast reconstruction using 3-dimensional surface imaging and a printed mold. *Plastic and Reconstructive Surgery - Global Open*, 3(3):1–5, 2015.
- [87] K. Tomita, K. Yano, M. Taminato, M. Nomori, and K. Hosokawa. DIEP flap breast reconstruction in patients with breast ptosis: 2-stage reconstruction using 3-dimensional surface imaging and a printed mold. *Plastic and Reconstructive Surgery - Global Open*, 5(10):1–4, 2017.
- [88] K. A. Tønseth, B. M. Hokland, T. T. Tindholdt, F. E. Åbyholm, and K. Stavem. Quality of life, patient satisfaction and cosmetic outcome after breast reconstruction using DIEP flap or expandable breast implant. *Journal of Plastic, Reconstructive and Aesthetic Surgery*, 61(10):1188–1194, 2008.
- [89] J. B. Troost. Usability study to obtain design and manufacturing recommendations for the optimal 3D printed mold for autologous breast reconstruction. Technical report, 2020.
- [90] C. H. J. Tzou, N. M. Artner, I. Pona, A. Hold, E. Placheta, W. G. Kropatsch, and M. Frey. Comparison of three-dimensional surface-imaging systems. *Journal of Plastic, Reconstructive and Aesthetic Surgery*, 67(4):489–497, 2014.
- [91] C. H. J. Tzou and M. Frey. Evolution of 3D Surface Imaging Systems in Facial Plastic Surgery. *Facial Plastic Surgery Clinics of North America*, 19(4):591–602, 2011.
- [92] D. Van Der Waal, A. L. Verbeek, G. J. Den Heeten, T. M. Ripping, V. C. Tjan-Heijnen, and M. J. Broeders. Breast cancer diagnosis and death in the Netherlands: A changing burden. *European Journal of Public Health*, 25(2):320–324, 2015.
- [93] T. J. Verhoeven, C. Coppen, R. Barkhuysen, E. M. Bronkhorst, M. A. Merckx, S. J. Bergé, and T. J. Maal. Three dimensional evaluation of facial asymmetry after mandibular reconstruction: Validation of a new method using stereophotogrammetry. *International Journal of Oral and Maxillofacial Surgery*, 42(1):19–25, 2013.
- [94] A. Verhulst, M. Hol, R. Vreeken, A. Becking, D. Ulrich, and T. Maal. Three-Dimensional Imaging of the Face: A Comparison between Three Different Imaging Modalities. *Aesthetic Surgery Journal*, 38(6):579–585, 2018.

- [95] T. Wachter, M. Edlinger, C. Foerg, G. Djedovic, C. Mayerl, J. Kinzl, T. Bauer, and D. Wolfram. Differences between patients and medical professionals in the evaluation of aesthetic outcome following breast reconstruction with implants. *Journal of Plastic, Reconstructive and Aesthetic Surgery*, 67(8):1111–1117, 2014.
- [96] R. G. Wade, F. Marongiu, E. M. Sassoon, R. M. Haywood, R. S. Ali, and A. Figus. Contralateral breast symmetrisation in unilateral DIEP flap breast reconstruction. *Journal of Plastic, Reconstructive and Aesthetic Surgery*, 69(10):1363–1373, 2016.
- [97] T. S. Wesselius, A. C. Verhulst, R. D. Vreeken, X. Tong, T. J. Maal, and D. J. Ulrich. Accuracy of Three Software Applications for Breast Volume Calculations from Three-Dimensional Surface Images. *Plastic and reconstructive surgery*, 142(4):858 – 864, 2018.
- [98] T. S. Wesselius, A. C. Verhulst, T. Xi, D. J. O. Ulrich, and T. J. J. Maal. Effect of skin tone on the accuracy of hybrid and passive stereophotogrammetry. pages 1564–1569, 2019.
- [99] T. S. Wesselius, R. D. Vreeken, A. C. Verhulst, T. Xi, T. J. Maal, and D. J. Ulrich. New software and breast boundary landmarks to calculate breast volumes from 3D surface images. *European Journal of Plastic Surgery*, 41(6):663–670, 2018.
- [100] F. N. Wilting, M. Hameeteman, H. J. Tielemans, D. J. Ulrich, and S. Hummelink. Three-dimensional evaluation of breast volume changes following autologous free flap breast reconstruction over six months. *Breast*, 50:85–94, 2020.
- [101] J. M. Yip, D. I. Watson, M. Tiggemann, S. Hsia, A. E. Smallman, and N. R. Dean. Determinants of breast reconstruction outcome: How important is volume symmetry? *Journal of Plastic, Reconstructive and Aesthetic Surgery*, 68(5):679–685, 2015.
- [102] L. Zhao, A. Cheong, G. P. Reece, M. C. Fingeret, S. K. Shah, S. Member, F. A. Merchant, and S. Member. Inferior Breast-Chest Contour Detection in 3-D Images of the Female Torso. 4(April), 2016.





# Appendix

## Appendix A

### Extended version DIEP flap procedure description and technical background

#### Patient requirements

Not every patient is suitable for DIEP flap surgery. Therefore, a patient must comply with some requirements. Smoking is one of the important contra-indication for a DIEP flap. Smoking causes a significantly higher chance of complications such as total flap loss. Therefore, the patient is being urged to stop smoking or use a nicotine substitute. Also, a healthy Body Mass Index (BMI) is important, but enough fat to transfer is also a requirement to perform the DIEP flap. Previous surgeries could lead to problems performing the DIEP, but luckily a caesarean section is not one of them. There is no age restriction, but the patient should be in good physical condition

#### Procedure

The skin and subcutaneous fat of the lower abdomen is adequate tissue for breast reconstruction because it gives a soft and natural shaped reconstruction. In short, during the DIEP flap procedure, abdominal skin and fat are transferred with blood vessels for blood supply. The vessels harvest in the abdominal region arise from the deep inferior epigastric artery (DIEA) which arise from the terminal aspect of the external iliac artery. The abdominal flap can be divided into four parts perfused by branched of the iliac artery, the Hartrampf perfusion zones (figure A.1) [42]. The higher number zones contain poorer vascularity, so the mid parts of the flap are the first choice for reconstruction. The abdominal flap must be harvested accurately in order not to damage vulnerable structures as the perforators or nerves to preserve the function and sensation of the abdominal muscle. Despite the precise work of the surgeons, affecting the musculus abdominal muscle for harvesting of the perforator vessels cannot be avoided. Finally, a vein and artery from the abdomen is the harvest which supplies the needed part of the abdominal flap with blood. [38]

After harvesting the abdominal flap, abdominal perforators and thoracal perforators, the perforators from the abdominal flap are cut through. Now, re-attaching of the small abdominal vessels to the mammary vessels is started with the microscope. Until the blood supply is restored, the abdominal flap is isolated from blood, called the ischemia time. Before constructing the anastomosis, the flap and vessels are flushed with heparin to prevent blood clots. The arteries are sutured to connect with a special suture set for microscopy. The vein anastomosis is connected with a small fast device named Coupler. The blood supply of the flap should be restored and is checked with a Doppler device to check the artery pulsating. Further, the capillary refill and colour are checked. If the surgeon thinks the flap is well supplied, the shaping of the flap to a breast can start. This is to insert the flap into the breast pocket and observe if the breast

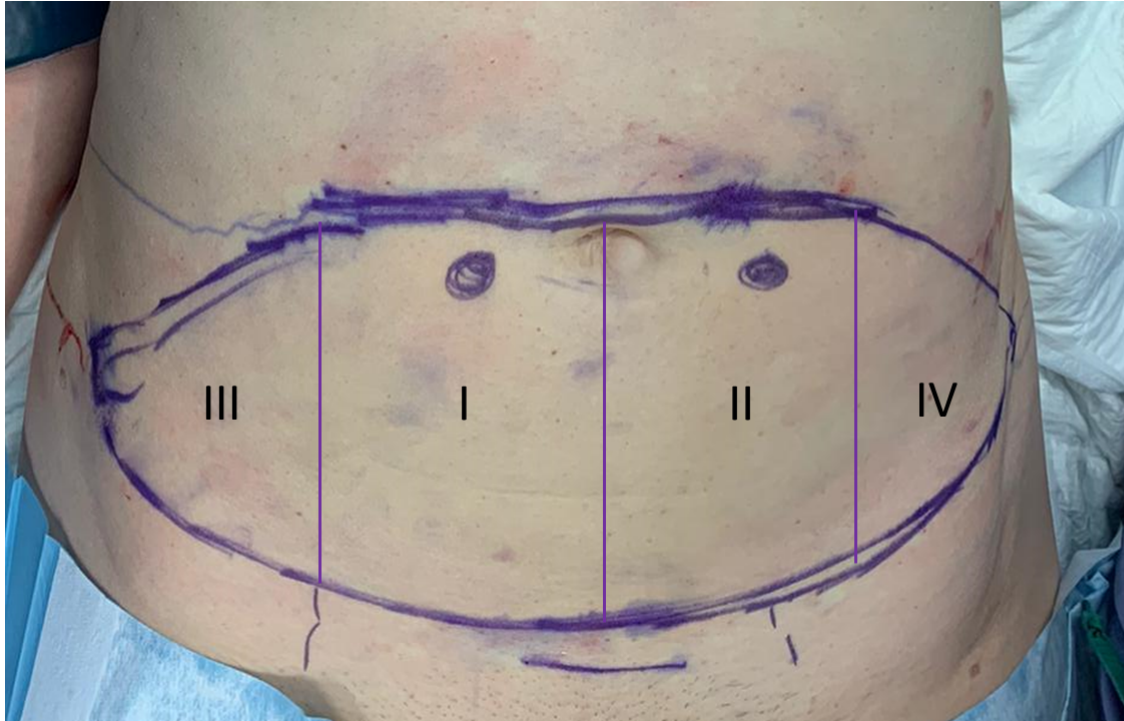


Figure A.1: Perfusion zones of the lower abdominal flap divided into four parts to Hartrampf. Before transferring the flap to the chest wall, the artery mammary internal and vein mammary internal have to be prepared for attaching the abdominal vessels and thorax vessels. These vessels, which normally provide the breasts with blood, lie under the thoracal ribs. The second or third rib is often sacrificed to create enough length.

is symmetrical to the contralateral side. Shaping a symmetrical breast is in some cases a challenge. After obtaining a satisfying volume and shape, the skin will be closed with sutures. A skin paddle is left to check the state of the flap on the nursing ward. Furthermore, staples were left on the place(s) where the artery vessel(s) could be heard with a Doppler device. After suturing the abdominal wound and stick steristrips, the time out procedure starts and the patient can be transferred to the recovery unit. [38] In figure A.2, a pre-and 2-week post-operative picture is displayed. The left breast was operated and a skin paddle was left for flap monitoring.

### Postoperative

Patients stay 3-5 nights at the ward after the surgery. The infuse will be removed after 1 -2 days after surgery if the patient drinks enough and the check-ups are sufficient. The patient receives pain resistance medication, such as morphine. Further cefazolin (antibiotic) and Dalteparine (antithrombotic) are given to the patient to prevent infections and thrombus forming. The use of vasoconstrictive medication should be avoided. The flap is monitored by clinical evaluation and a handheld doppler device. The clinical evaluation consists of monitoring the colour, capillary refill and temperature of the skin island. With a handheld Doppler probe, the anastomoses are monitored for a pulsating sound. This suggests that the flap is supplied with blood and oxygen. [49]



Figure A.2: A pre- and 2-week postoperative photo of a patient that underwent a DIEP flap at the ZGT. The left breast was operated and a skin paddle was left to monitor the flap.

### **Advantage**

The most important advantage of the DIEP flap procedure compared with silicone implants is that the reconstructed breast consists of the patient's own tissue. The breast is numb, but the breast is warm and feels like the patient's own breast. Another important advantage is that a DIEP flap reconstruction is for the rest of a patient's life compared to silicone implants which have to be substituted at a given moment. Also, the breast changes with weight changes preserving the breast symmetry. An additional advantage for corpulent women is a flatter stomach through abdominoplasty. [49]

### **Disadvantage**

Compared to a reconstruction with implants, the DIEP flap procedure is time-consuming and a major surgery. A scar across the entire abdominal width arises with sometimes permanent loss of skin feeling. Moreover, a scar around the umbilicus arises. Due to the weakness of the large wound and incision in the abdominal muscle the chances of an incisional hernia increase. Finally, the recovery will take six weeks or longer. [49]

### **Complications**

Every surgery has a risk for minor or major complications. Examples of minor complications are dehiscence, seroma, infection and fat necrosis. Major complications are total flap loss, partial flap loss and compromised flap. Fortunately, complications do not occur often. A recent study performed into the Ziekenhuisgroep Twente (ZGT) to the complications in unilateral and bilateral DIEP flap surgeries found a complication rate of 7.4% in the unilateral group and 6.7% in the bilateral group between 2017 and 2019. This is a large decrease in comparison with the rates between 2013 and 2017 with 16.7% for unilateral and 26.7% for the bilateral group. In the total interval from 2013 to 2019, only 1.2% of

the patient flap loss occurred. In 5.3% a compromised flap was seen. 12.9% of the patients needed reoperation in the theatre. [47]

## Appendix B

### Extended technical background

#### 3D photography

Different 3D imaging techniques are available such as laser imaging, structured light and 3D stereophotogrammetry (3D photography). Laser imaging obtains 3D data by scanning the object's surface with a laser beam. The scattered light by the scanned object is collected at a known triangulation distance from the laser. The x, y, and z of the surface points are calculated using trigonometry.[91] Two other techniques based on visible light are structured light and stereophotogrammetry 3D imaging. Structured light technology projects an organized white light pattern on the object surface during photographing the object with a calibrated camera. The shape data, including colour and texture, is determined by a sensor due to the distortion of light. To avoid pattern interference and create an accurate 3d model, a two viewpoint capture must be taken.[91] With equation 6.1, a 3D surface can be calculated.

$$R = B \frac{\sin(\theta)}{\sin(\theta + \alpha)} \quad (6.1)$$

$R$  is the distance between a point  $P$  and the camera, the depth  $B$  is the baseline between the projector and camera.  $\theta$  is the angle between the baseline and the line between  $P$  and the projector.  $\alpha$  is the angle between the baseline and the line between point  $P$  and the camera (Figure B.1).[35]

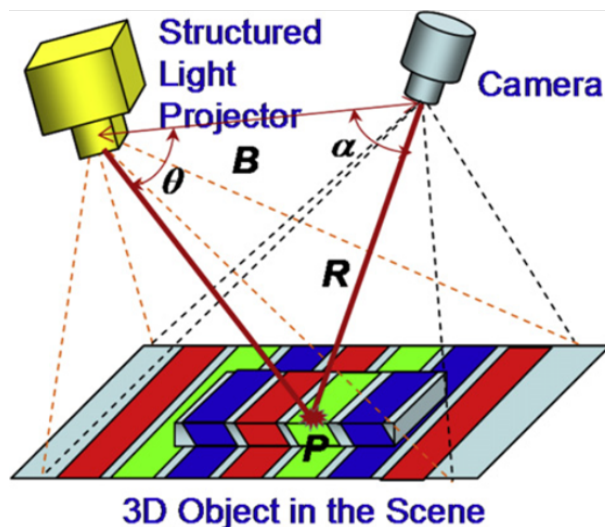


Figure B.1: Illustration of structured light camera. With  $B$  the baseline, the distance from the camera to point  $P$ . and the angles between the baseline and point  $P$  to respectively the projector and camera.

3D Stereophotogrammetry (3D photography) is an imaging technique that creates 3D surfaces of patients by using multiple cameras. The 3D model is generated by an algorithm based on the recorded pattern of the surface. After

producing the geometry model, colour and texture are added onto the model.[78, 90, 91, 98] Three techniques can be differentiated in 3D photography: active, passive and hybrid. Active stereophotogrammetry is based on structured light. A pattern is projected on a surface and used two or more cameras to capture the deformation of the pattern caused by the objects surface. Through a triangulation process, the 2D pixels in the cameras are used to calculate the 3D coordinates and generate a 3D surface. With the knowledge of the camera position, distances of camera and pairs of 3D pixels the surface could be generated by combining this information. The projected pattern simplifies the finding of corresponding points and no additional light is needed.[78]

In contrast, the 3D surface image with passive stereophotogrammetry is only based on the photos taken by the two or more cameras of the system. No pattern is projected on the surface. Although it is more difficult to find corresponding points between the photos, a high qualitatively 3D surface can be obtained. Important requirements for obtaining a 3D surface of good quality are high-quality cameras to capture surface details and sufficient texture patterns, such as pores, freckles, scars and rhytids. Ambient light may lead to glare which lowers the surface details. An example of a passive system is the Canfield Vectra XT system which is used in this paper to take 3D photos.[78, 90, 91, 98]

Some systems combine active and passive stereophotogrammetry, called hybrid stereophotogrammetry. This technique uses a combination between light patterns and the natural surface with pores and freckles to generate the 3D surface object.[90, 98] An example of this hybrid system is the 3dMD (Dimensional Imaging Ltd, Glasgow, Scotland) that is used in the TechMed Centre at the University of Twente. Figure B.2. shows the Vectra XT system and the hybrid 3DMD system around the Vectra.



Figure B.2: A photo of the passive Canfield Vectra XT system and the hybrid 3DMD system around the Vectra

### **B1. 3D printing techniques**

3D printing in medical setting can be deployed in a lot of applications such as patient-specific anatomical prints, surgical planning, surgical instruments and bioprinting. 3D printing techniques could be divided into three main groups: Powder based printing, Liquid-based printing and fused deposition modelling. Although only the last one is used for this research, all three groups will be described shortly underneath in this section as a background to show the diversity of options for medical 3D printing.

#### **Fused deposition modelling (FDM) printing**

FDM is the classic form of 3D printing. A thin solid filament wire on a roller is melted by a heating element to a semi-liquid state and extruded layer by layer through a tiny hole (typically 200 micron) on a building plate where it solidifies.[32, 66, 84]. The characteristics of the prints are affected by the layer thickness, orientation and width of the filament. The extrusion head moves in the horizontal x- and y-direction while the building platform moves in the z-direction during the building phase (Figure B.3). Software regulates the head and platform during the process to generate the 3D model.[32, 84] The major advantages of this technique are the acceptable printing speed, low costs and simplicity of the process. Disadvantages could be poor quality, the appearance of the layers and limited choice for thermoplastic filaments. Nevertheless, FDM could be applied in the printing of metals, polymers and bioprinting[96]. Thermoplastic filaments such as PolyLactid acid (PLA) are most used and have biocompatible and biodegradable

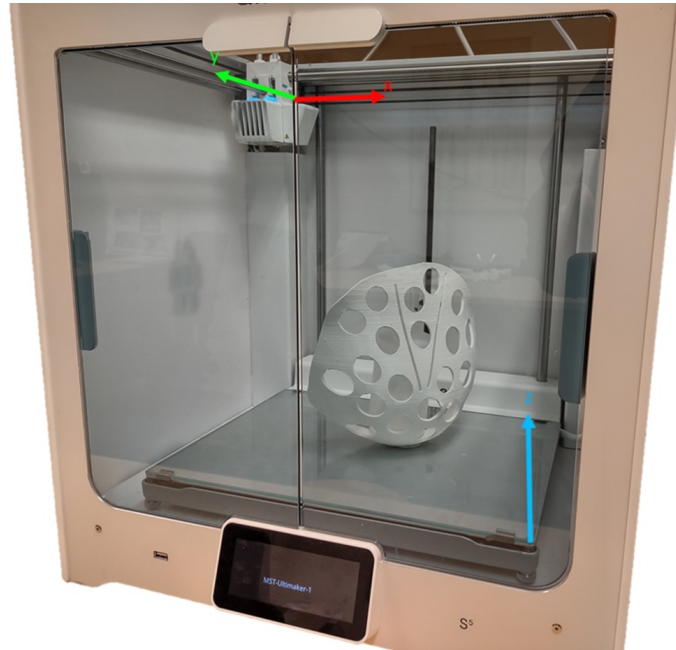


Figure B.3: Photo of the Ultimaker S5 used for printing breast moulds in this thesis. The red and green arrow indicates the horizontal movement of the extruder (x- and y-direction). The building plate moves in the z-direction (blue arrow).

properties. The thermoplastic materials melt at a relatively low temperature, for PLA at 175°C.[66] FDM is a potential technique to produce surgical instruments, implants and specific surgical guides.[50, 66]

### Powder based printing

This technique uses a laser or an electron beam to melt powder to obtain a 3D model. The beam melts and draws a pattern in the powder bed per layer. [50, 84] A roller in the printer applies a new layer of powder onto the surface if the previous layer is completed. Unreacted resin is removed.[50] Four common powder based techniques could be distinguished: selective laser sintering (SLS), direct metal laser sintering (DMLS), selective laser melting (SLM) and electron beam melting (EBM). SLS and DMLS melt the powder not completely while SLM and EBM do. For an electron beam temperatures  $>600\text{ }^{\circ}\text{C}$  are required for the working process. Despite the high temperature, the prints maintain higher tribological, mechanical and corrosion properties [32]. SLS and DMLS utilize a laser beam to bond particles. The techniques with fully melting the powder have a less rough surface, but SLS and DMLS have a wide range of materials that can be used, such as plastic powders, ceramic powders and metal powder. Unfortunately, the surface is rough.[32, 50]

### Liquid based printing

This technique uses a basin of liquid photosensitive polymer resin that is exposed to a laser or light beam causing triggering the solidifying process in a thin surface layer. The light or laser connects connected molecules to obtain object, a process called photopolymerization.[32, 50, 84] Resolutions of  $10\text{ }\mu\text{m}$  can be obtained, but the technique is



slow, expensive, involves of toxic chemicals and a limited amount of materials are available, but flexible resins are available [74]. Objects that can be printed are valves, lenses and fluidic interconnections. Such as in the FDM process the platform moves along the x-axis and the object where printed layer by layer in the xy-plane.[32] Product printed with this technique have to be exposed to light after printing to enhance stability. Examples of liquid based printing processes are stereolithography and laminated object manufacturing.[50]

## **B2. 3D mesh/object**

A digital 3D object, also called a polygon mesh, consists of vertices, faces and edges that defines a polyhedral object. A vertex is a node where two or more edges come together. An edge is a connection between two vertices. Edges and vertices form faces, which is a closed set of edges and can have different shapes. For example a triangle face has three edges (used in this research) and a quad face four edges, an example of a triangular mesh is shown in figure B.4. Faces in the same plane (coplanar) are polygons. Multiple polygons form a 3D surface, but these data can be stored in multiple ways. A set of faces and vertices were used to represent the 3D object. Every face in a triangular object must connect three vertices, but not every vertex must connect three faces. The most used representation of a 3D object is the Face-vertex mesh. With this representation it is easy to find the information of the mesh. The vertex list contains a list of faces connected to each vertex. Disadvantage of this mesh is the difficulty to split or merge the surface.

Storage of 3D meshes are available in a lot of 3D files. In this thesis wavefront OBJ (.obj) and Stereolithography format (.stl) files are used. The OBJ format is a simple data-format that represents 3D geometry. The information that the format contains the position of each vertex, UV position, vertex normal, face information and texture. Comparing with STL, OBJ can expose the colour information such as the skin in patient photos.

STL is a widely used format for 3D modelling applications and 3D printing. STL files describe only the geometry of a 3D object without any colour or texture representation. The files are often binary, because these are more compact. The STL describes a surface in triangles, therefore it is always a raw approach of the original surface. More triangles result to better accuracy of the STL file, however the file size will increase.[11] Figure B.5 shows the difference between a binary STL (right) and an colour overlay OBJ file (left).

## **Symmetry**

Symmetry is a universal concept in nature, science and art and occurs at all scales, from crystal lattice structures to the human body. Symmetry is in fact when two halves of an object are each other reflections and can occur relative to a point (1D), line (2D) or plane (3D). Mathematically, the symmetry of an object is the invariance of a translation, rotation, scaling or reflection. These operations are also called geometric transformations (T), which lead to the equation for a geometric object M to a transformation,  $M = T(M)$ . In breasts, symmetry is mainly focused on volume symmetry. However, the shape and location of the volume are other factors that important for womens satisfaction with

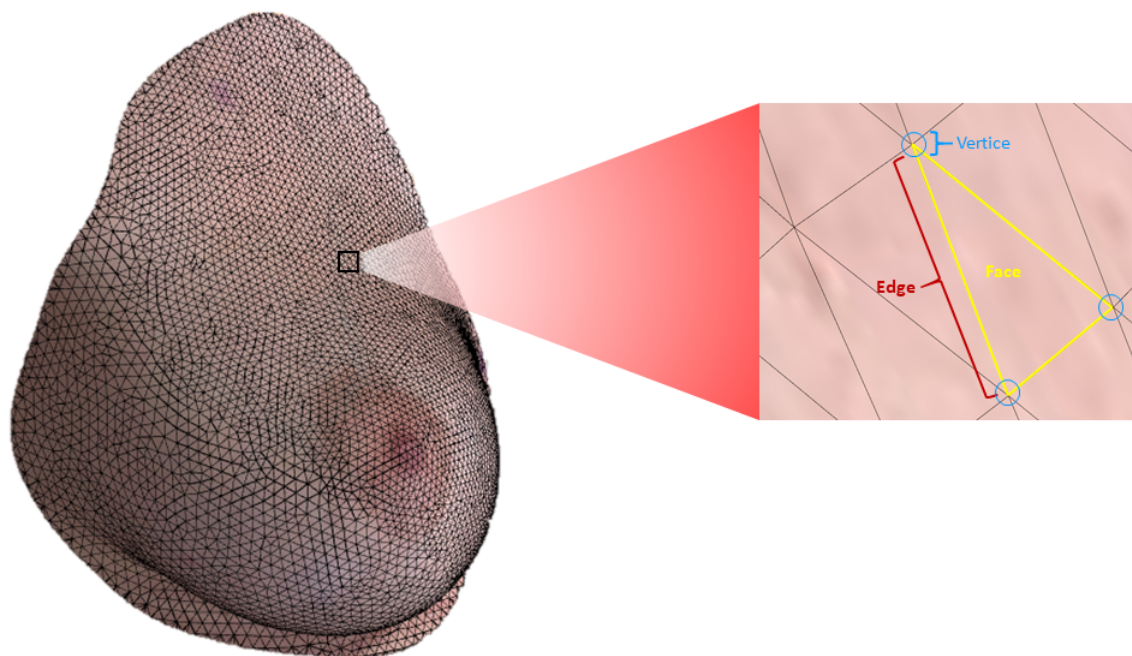


Figure B.4: OBJ file of a patients breast with triangular mesh. The blue circles indicates a vertex. The yellow lines connect the vertices and create a face. The face consists of three edges indicated with red.

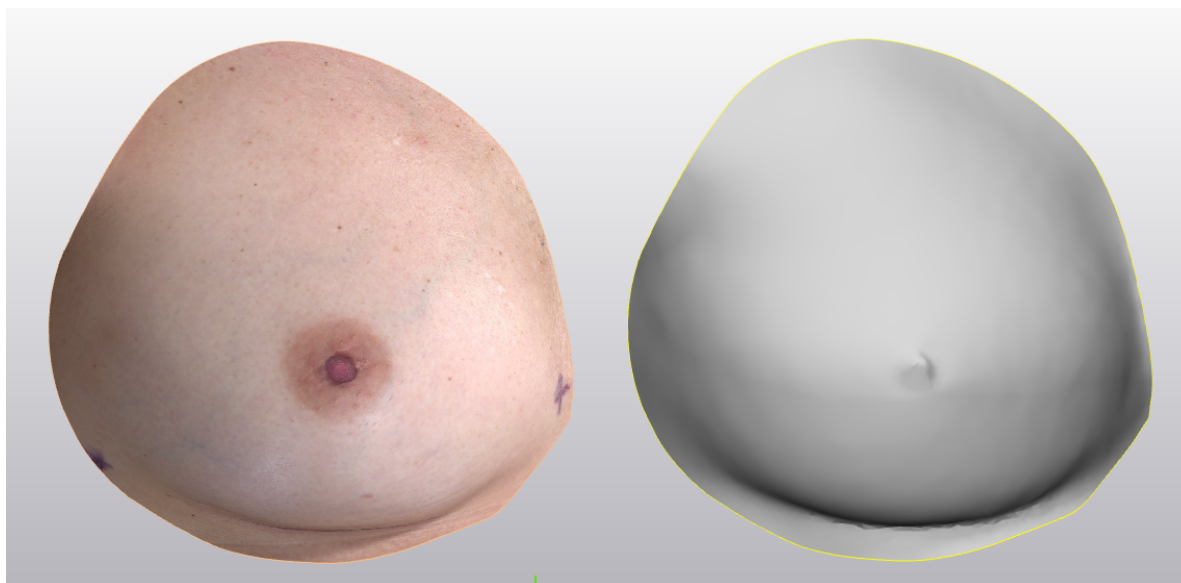


Figure B.5: An example of the same breasts. The left breast is in OBJ format and contains the colour information. The right is a binary STL file.

their breasts. Therefore, describing the breasts with a shape index could lead to more reliable satisfaction rates and insight into the symmetry between breasts.

### B3. Curvature

In this section multiple curvatures for surfaces embedded in  $\mathbb{R}^3$  are described with its advantages and disadvantages. To understand what curvature is this will be explained by the oscillating curve C in figure B.6, a two times differentiable 2D curve. There are three points, K, L and M, illustrated on the curve C. The curvature of these points can be calculated. Mathematically the curvature of a specific point on a line, figure B.6, in this example K, L or M, is the inverse radius (R) of a circle through a point. The formula is given by  $\kappa = 1/R$ . From this can be argued that a larger radius results in a small curvature and a small radius to a large curvature. The curve C consists of multiple points and for every point on the curve C a unique circle could be defined. With the radii of these circles the curvature can be calculated to approximate the curvature in that specific point.

For 3D surfaces the curvature on every coordinate can vary in every direction. The principal curvatures are the values for the minimum and maximum bending on a coordinate. The principal curvatures are indicated by  $\kappa_1$  and  $\kappa_2$  and are perpendicular to each other. Let M be a smooth surface with a point p as in figure B.7.  $\vec{N}$  is the unit normal vector of point p on the surface M.  $\vec{T}$  is the unit tangent vector of p at surface M. The unit vectors could also be called as the eigenvectors of point p. Of the eigenvectors, the eigenvalues can be calculated. The two calculated eigenvalues are the principal curvatures.[59] With the calculated principal curvatures, the mean- (M) and Gaussian curvature (G) could be determined, such as Koenderink's shape index (S) and magnitude of curvedness (MC). The formulas can be found below:

1. Gaussian:  $G = \kappa_1 * \kappa_2$
2. Shape index:  $S = \frac{2}{\pi} * \arctan\left(\frac{\kappa_1 + \kappa_2}{\kappa_1 - \kappa_2}\right), \kappa_1 \geq \kappa_2$
3. Mean:  $M = \frac{\kappa_1 + \kappa_2}{2}$
4. Magnitude Curvedness:  $C = \sqrt{\frac{\kappa_1^2 + \kappa_2^2}{2}}$

The Gaussian, given by the product of the principal curvatures, and the mean, given by the sum of the principal curvature divided by two, are the most widely used indicators for shape classification. The Gaussian curvature is intrinsic to the surface and is not dependent of the embedding of the surface.[51] Koenderink developed another shape indicators from the principal curvatures, because his thought was that these indicators represent the surface better. His approach with the shape index and curvedness divided the shape and size. This resulted in a scale invariant shape index with a range between [-1, 1] and thus specifies the shape. The curvedness is a positive number that describes the magnitude of the curvedness at a point. In other words, how highly the bending is on a point. It specifies the size.[51]

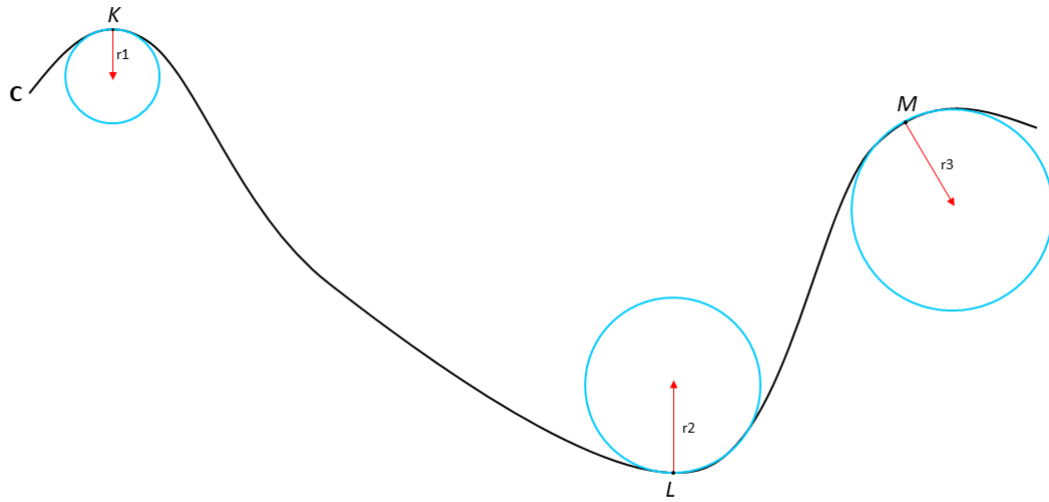


Figure B.6: Image of the curvature in 2D. A curve with three points K, L and M. On these points is a circle determined with corresponding radius of that point. The curvature can be calculated by the inverse radius.

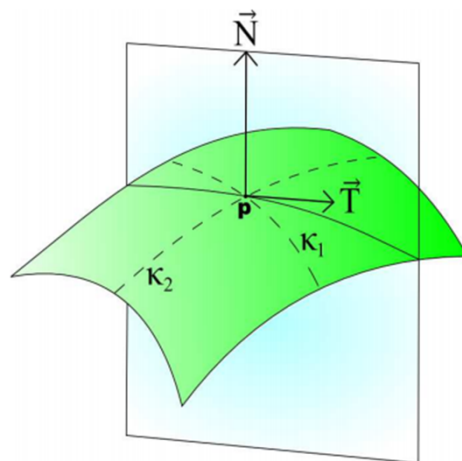


Figure B.7: Surface M with normal vector  $\vec{N}$  and unit tangent vector  $\vec{T}$  of point p. The principal curvature are  $\kappa_1$  and  $\kappa_2$  determined from the vectors. The principal curvatures are the eigenvalues of point p

## Appendix C

### Matlabcode

```
1 % Start with a clean workspace
2 clear all;
3 close all;
4
5 %% Calculating the left side
6 %%
7 filename = uigetfile( '*.stl' ); % Load in the left breast
8
9 %% Vertices en faces extract from struct
10 [fv.vertices,fv.faces] = stlread(filename);
11 vertices = fv.vertices;
12 faces = fv.faces;
13
14 %% Compression phase
15 [fv.vertices, indexm, indexn] = unique(fv.vertices, 'rows' );
16 fv.faces = indexn(fv.faces);
17
18 %% calculate curvatures
19 getderivatives=0;
20 [PrincipalCurvatures,PrincipalDir1,PrincipalDir2,FaceCMatrix,VertexCMatrix,Cmagnitude]= ...
    GetCurvatures(fv ,getderivatives);
21 mean_princ1 = mean(PrincipalCurvatures(1,:));
22 mean_princ2 = mean(PrincipalCurvatures(2,:));
23
24 GaussianCurvature = PrincipalCurvatures(1,:).*PrincipalCurvatures(2,:);
25
26 min_Gauss = min(GaussianCurvature);
27 max_Gauss = max(GaussianCurvature);
28
29 %% Draw the mesh to the screen
30 figure( name , 'Triangle Mesh Curvature Example' , numbertitle , off , color , w );
31 colormap turbo
32 %caxis([min(GaussianCurvature) max(GaussianCurvature)]); % color overlay the gaussian curvature
33 caxis([min_Gauss max_Gauss]);
```

```

34 surface = patch(fv, FaceVertexCdata ,GaussianCurvature , facecolor , interp , ...
    edgecolor , interp , EdgeAlpha ,0.2);
35 %set some visualization properties
36 set(surface, ambientstrength ,0.35);
37 axis on
38 view([-45,35.2]);
39 camlight();
40 lighting phong
41 grid on
42 colorbar();
43
44 %print -r150 -dpng .png
45
46 %%
47 %Calculate area of each face, and sum them
48 A = vertices(faces(:,2),:) - vertices(faces(:,1),:);
49 B = vertices(faces(:,3),:) - vertices(faces(:,1),:);
50 c = cross(A,B,2); % Cross product calculation of A and B, treating the rows as vectors
51 area = 1/2 * sum(sqrt(sum(c.^2, 2)))/100; % Calculate the area in cm^2
52
53 fprintf( \nThe surface area is %f\n\n , area); % Display the result
54
55 %% Calculating the right side
56 %%
57 filename2 = uigetfile( *.stl ); % Load in the right breast
58
59 %% Vertices en faces extract from struct
60 [fv2.vertices,fv2.faces] = stlread(filename2);
61 vertices = fv2.vertices;
62 faces = fv2.faces;
63
64 %% Compression phase
65 [fv2.vertices, indexm, indexn] = unique(fv2.vertices, rows );
66 fv2.faces = indexn(fv2.faces);
67
68 %% calculte curvatures
69 getderivatives=0;
70 [PrincipalCurvatures,PrincipalDir1,PrincipalDir2,FaceCMatrix,VertexCMatrix,Cmagnitude]= ...
    GetCurvatures(fv2 ,getderivatives);
71 mean_princ1 = mean(PrincipalCurvatures(1,:));
72 mean_princ2 = mean(PrincipalCurvatures(2,:));

```

```
73
74 GaussianCurvature2 = PrincipalCurvatures(1,:).*PrincipalCurvatures(2,:);
75
76 min_Gauss2 = min(GaussianCurvature2);
77 max_Gauss2 = max(GaussianCurvature2);
78
79 %% Draw the mesh to the screen
80 figure( name , Triangle Mesh Curvature Example , numbertitle , off , color , w );
81 colormap turbo
82 %caxis([min(GaussianCurvature) max(GaussianCurvature)]); % color overlay the gaussian curvature
83 caxis([min_Gauss2 max_Gauss2]);
84 Surface2 = ...
    patch(fv2, FaceVertexCdata ,GaussianCurvature2, facecolor , interp , edgecolor , ...
        interp , EdgeAlpha ,0.2);
85 %set some visualization properties
86 set(surface2, ambientstrength ,0.35);
87 axis equal
88 view([-45,35.2]);
89 camlight();
90 lighting phong
91 colorbar();
92
93 print -r150 -dpng .png % Print the 3D image to a 2D PNG image
94
95 %%
96 %Calculate area of each vertice, and sum them
97 A = vertices(faces(:,2),:) - vertices(faces(:,1),:);
98 B = vertices(faces(:,3),:) - vertices(faces(:,1),:);
99 c = cross(A,B,2); % Cross product calculation of A and B, treating the rows as vectors
100 area2 = 1/2 * sum(sqrt(sum(c.^2, 2)))/100; % Calculate the area in cm^2
101
102 fprintf( \nThe surface area is %f\n\n , area2); % Display the result
103
104 %% Calculation the ratio between left and right
105 % A factor between 0 and 1 will be obtained. 0 is no symmetry, 1 is perfect symmetry.
106 Symmetry_area = abs((area - area2)/ (area + area2));
107 Symmetry_area = 1 - Symmetry_area;
108
109 %%
110 mean_Gauss1 = mean(GaussianCurvature);
111 mean_Gauss1 = abs(mean_Gauss1);
```

```
112 mean_Gauss2 = mean(GaussianCurvature2);
113 mean_Gauss2 = abs(mean_Gauss2);
114 Symmetry_Gauss = abs((mean_Gauss1 - mean_Gauss2) / (mean_Gauss1 + mean_Gauss2));
115 Symmetry_Gauss = 1 - Symmetry_Gauss
116
117 %%
118 Symmetry = (Symmetry_area + Symmetry_Gauss)/2
```



## Appendix D

### Protocols

In this appendix there can be found three separate protocols. These protocols are written in Dutch. The protocols are presented in the following order:

1. Protocol 1: 3D mammafotografie met de Canfield Vectra XT
2. Protocol 2: Protocol voor het maken van patiënt specifieke borstmallen in Materialise 3-Matic en MeshMixer
3. Protocol 3: Bepaling van de ROI in 3-matic AHV 3D foto's



## PROTOCOL 1:

# 3D MAMMAFOTOGRAFIE MET DE CANFIELD VECTRA XT

T. van Kuipers, A. Ooms, J.B. Troost

## Inhoud

Doelstelling.....	2
Toepassingsgebied .....	2
Benodigheden .....	2
Vorbereiding.....	2
Opstarten systeem & software .....	2
Kalibratie .....	3
Draadloze afstandsbediening.....	3
Werkwijze.....	4
Selecteren of maken een (nieuwe) patiënt.....	4
3D foto maken van de patiënt.....	4
Patiënt positioneren voor een borstfoto .....	7
Fotograferen.....	8
Nazorg .....	8
Selecteren landmarks.....	8
Opslaan van foto's.....	9
Exporteren van de foto's.....	9
Afsluiten van het systeem .....	9
Schoonmaken camera's.....	9
Arbo/ veiligheid .....	9
Veiligheid.....	9
Verslaglegging/ rapportage.....	<b>Fout! Bladwijzer niet gedefinieerd.</b>
Complicaties .....	9
Definities en afkortingen.....	<b>Fout! Bladwijzer niet gedefinieerd.</b>
Storingen/ Probleemoplosser .....	9
Documentstatus .....	10
Gerelateerde documenten.....	10
Literatuur en bronvermelding.....	<b>Fout! Bladwijzer niet gedefinieerd.</b>
Disclaimer .....	10

## Doelstelling

Het verkrijgen van een eenduidige veilige werkwijze bij het uitvoeren van 3D fotografie en plaatsen van borstmarkeringen voor de productie van een gepersonaliseerde 3D geprinte borstmal.

### Primaire doelstellingen

- Eenduidig uitvoeren van de handelingen
- Toetsbaar maken van de handeling

### Secundaire doelstellingen:

- Hulpmiddel bij inwerken van nieuwe collega's

## Toepassingsgebied

Dit document beschrijft het veilig en op de juiste manier maken van 3D afbeeldingen. Daarnaast wordt het plaatsen van markeringen beschreven ten behoeve van patiënten die in aanmerking komen voor een gepersonaliseerde 3D geprinte borstmal.

### Uitvoerende:

- Technisch Geneeskundige/ Klinisch Technoloog
- Medisch Fotograaf
- Plastisch chirurg
- Verpleegkundig specialist

## Benodigheden

### Apparatuur

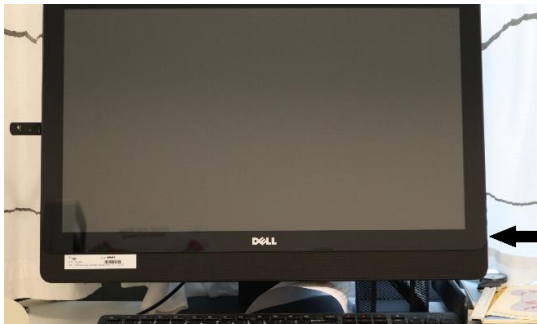
- Canfield Vectra XT systeem
- Computer met Canfield Vectra software
- Markeerstift (niet permanente)


## Vorbereiding

Onderstaande stappen zijn zowel gebaseerd op de handleiding van Canfield als de eigen ervaringen.

### Opstarten systeem & software

1. Zet de computer aan door de *power button* rechtsonder op het scherm in te duwen. In onderstaande afbeelding bij de *zwarte pijl*.





2. Als de computer volledig is opgestart, kun je op het Windows bureaublad de *Vectra software* openen door op logo  te klikken. Het camerasysteem zal nu ook opstarten.

## Kalibratie

Kalibratie van het systeem zorgt ervoor dat de camera's en andere componenten van het systeem op de juiste manier met elkaar samenwerken. Dit is erg belangrijk om accurate geometrisch juiste 3D modellen te krijgen. Het systeem kalibreren moet gedaan worden als het camerasysteem is verplaatst of de kalibratie verouderd. Er staat geen termijn genoemd wanneer de kalibratie verouderd is. Advies is om maandelijks te kalibreren.

Het kalibratieproces duurt enige minuten en is het makkelijkst met zijn tweeën, maar kan ook alleen worden uitgevoerd met de draadloze afstandsbediening.

3. Klik op de *set-up* button rechtsonder in het scherm. 
4. Selecteer het tabblad *Capture* en selecteer VECTRA XT in het drop-down menu.
5. Klik op *Calibrate now*
6. Ga met het kalibratiebord ongeveer 70 centimeter van het VECTRA systeem staan en houdt het bord loodrecht ten opzichte van de grond en de *L* rechtop.
  - Beweeg naar voren of achteren om het lange gedeelte van de *L* tussen de verticale balken te krijgen op het preview scherm.
  - Beweeg het bord omhoog en omlaag om het korte gedeelte van de *L* in de horizontale balk te krijgen op het preview scherm.
7. Klik op *take picture* op het scherm of druk de rechterpijl in op de draadloze afstandsbediening.
8. Positioneer het kalibratiebord voor het tweede deel van de kalibratie door ongeveer 70 centimeter vanaf het VECTRA systeem te gaan staan. Zie ook het computer scherm voor instructies.
  - Zorg dat de *L* recht opstaat en het korte gedeelte van de *L* is tussen de horizontale balk.
  - Kantel het bord ongeveer 30° voorover.
  - Zorg ervoor dat de lange kant van de *L* tussen de schuine horizontale balken komt te liggen in de preview images.
9. Klik op *take picture*  op het scherm of de rechterpijl op de draadloze afstandsbediening
10. Als de kalibratie afbeeldingen zijn verwerkt is het kalibratie proces voltooid. Klik op OK.

## Draadloze afstandsbediening

**Select knop:** Werkt hetzelfde als de linkermuisknop van een 'normale' computermuis

**Ontspanknop:** Door de rechterpijl in te duwen zal de foto genomen worden.




**Height control:** Druk omhoog of omlaag en houdt vast om het systeem omhoog of omlaag te bewegen.

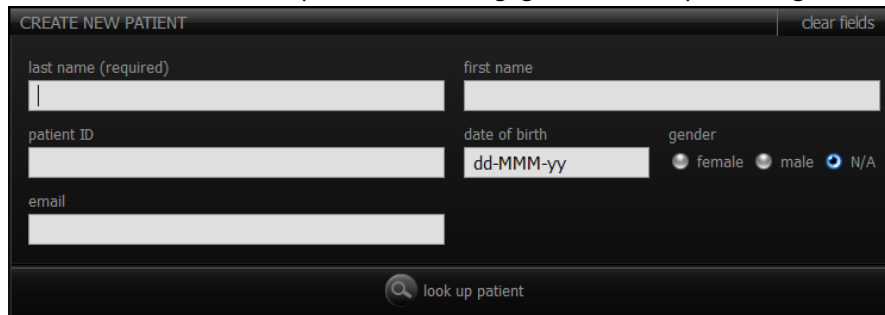
**Cursor:** Druk en beweeg voorzichtig om de positie van de cursor pijltje op het scherm te verplaatsen.


## Werkwijze

### Selecteren of maken een (nieuwe) patiënt


#### Aanmaken nieuwe patiënt

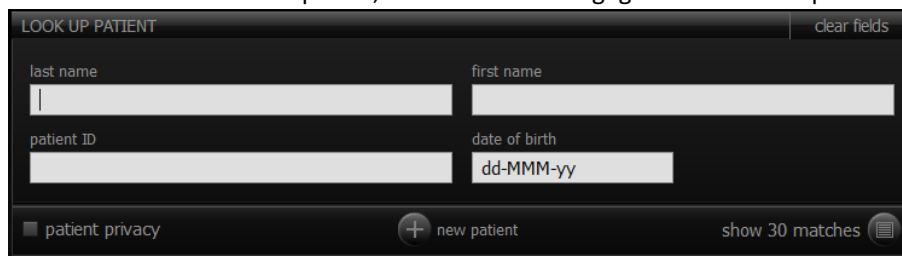
1. Klik op de button *new patient*  in de rechterbovenhoek van het VECTRA home scherm
2. Onderstaand venster zal openen waarin de gegevens van de patiënt ingevuld kunnen worden.



3. Klik op *XT capture*  om een 3D foto te maken, de gegevens van de patiënt zullen automatisch opgeslagen worden.

#### Openen/vinden van een bestaande patiënt

1. Klik op de button *look up patient*  in de rechterbovenhoek van het VECTRA home scherm
2. Onderstaand venster zal openen, vul 1 of meerdere gegevens in van de patiënt.



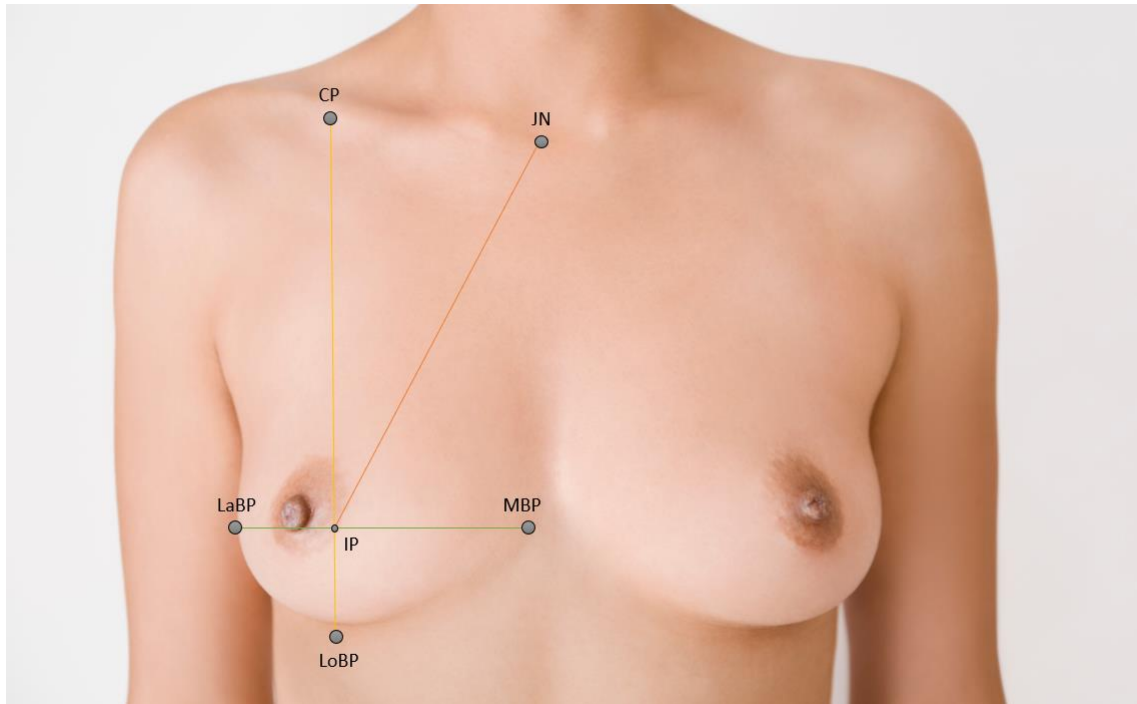
3. Door op Enter te drukken of *show matches* aan te klikken krijg je een lijst met corresponderende patiënt(en).
4. Dubbelklik op de juiste patiënt, eerder gemaakte 3D foto's zullen worden weergegeven. Staat de juiste patiënt er niet tussen, maak dan een nieuwe patiënt aan.
5. Klik op *XT Capture* om een nieuwe 3D foto te maken.

### Plaatsen van borstmarkeringen

Maak voordat je de borstmarkeringen aanbrengt een schone foto van de patiënt. Dat wil zeggen zonder iets op de patiënt afgetekend. Voor instructie van het nemen van een foto, ga door naar '3D foto maken van de patiënt' op pagina 7.

1. Gebruik een (niet-permanente) markeerstift om de landmarks uit te tekenen. Teken op elke landmark een kruisje (X), zodat deze ook nog te herkennen is als de borst wordt afgetekend voor het maken van een mal.
2. Begin met de landmarks die je duidelijk ziet met markeren. Dit zijn de Jugular notch (JN), Lowest breast point (LoBP) en Medial breast point (MBP). De MBP is de (laagste) meest mediale punt van de borst. Deze is te vinden door de borst opzij te duwen en de ontstane huidplooi te bekijken. Zet op deze punten een markering.

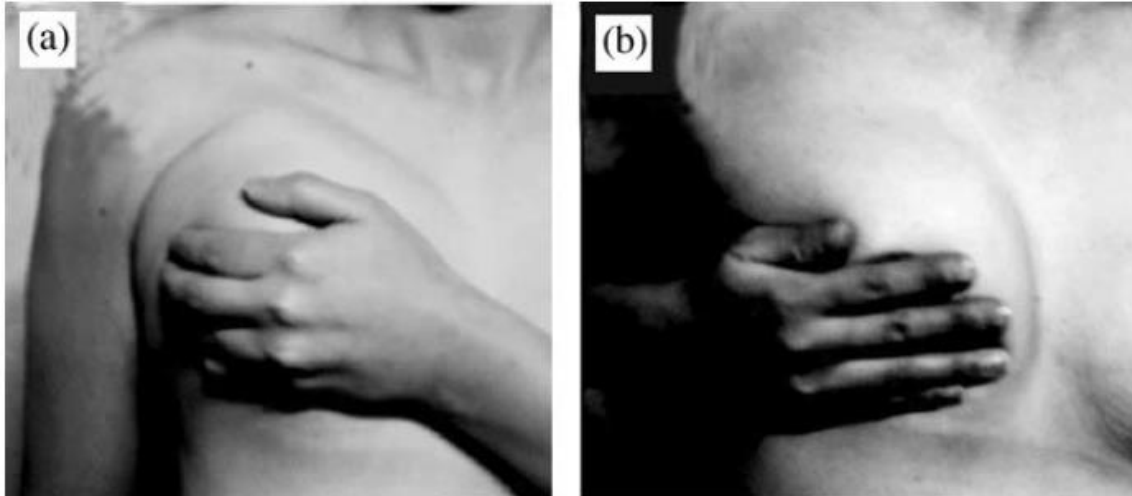
3. Loodrecht opzij naar lateraal, vanaf de MBP, kan het lateral breast point (LaBP) worden gevonden. Bepaal waar de IMF stopt aan de laterale zijde en zorg da de LaBP daar recht boven zit.
4. Loodrecht omhoog vanaf het LoBP naar de clavicula wordt het clavculaire point (CP) gevonden.



*Figuur 1: Landmarks zoals na het volgen van de stappen wordt verkregen*

## Bepaling borstcontour

1. Gebruik een (niet permanente) markeerstift om de contouren van de 'gezonde' contralaterale borst te markeren. Dit is dus de borst die niet geopereerd wordt.
2. Vraag de patiënt haar borst omhoog te duwen of doe dit zelf zoals in onderstaande foto. Er zal een huidplooi ontstaan die de bovenste borstcontour representeert.



Figuur 2: Voorbeeld van hoe de *fold line method* uit te voeren.[1]

3. Begin met het plaatsen van markeringen bij het meest mediale punt van de inframammary plooï (IMF), en volg de bovenzijde van de borst tot het meest laterale punt van de IMF. Neem ongeveer 2-3 cm tussen elk markeer punt. Er zal nu een patroon ontstaan zoals in onderstaande figuur.



Figuur 3: Voorbeeld hoe de landmarks en borstcontour eruit kan zien na plaatsing van de landmarks

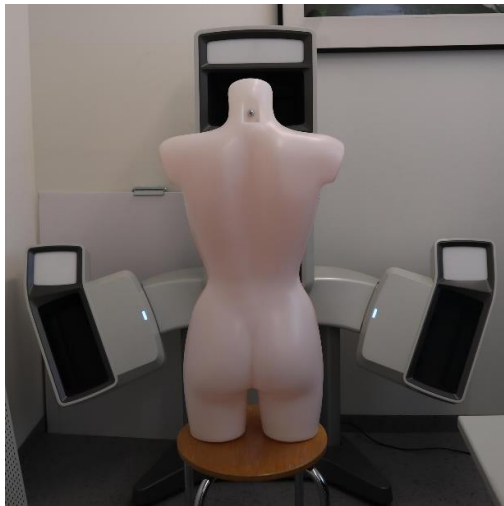


### 3D foto maken van de patiënt

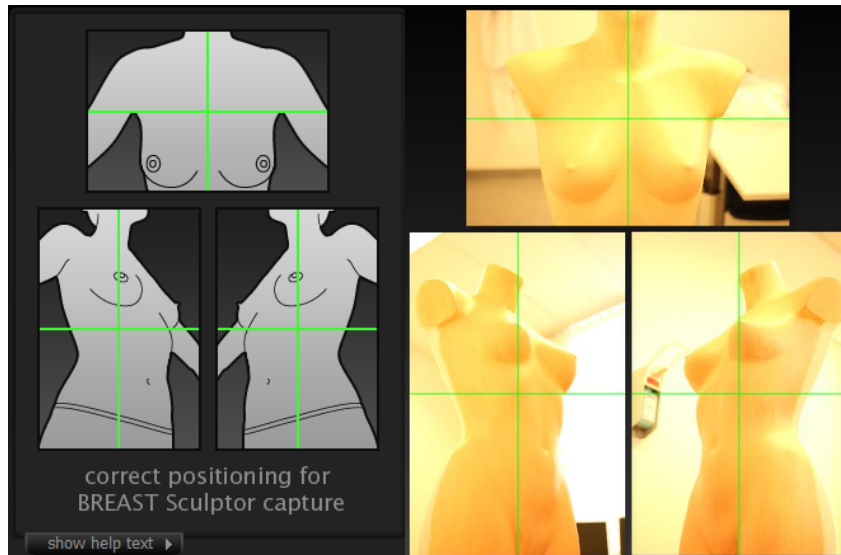
1. Selecteer *3D breast capture* in de tabbladen bovenin het scherm.
2. Instrueer de patiënt om haar juwelen af te doen, verwijder zweet, olie of ander glimmend van de huid. Vraag de patiënt om, bij langer haar, het haar naar achteren te doen. Instrueer de patiënt om haar bovenkleding uit te doen, ook de BH. Eventueel de patiënt haar broek laten uittrekken bij metalen knopen etc., dit kan voor weerkaatsing zorgen in de foto door de flits.

### Patiënt positioneren voor een borstfoto

1. Check nogmaals of de goede patiënt geselecteerd staat.
2. Laat de patiënte in het midden met haar gezicht richting het Vectra systeem staan zoals in onderstaande foto. De afstand tussen patiënte en systeem kan per patiënt verschillen, een afstand van  $\pm 70$  centimeter om te beginnen kan worden aangehouden.
  - Laat de patiënte zo rechtop mogelijk staan
  - Beide voeten moeten op gelijke afstand van het systeem staan.
  - Indien sprake is van meerdere sessies kunnen markeringen op de grond helpen om de patiënt op dezelfde plaats te laten staan.



3. De positie zoals in onderstaande foto's moet verkregen worden voor het verkrijgen van een goede foto.
  - Door de afstand tussen systeem en patiënt groter of kleiner te maken, kan de 'side preview images' worden aangepast. Zorg ervoor dat de verticale lijnen over de tepels lopen. Check of beide borsten en de abdominale *midline* volledig in beeld zijn. De foto's links en rechts moeten een spiegelbeeld van elkaar kunnen zijn.
  - Met de *height control* rechts op het beeldscherm kan het systeem omhoog en omlaag gebracht worden. Zorg ervoor dat de schouders en areola volledig in beeld zijn in de frontale preview image. Als het niet lukt om de schouders en areola volledig in beeld te krijgen, laat de patiënt dan een stap terug doen.



4. Laat de patiënte nu haar armen wijd houden, waarbij de hoek tussen lichaam en armen ongeveer 45°. Zorg ervoor de borsten niet omhoog gaan bij het spreiden van de armen. Laat de patiënt uitademen vlak voor het maken van de foto, maar zorg er voor dat de schouders niet zakken.

### Fotograferen

1. Om een foto te nemen, klik op *take picture* of druk de rechter pijl in op de draadloze afstandsbediening (zie gebruik van de draadloze afstandsbediening). Na de flits, zal het systeem de foto's converteren tot een 3D foto. Vergeet niet de patiënt te vertellen dat zij weer mag ontspannen.
2. Check als de software klaar is met verwerken of alle benodigde structuren in de 3D foto worden weergegeven.
  - Ja, laat de patiënte zich weer aankleden, indien er geen andere foto gemaakt hoeft te worden.
  - Nee, vraag de patiënt voor toestemming om nogmaals een foto te maken. Doorloop bovenstaande stappen om de patiënt wederom te positioneren en de foto te maken. Kijk eventueel in sectie troubleshooting voor een aantal voorkomende fouten en hun oplossing.

### Nazorg

#### Bepalen borstvolume met behulp van digitale landmarks


1. Op twee manieren kunnen er *landmarks* geplaatst worden, automatisch en handmatig. De software zal automatisch aangeven of het lukt om de *landmarks* automatisch te plaatsen. Als dit gelukt is, ga dan naar stap 3.
2. De *landmarks* kunnen ook handmatig geplaatst worden en is nodig als de automatische landmark plaatsing niet werkt. Het systeem geeft aan op welke plaatsen je de *landmarks* moet plaatsen. Enige nauwkeurigheid is hierbij gewenst i.v.m. het bepalen van de vorm van de borstkas en het volume van de borst.
3. Na het plaatsen van de *landmarks* kun je links op het scherm verschillende buttons aanklikken. Klik op *Assessment* en daarna *Chest wall*. De software berekent nu het volume van de borst en waar de borstkas zit aan de hand van de *landmarks*.

## Opslaan van foto's

1. Klik linksboven op de *VECTRA home* button.
2. Er verschijnt een pop-up met *updated surface*, geeft het bestand een naam en druk op *save*.
3. De foto inclusief *landmarks* is opgeslagen onder de patiënt. Deze ziet u nu terug in het hoofdmenu.

## Exporteren van de foto's

Als de eerste 2 stappen al zijn doorlopen bij 'Opslaan van foto's, ga dan door naar stap 3.

1. Klik linksboven op *3D analysis*. Een nieuw scherm opent.
2. Zorg dat je object geselecteerd staat, dit zie je linksboven door een ingedrukt  object.
3. Om het object te exporteren ga linksboven naar *File* → *Export*.
4. Selecteer een bestandstype om in op te slaan, *.obj* of *.stl*.
5. Kies zelf de bestandslocatie waarin je het object wil opslaan. Geef je bestand een naam.

## Afsluiten van het systeem

1. Klik op de *VECTRA home* button in de linkerbovenhoek om terug te gaan naar het hoofdmenu
2. Klik op de *exit* button rechtsonder in het scherm van het hoofdmenu
3. Als alles is opgeslagen en geen andere programma's draaien kan de computer worden uitgeschakeld zoals bij een normale Windows computer.

## Schoonmaken camera's

De buitenkant van het systeem (niet het glas van de camera's) kan worden afgenomen met een schone lichtvochtige doek of spons waarop een mild schoonmaakmiddel is aangebracht. Het (herhaaldelijk) gebruik van alcohol, benzeen, verfoplosmiddelen zoals thinner, of andere licht ontvlambare middelen, kunnen brand of een elektrische schok veroorzaken.

Het glas van de camera's kan worden schoongemaakt met een optische glasreiniger en gebruik van een zachte doek. Vermijdt het gebruik van harde materialen want deze kunnen krassen geven op het glas. Raak het glas niet aan met je vingers, dit geeft vet afdrucken op het glas wat het fotograferen kan belemmeren.

## Arbo/ veiligheid

### Veiligheid

Het 3D fotosysteem maakt de foto met een flits vanuit 4 punten. Dit kan een risico vormen bij patiënten met lichtflitsgevoelige epilepsie, hierbij zal overwogen moeten worden om de foto niet te maken.

## Complicaties

Door het gebruik van 3D stereolithografie zijn geen complicaties bekend.

## Storingen/ Probleemoplosser

Probleem	Oplossing
Camerasysteem gaat niet meer omhoog	Het systeem via de knop omhoog/ omlaag helemaal omlaag laten gaan. Houdt de knop 10 seconden vast, het lift systeem zal hierdoor gereset worden en zal weer omhoog en omlaag gaan.
3D objecten bevatten geometrische oneffenheden, bijvoorbeeld dislocaties.	De kalibratie van het systeem kan verouderd zijn. Kalibreer het systeem volgens het 'Kalibratie stappenplan'.

Oppervlakte kleur is vlekkelig/ niet gelijk op de rechterhelft en linkerhelft van het 3D object.	Reflecterende oppervlakten in de omgeving hebben invloed op de uiteindelijk 3D afbeelding. Verwijder reflecterende objecten, zoals spiegels en schilderijen, die licht kunnen reflecteren op het object.
Kalibratie <ul style="list-style-type: none"> <li>- Donkere afbeeldingen</li> <li>- Fel omgevingslicht</li> <li>- Kalibratie bord niet goed gepositioneerd</li> </ul>	Bij donkere afbeeldingen kan het zijn dat de flitsers het niet goed doen. Probeer nogmaals te kalibreren. Als de flitsers kapot zijn, zal Canfield deze moeten vervangen. Bij overbelichting zorg ervoor dat het teveel aan omgevingslicht wordt verminderd. Positioneer het kalibratie bord zoals beschreven en afgebeeld in het stappenplan.
Software geeft foutmelding over het vinden van de patiëntendatabase	Soms geeft de software aan dat de patiëntendatabase niet gevonden kan worden. Start de software opnieuw op, vaak wordt de patiëntendatabase dan wel gevonden.

## Documentstatus

Dit document is een kwaliteitsdocument dat de algemeen geldende norm voor goed handelen beschrijft.

Indien hier in het belang van de patiënt van wordt afgeweken moet dit gemotiveerd in het elektronisch verpleegkundig en/of medisch dossier van de patiënte worden vermeld.

## Gerelateerde documenten

User Guide Canfield Vectra XT

## Disclaimer

De inhoud van dit document kan vertrouwelijk zijn. Het is niet toegestaan om dit document of delen daarvan zonder uitdrukkelijke toestemming te gebruiken, te verspreiden of op te slaan in een voor meerdere personen toegankelijke gegevensdrager. Uitzondering hierop vormt het overdragen van ZGT- en MST-protocollen aan zorginstellingen die een zelfstandige ketenrol vervullen bij patiënten van ZGT/MST. ZGT/ MST sluit elke aansprakelijkheid uit inzake het gebruik van dit document, ook wanneer hiervoor toestemming is gegeven.

## Referenties

- [1] H. Y. Lee, K. Hong, and E. A. Kim, "Measurement protocol of women's nude breasts using a 3D scanning technique," *Appl. Ergon.*, vol. 35, no. 4, pp. 353–359, 2004, doi: 10.1016/j.apergo.2004.03.004.

Protocol 2: voor  
het maken van  
patiënt specifieke  
borstmallenIn  
Materialise 3-  
Matic en  
MeshMixer

## Inhoudspagina

Hoofdstuk 1: Inleiding .....	3
Hoofdstuk 2: Voorbereiden STL-object voor segmentatie .....	4
Importereren van een 3D object .....	4
Hoofdstuk 3: Segmenteren van de borst .....	5
Het plaatsen van landmarks .....	5
Segmenteren .....	7
Spiegelen .....	9
Hoofdstuk 4: Het maken van de mal .....	9
Mal 1: Basis mal .....	9
Mal 2: Mal met cilinder gaten .....	12
Mal 3: Mal met gleuven .....	15
Mal 4: Mal met Voronoi patroon .....	17
Hoofdstuk 5: Afronden .....	23
Afmetingen vinden van de mal .....	23
Label toevoegen .....	23
Mal exporteren als STL-bestand .....	24

## Hoofdstuk 1: Inleiding

In dit werkprotocol wordt uitgelegd hoe verschillende designs van borstmallen ontworpen worden. Het doel hiervan is om duidelijk te documenteren hoe verschillende borstmallen zijn gemaakt, zodat nieuwe gebruikers dit protocol als handvat hebben om de mallen zelf te kunnen maken. Daarnaast zorgt dit protocol ervoor dat er zo min mogelijk verschil is tussen de mallen en kan deze documentatie bijdragen aan het optimaliseren van het maken van 3D geprinte borstmallen.

Dit protocol is gebaseerd op onderzoek naar het maken van borstmallen voor patiënten die een unilaterale DIEP lap reconstructie zullen ondergaan. Hierbij wordt gebruik gemaakt van de goede borst om een mal te vormen. Het kan zijn dat voor bilaterale reconstructies dit protocol niet geschikt is. In dit protocol wordt gebruik gemaakt van een preoperatieve 3D mammafotografie, gemaakt met de Canfield Vectra XT systeem.

Dit protocol bestaat uit verschillende delen. In Hoofdstuk 2 wordt het STL-object ingeladen en voorbereid op segmentatie. In Hoofdstuk 3 wordt de goede borst gesegmenteerd van de torso. Hoofdstuk 4 laat zien hoe de gesegmenteerde borst wordt omgezet naar verschillende soorten mallen. In Hoofdstuk 5 worden de laatste stappen om de mal te printen besproken.


Om dit protocol door te kunnen gaan heeft u het volgende nodig:

- Computer
  - Windows 7 of hoger met 64 bit (Materialise werkt niet op een MAC)
  - CPU: Intel Core i7 of AMD Phenom II X4/ X6 (3 GHz of hoger) met SSE2 technologie
  - 2 GB vrije schijfruimte
- Software
  - Materialise 3-Matic (Materialise, Leuven, Belgium)
  - Meshmixer (Autodesk Inc., San Rafael, USA) (Alleen als u een Voronoi patroon wilt maken)
- 3D-object
  - STL-object van preoperatieve torso

## Hoofstuk 2: Voorbereiden STL-object voor segmentatie

Allereerst moet het 3D object worden ingeladen in Materialise 3-Matic. Zorg ervoor dat u het 3D-object als STL-bestand heeft opgeslagen op de computer waarop u werkt. Zorg er verder voor dat 3-Matic is geïnstalleerd op de computer en klaar is voor gebruik.


### Importeren van een 3D object

1.  Links ziet u een verticale werkbalk met verschillende icoontjes. Klik op het icoon wat hoort bij *Import part*
2. Selecteer het STL-bestand wat u wilt gebruiken
3. Een venster wordt geopend. Alle standaard instellingen zijn hierbij goed. Belangrijk is dat *Scale coefficient* op *mm* staat
4. Druk op *OK*
5. U ziet nu uw 3D model

Inspecteer uw object op oneffenheden of artefacten. Hierbij is vooral de goede borst en de directe torso eromheen van belang. Aan artefacten op de buik hoeft u niets te doen, maar wees er wel alert op dat er dan ook kans is dat de borst een artefact kan hebben. Als het object veel artefacten blijkt te hebben, kan het zijn dat uw object onbruikbaar is. Het bewerken van het object zal de vorm dan zoveel aantasten dat de mal niet meer te gebruiken is.

Voordat u verder gaat met uw object, willen we eerst onnodige data verwijderen. Dit kost namelijk een hoop extra rekenkracht. In dit geval gaan we de buik verwijderen, maar u kunt ook de armen verwijderen.

#### 1.2.3.1 Verwijderen van onbelangrijke data

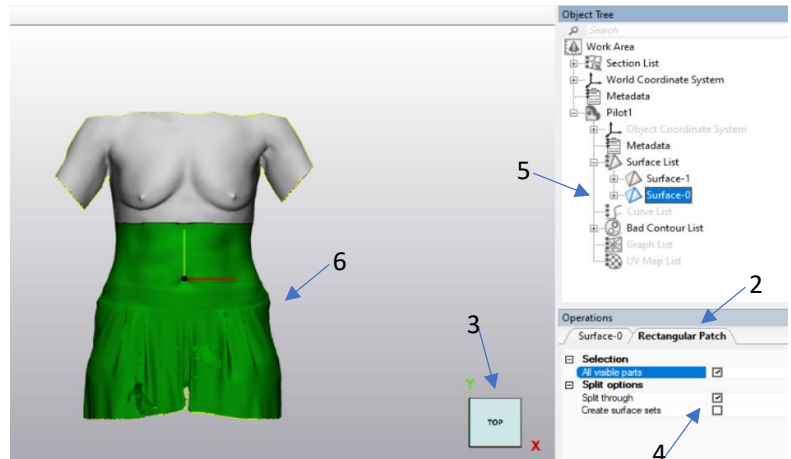
1. Ga naar het tabblad *Surface*, te vinden in het blauw in de tweede horizontale werkbalk
2.  Klik op het icoon wat hoort bij *Rectangular Patch*. U ziet nu rechtsonder onder *Operations* het tabblad *Rectangular Patch* verschijnen
3. Zorg ervoor dat u recht op uw object kijkt. Dit doet u door op *Top* te klikken op de kubus in de *Work Area*



- Zorg ervoor dat bij *Split options*, onder het kopje *Rectangular Patch*, de optie *Split through* is aangevinkt

- Selecteer nu de regio onder de borsten. Let hierbij op dat u het niet per ongeluk data van de borsten selecteert. U heeft nu een nieuwe surface aangemaakt. Deze is terug te vinden in de *Object Tree* – “Uw object” – *Surface list*

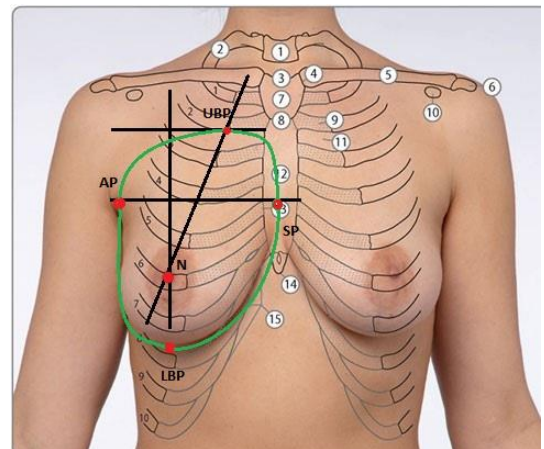
- Selecteer nu de surface die niet de borsten bevat. Hetgeen wat u heeft geselecteerd is groen. Klik op *delete* op uw toetsenbord. U heeft nu alleen het bovenste gedeelte van de torso over



Stappen gevisualiseerd voor verwijderen surface


### Hoofdstuk 3: Segmenteren van de borst

Het segmenteren van de borst is uitdagend, aangezien de borst geen duidelijke begrenzing heeft. Om de segmentatie toch enigszins te standaardiseren wordt er in dit protocol gebruik gemaakt van landmarks. Dit is gebaseerd op de afbeelding hiernaast. Let hierbij goed op dat de door u gemaakte lijnen straks gezien moeten worden als projecties op de borst. Als u deze lijnen gebruikt om de locatie van een punt te bepalen, moet de oriëntatie dan ook goed zijn. Zorg er dus altijd voor dat de oriëntatie op *Top* staat, voordat u punten zet.



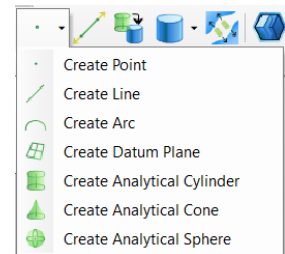
Overzicht verschillende landmarks en begrenzing borst, van Van Kuipers, et al. (2020)

#### Het plaatsen van landmarks

- Ga naar het tabblad *Design*, te vinden in het rood in de tweede horizontale werkbalk
-  Klik op het icoon wat hoort bij *Create point*. Er verschijnt nu onder *Operations* het tabblad *Create Points*
- Controleer of in dit tabblad de *Method* staat op *Coordinates*. Dit moet zo zijn voor elk punt wat u maakt. Zet elke keer dat u een nieuw punt maakt uw focus op het kopje *Coordinates*
- Selecteer nu de volgende vier punten:
  - Nipple (N)*: selecteer de tepel op de goede borst. Kies *Triangle node* voor selectie. Als u tevreden bent klinkt u op *Apply*

Let op: zorg ervoor dat u voor dit punt de z-coördinaat – het laatste getal – ergens opschrijft. Dit is  $z_N$

- b. *Axil point (AP)*: selecteer het hoogste punt van de oksel, aan de kant van de goede borst. Kies *Triangle node* voor selectie. Als u tevreden bent klinkt u op *Apply*  
Let op: Neem dit punt liever te ver ventraal dan te ver dorsaal.
  - c. *Upper point (UP)*: Probeer de clavicula te vinden in het model. Selecteer een punt op de clavicula aan de kant van de goede borst. Kies *Triangle node* voor selectie. Trek voordat u bevestigt 20 mm van de y-coördinaat van dit punt – het tweede getal – af.<sup>1</sup> Als u tevreden bent klinkt u op *Apply*
  - d. *Clavicula (C)*: selecteer de mediale kant van de clavicula aan de kant van de goede borst. Kies *Triangle node* voor selectie. Als u tevreden bent klinkt u op *Apply*
5. In de *Object Tree* ziet u nu de gemaakte punten. Hernoem ze door dubbel op de naam te klikken. Dit geldt ook voor alle lijnen die u hierna gaat maken
  6. Klik op het pijltje naast het icoon wat hoort bij *Create point*. Er verschijnt nu een drop down menu. Selecteer *Create line*. Dit verschijnt nu onder *Operations*
  7. Selecteer als *Method Direction and length*. *Length* maakt niet heel veel uit, 250 is een goede indicatie. Zolang de lijnen maar langer zijn dan de borst zelf
  8. Maak nu de volgende vier lijnen:
    - a. *Nipple line (NL)*: Kies als *Direction (0,1,0)*, dit is een verticale lijn. Selecteer voor uw *Origin N*, maar trek een aantal centimeter van de y-coördinaat af zodat de onderkant van de lijn onder de borst uitkomt. Klik op *Apply* ter bevestiging
    - b. *Middle breast line (MBL)*: Kies als *Direction (1,0,0)*, dit is een horizontale lijn. Selecteer voor uw *Origin AP*, maar vul voor de z-coördinaat  $z_N$  in, zodat de lijn aan de voorkant van het object uitkomt. Klik op *Apply* ter bevestiging
    - c. *Upper breast line (UBL)*: Kies als *Direction (1,0,0)*, dit is een horizontale lijn. Selecteer voor uw *Origin UP*, maar trek een aantal centimeter van de x-coördinaat af zodat de linkerkant van de lijn voorbij de goede kant van de borst komt, ter hoogte van *AP*. Vul voor de z-coördinaat  $z_N$  in, zodat de lijn aan de voorkant van het object uitkomt. Klik op *Apply* ter bevestiging



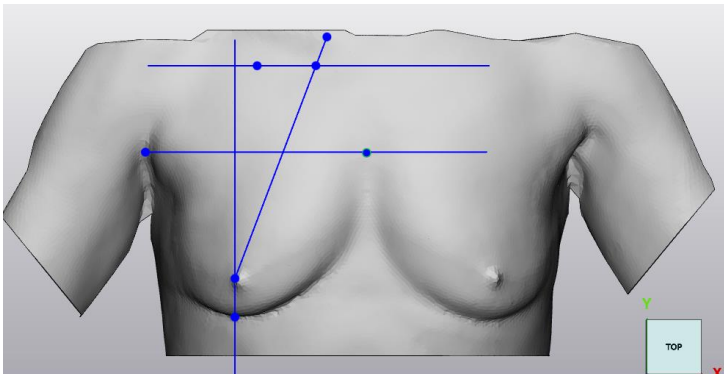
Drop down menu van create point

---

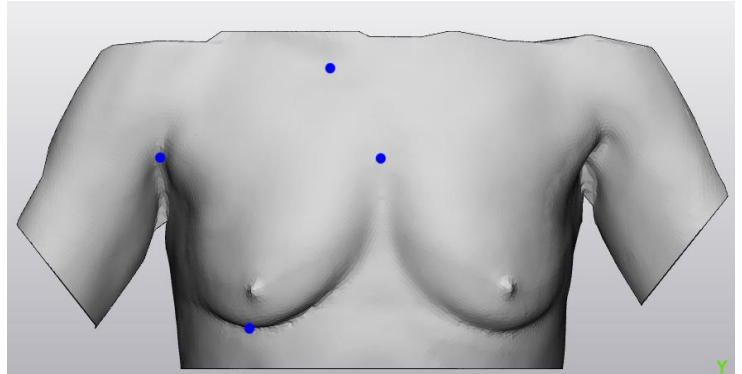
<sup>1</sup> De afstand tussen clavicula en bovenste punt van de borst wordt als constante gezien door plastische chirurgen, namelijk 2cm

- d. *Clavicula – Nipple line (CNL)*: Voor deze lijn moet u de *Method* op *Coordiantes* zetten. Selecteer bij *From* uw *C*-punt en bij *To* uw *N*-punt. Verander uw *z*-coördinaat van uw *From*-punt naar  $z_N$ , zodat de lijn aan de voorkant van het object uitkomt. Klik op *Apply* ter bevestiging
9. Ga nu weer terug naar *Create point* en selecteer de volgende drie punten:
    - a. *Upper Breast Point (UBP)*: Zoom in op de intersectie tussen de *UBL* en de *CNL* en selecteer hier uw nieuwe punt. Klik op *Apply* als u tevreden bent
    - b. *Lower Breast Point (LBP)*: Zoom nu in op de onderkant van uw *Nipple Line*. Selecteer hier het punt dat de kruising tussen de *NL* en de inframammairplooi is. Klik op *Apply* als u tevreden bent
    - c. *Sternum Point (SP)*: Volg nu de *Middle Breast Line* en selecteer het punt waar deze lijn het sternum kruist. Klik op *Apply* als u tevreden bent
  10. U kunt nu alle lijnen onzichtbaar maken, door met de rechtermuisknop op deze lijnen te klikken in de *Object Tree* en op *Hide* te klikken. Doe hetzelfde voor de punten *Nipple*, *Upper Point* en *Clavicula*

U heeft nu de vier landmark punten die nodig zijn voor de segmentatie. Hieronder ziet u het object met alle getekende lijnen en punten (links) en alleen de vier overgebleven landmarks (rechts). Nu kunt




Overzicht van de getekende lijnen en punten u de borst segmenteren van de thorax

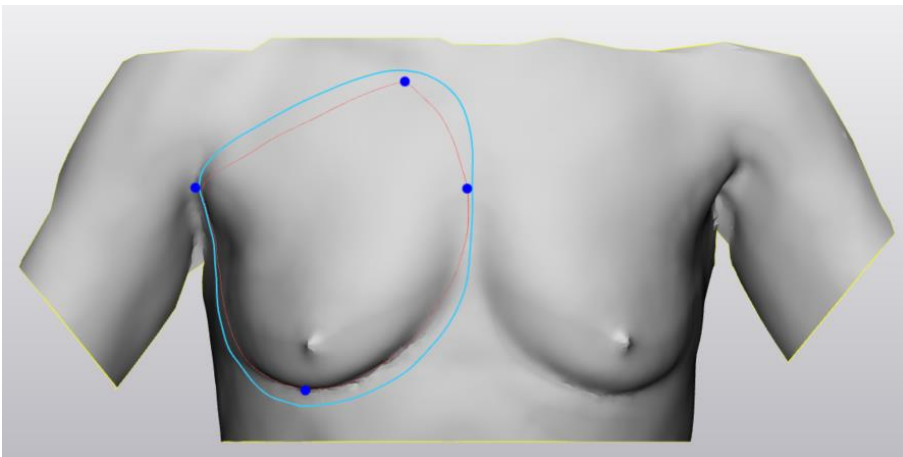


Overzicht van de uiteindelijk benodigde landmarks

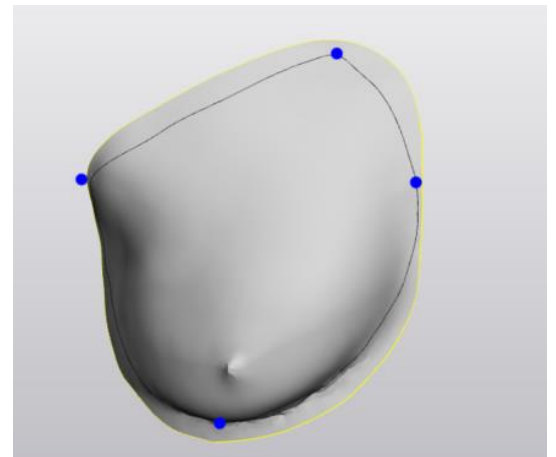
### Segmenteren

1. Ga naar het tabblad *Curve*, te vinden in het rood in de tweede horizontale werkbalk
2.  Klik op het icoon wat hoort bij *Create curve*. Er verschijnt nu onder *Operations* het tabblad *Create Curve*
3. Zorg dat de volgende opties aangevinkt zijn:
  - a. *Close curve*

- b. Curve creation method: Smooth curve
  - c. Attract curve
  - d. Attach curve
  - e. Split surfaces
4. Zoom goed in op de lower breast point en zet hier het begin van uw curve. Volg nu de borstcontouren, waarbij u uw vier landmarks gebruikt als begrenzing. Ga de hele borst rond en dubbelklik als laatste punt dicht bij uw beginpunt, waardoor de curve sluit
  5. Controleer nu of de curve mooi gesloten is. Als dit niet zo is moet u de huidige curve verwijderen en het opnieuw proberen. Let hierbij op dat u uw punten dicht bij elkaar zet. Op deze manier zal er één curve uitkomen
  6. Maak nu een tweede curve, met dezelfde instellingen, rondom de thoraxwand. Probeer een afstand van één à twee centimeter van de borstcurve aan te houden. Let er hierbij op dat dat niet mogelijk is rond het sternum punt en rond het axilair punt, sluit hier zo netjes mogelijk aan bij de borstcurve.
  7. In uw *Object tree* ziet u nu in de *Surface List* van uw object drie verschillende surfaces. Klik op de surface en zie waar deze bij hoort. Hernoem de surface voor uw eigen gemak
  8. Selecteer in uw *Object tree* nu de twee surfaces die u gemaakt heeft met uw curves. Klik erop met uw rechtermuisknop en selecteer *Separate* → *Copy to part* → *Create new*. U heeft nu een nieuw object wat alleen uit uw mal bestaat
  9. Klik nu met uw rechtermuisknop op uw originele object en selecteer *Hide*. U ziet nu alleen uw gesegmenteerde borst



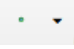

Resultaat van de twee getekende curves



Gesegmenteerde borst

Als u een mal aan het maken bent voor een geplande unilaterale DIEP lap reconstructie, moet de mal nog gespiegeld worden. U maakt hierbij gebruik van het *Sternum Point (SP)*, aangezien die precies in het midden zou moeten liggen

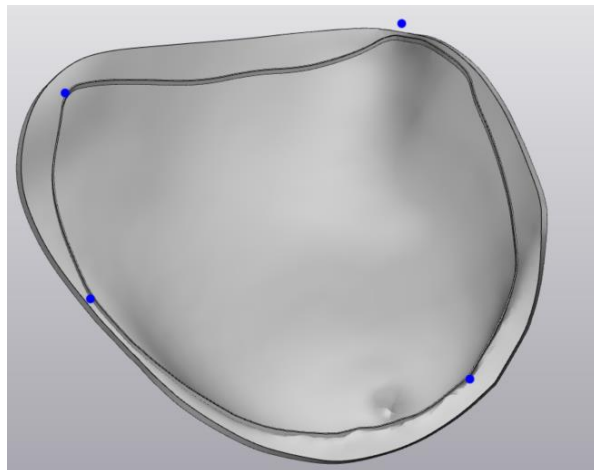
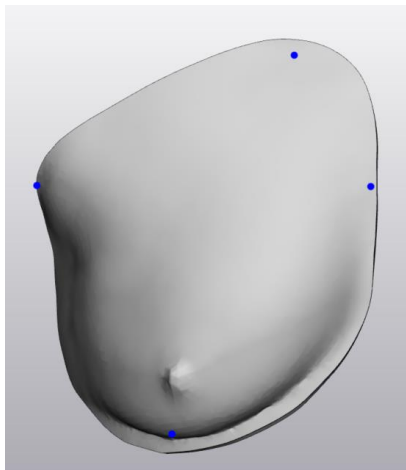
## Spiegelen

1. Ga naar het tabblad *Design*, te vinden in het rood in de tweede horizontale werkbalk
2.  Klik op het pijltje naast het icoon dat hoort bij *Create point*. Er verschijnt nu een drop down menu
3. Selecteer *Create Datum Plane*
4. Selecteer als *Methode* de optie *Normal and origin*
5. Kies als *Normal* (1,0,0)
6. Kies als *Origin* het *Sternum Point (SP)*
7. Selecteer *Apply*. In uw *Object Tree* is er nu een *DatumPlane* toegevoegd
8. Ga naar het tabblad *Align*, te vinden in het blauw in de tweede horizontale werkbalk
9.  Klik op *Mirror*
10. Selecteer als *Entities* uw gesegmenteerde borst
11. Selecteer als *Mirror plane* het vlak doet u zojuist hebt gemaakt
12. Klik op *Apply*. De gesegmenteerde borst zal nu over de y-as moeten zijn gedraaid

## Hoofdstuk 4: Het maken van de mal

Er zijn verschillende soorten mallen die u kunt maken. In dit hoofdstuk worden er een aantal beschreven. Elk kopje staat dus voor een andere soort mal en u moet alleen de instructies volgen voor de soort mal die u wilt maken. De eerste mal bevat wel alle stappen die bij andere mallen ook nodig zijn. Daarom zal aan het einde van die mallen aangegeven worden dat u nu alle stappen van de Basis mal moet doorlopen om uw mal af te ronden. Bij elke mal wordt als beginsituatie uitgegaan van het resultaat van Hoofdstuk 3.




### Mal 1: Basis mal






Resultaat na het doorlopen van alle stappen van mal 1, de basis mal. Links ziet u de voorkant, rechts ziet u de achterkant, inclusief opstaand randje

1. De eerste

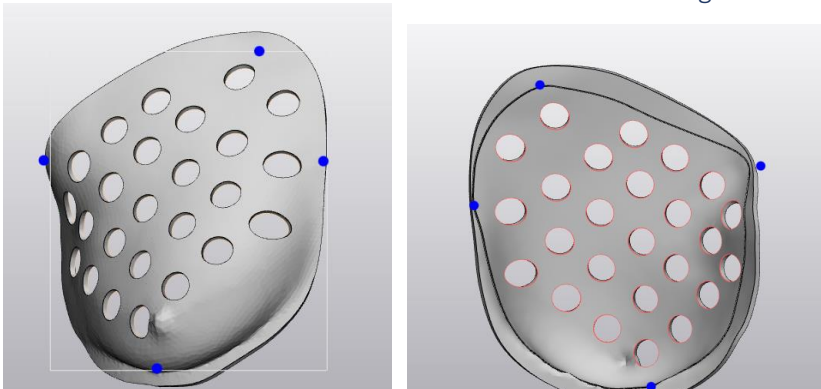
stap is om de mal een dikte te geven. U zult zien dat uw mal dikker zal worden, zonder dat de binnenkant van de mal zijn vorm zal verliezen

- a. Ga naar het tabblad *Design*, te vinden in het rood in de tweede horizontale werkbalk
  - b.  Klik op het icoon wat hoort bij *Uniform offset*. In het rechthoek van uw scherm, onder het kopje *Operations*, ziet u nu het tabblad *Uniform Offset*
  - c. Klik hier op *Entities* en selecteer uw object. De naam van dit object is nu zichtbaar bij *Entities*
  - d. Zorg ervoor dat bij de *Offset parameters*:
    - i. *Direction* op *External offset* staat
    - ii. *Distance* op de gewenste dikte staat. 3 mm is een goede dikte voor een mal
    - iii. *Preserve sharp features* uit staat
    - iv. *Solid* aangevinkt is
  - e. Klik op *Apply*.
2. Door de verdikking heeft de voorkant van de mal nu een overschot aan driehoeken, die geen toegevoegde waarde hebben en het proces alleen maar vertragen. Daarom gaan we deze verwijderen. Doe voor goede visualisatie het volgende: Selecteer uw mal → selecteer onder *properties* het eerste tabblad → Klik op *Filled with Triangle Edges* bij *General – Visualisation – Shading Mode*. U ziet nu een grote hoeveelheid driehoeken aan de voorkant van de mal
- a. Ga naar het tabblad *Fix*, te vinden in het blauw in de tweede horizontale werkbalk
  - b.  Klik op het icoon wat hoort bij *Reduce*
  - c. Klik hier op *Entities* en selecteer het oppervlak wat bij de voorkant van uw mal hoort. De naam van dit oppervlak is nu zichtbaar bij *Entities*
  - d. Kies voor de *Geometrical error* 0.03
  - e. Selecteer *Apply*. U ziet dat uw voor kant nu weer een normale hoeveelheid driehoeken heeft. U kunt uw visualisatie nu weer terugzetten naar *Smooth shaded*
3. De volgende stap is om een voelbaar randje te maken aan de binnenkant, zodat de grens tussen de borst en de thoraxrand goed te zien is
- a. Ga naar het tabblad *Design*, te vinden in het rood in de tweede horizontale werkbalk
  - b.  Klik op het icoon wat hoort bij *Extrude*
  - c. Klik hier op *Entities* en selecteer het contour dat u op de achterkant van uw mal ziet als grens tussen borst en thoraxwand. De naam van deze contour is nu zichtbaar bij *Entities*
  - d. Zorg voor de volgende instellingen:

- i. *Solid* staat uit
    - ii. Kies voor de *Direction* een richting die voor elk punt gunstig is. Dit is een uitdaging omdat het een soort cirkel is, dus probeer verschillende dingen. Begin als uitgangspunt met een richting alleen in de negatieve z-richting (0,0,-1). Evalueer aan het contour of er nog veel rood te zien is. Rode stukken geven aan dat hier geen randje gevormd gaat worden. Probeer dan de z-richting iets te verminderen en ook een beetje de y-richting op te gaan. Voor het mooiste resultaat moet u een richting vinden waarbij het hele contour geel gekleurd is
    - iii. Kies voor *Depth* 2 mm
    - iv. *Draft angle* en *Draft outwards* mogen op nul / uit
  - e. Klik op *Apply*. Er is nu een nieuw object ontstaan, wat het opstaand randje is. Dit randje heeft nu nog geen dikte
  - f.  Geef het randje een dikte door weer op *Uniformal offset* te klikken
  - g. Selecteer als *Entities* het nieuw gevormde object, wat je randje is
  - h. Gebruik dezelfde instellingen als bij het verdikken van de mal, alleen gebruik nu al *Distance* van 0.5 mm
4. Voeg nu het gemaakte randje toe aan uw mal, zodat het één geheel wordt
- a. Ga naar het tabblad *Design*, te vinden in het rood in de tweede horizontale werkbalk
  - b.  Klik op het icoon wat hoort bij *Boolean Union*
  - c. Selecteer als *Entities* het object wat uw mal is en het object wat uw zelfgemaakte opstaande randje is. Beide verschijnen nu bij *Entities*
  - d. Klik op *Apply*. Er kan eventueel een waarschuwing komen die waarschuwt over 'bad edges', maar dat kan u negeren. U heeft nu een nieuw object, waarbij uw mal compleet is
5. Als laatste moet uw mal gecontroleerd worden op fouten. Als er veel fouten zijn is de kans groter dat die print mislukt
- a. Ga naar het tabblad *Fix*, te vinden in het blauw in de tweede horizontale werkbalk
  - b.  Klik op het icoon wat hoort bij *Fix wizard*. Er verschijnt nu een pop-up venster
  - c. Zorg ervoor dat uw object geselecteerd is. Dit kunt u controleren in het venster bij *Selection – Part*. Als dit leeg is moet u in het hoofdscherm uw object selecteren. De naam van uw object verschijnt dan in het venster, bij *Part*
  - d. Zorg ervoor dat het vinkje *Full analysis* aanstaat


- e. Boven in het venster ziet u *Advice* met in het geel een tekst erbij. Dit advies helpt u door de Fix Wizard. Klik op *Follow advice*, nu volgt het programma het advies zelf op. Allereerst controleert hij op er fouten in het object aanwezig zijn. Dit laat hij zien aan groene en rode getallen bij *# detected*.
  - f. Als er errors aanwezig zijn zal hij adviseren om naar de fout op te lossen. U kunt dit doen door te klikken op *Follow advice*. Het kan zijn dat alles groen is. Dan is het object goed en bent u klaar met deze stap.
  - g. Als hij een fout vindt en wil oplossen, zal hij nu een advies geven om iets uit te voeren. U klikt wederom op *Follow advice*, om dit uit te voeren. Als het goed is heeft het programma nu een specifiek probleem opgelost.
  - h. Het nieuwe advies is om terug te gaan naar *Diagnotics* om te zien wat de volgende stap is. U kunt hiervoor wederom op *Follow Advice klikken*
  - i. Blijf dit herhalen tot er geen rode getallen meer zijn en het programma tevreden is. Soms zijn er fouten die de fix wizard er niet uitkrijgt. Probeer hierbij zelf te beoordelen of dit acceptabel is om toch te printen
6. Uw mal is nu zo goed als klaar. Ga verder naar het hoofdstuk *Afronden* om de laatste stappen te doorlopen

Mal 2: Mal met cilinder gaten




Resultaat na het doorlopen van alle stappen van mal 2, de mal met cilinder gaten. Links ziet u de voorkant, rechts ziet u de achterkant, inclusief opstaand randje


Om de gaten in de mal te maken, maakt u gebruik van een schets. U maakt eerst de cirkels in 2D, waarna ze geprojecteerd worden op de mal.

1. Allereerst moeten een sketch openen waarop de cirkels getekend moeten worden
  - a.  Ga naar het tabblad *Sketch*, te vinden in het rood in de tweede horizontale werkbalk
  - b. Klik op het icoon wat hoort bij *New*




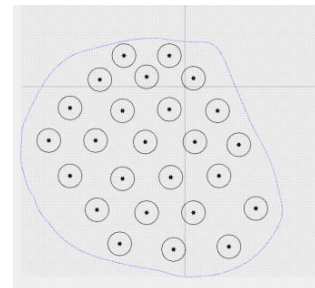
- i. Kies voor *Method* de *Fit plane*
- ii. Kies als *Fitting entities* uw object

- c.  Het is belangrijk dat uw sketch achter uw mal uitkomt. Ga hiervoor naar het tabblad *Align*, en selecteer *Interactive Translate*
- i. Selecteer als *Main entity* uw sketch
  - ii. Laat voor de rest alle parameters zoals ze zijn
  - iii. Klik op de blauwe pijl die u ziet en beweeg daarmee uw sketch naar achteren (in de negatieve z-richting). Zorg ervoor dat de schets netjes vlak achter uw mal uitkomt

- d.  Ga nu terug naar het tabblad *Sketch* en selecteer *Import References to Sketch*
- i. Selecteer als *Selection* uw sketch
  - ii. Selecteer bij *Projection* uw curve die de afscheiding is tussen borst en thoraxwand
  - iii. Selecteer *Apply*. Als u nu op de sketch klikt, naast het tabblad *Word Area*, ziet u uw 2D sketch met uw curve erop getekend


2. U kunt nu beginnen met het tekenen van de cirkels. Het patroon, de grootte en het aantal mag u zelf bepalen, houdt alleen in de gaten dat de mal stevig genoeg moet zijn. Te veel cirkels dicht bij elkaar kan de mal verzwakken. De onderstaande stap doet u in het tabblad "*Uw Sketch naam*", te vinden naast het tabblad *Workplace*. Hier ziet u uw mal niet meer, maar een 2D tekening.

- a.  Ga weer terug naar het tabblad *Sketch* en selecteer *Create cirkel*. Let er bij de instellingen vooral op dat de *Enabled* en *Equal radius* aan staat, voor gelijke grootte van de cirkels
- b. Teken nu de cirkels die u wilt hebben op uw mal. Zorg ervoor dat u niet buiten de projectie komt van uw contour. Let erop dat de cirkels groot genoeg zijn om met de vingers de lap te kunnen manipuleren

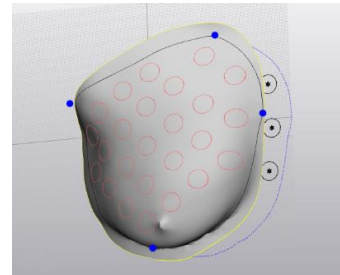


Voorbeeld van een sketch van de mal met cirkels

3. Nu kunt u de getekende cirkels projecteren op uw mal. Ga hiervoor terug naar de *Work Area*, waar u uw mal weer ziet

- a.  Ga naar het tabblad *Curve* en selecteer de optie *Project curve*

- i. Selecteer als *Entities* uw schets en selecteer als *Target entities* uw mal
- ii. Als *Direction* wilt u dezelfde richting als de schets. Selecteer hiervoor *Direction* en vouw in uw *Object*

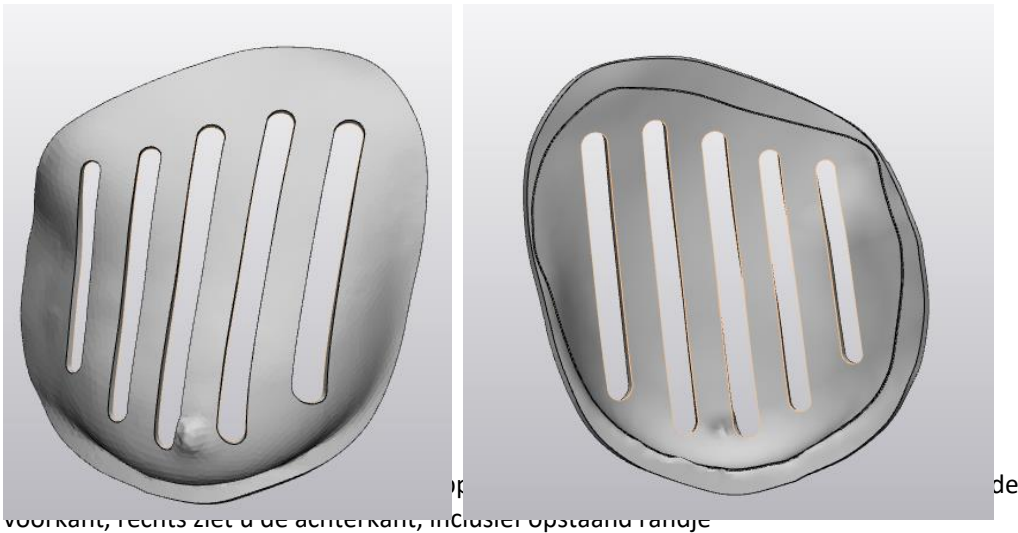


- Tree uw schets uit. Klik dan op het plusje naast de *Object Coordinate System* en selecteer de *Z-axis*. Het gele pijltje in het midden van uw schets zal nu loodrecht op de schets moeten staan, wijzend naar de mal
- iii. Zorg dat de vinkjes bij *Project through*, *Attach curve* en *Split surfaces* aan staan
  - iv. Selecteer *Apply*. U moet nu de cirkels op de mal terugzien




Voorbeeld van de geprojecteerde cirkels op de mal

4. Nu moeten de cirkels nog van de mal afgehaald worden. U kunt ondertussen uw schets verbergen, aangezien u deze niet meer nodig zult hebben
  - a. Zorg ervoor dat in de *Object Tree* uw mal uitgevouwen is, door op het plusje naar de naam van de mal te klikken. Vouw dan de bijbehorende *Surface List* uit
  - b. U ziet nu dat elke geprojecteerde cirkel een nieuwe surface heeft gemaakt. Als u op één van de surfaces klikt kunt u op uw mal in het groen zien welke gedeelte daarbij hoort. Vind nu de surfaces die bij de cirkels horen
  - c. Selecteer al deze surfaces tegelijk en verplaats ze naar een nieuw object. Dit doet u door met uw rechtermuisknop erop te klikken → *Seperate* → *Move to Part* → *Create New*. Onderin de *Object Tree* ziet u nu een nieuw object, wat uit alle cirkels bestaat
  - d. Klik met uw rechtermuisknop op dit object en verberg het door op *Hide* te klikken. U heeft nu een mal met gaten
5. Volg nu alle stappen van *Mal 1: Basis mal* op de mal verder af te maken


### Mal 3: Mal met gleuven

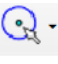


Om de gleuven in de mal te maken, maakt u gebruik van een schets. U maakt eerst de gleuven in 2D, waarna ze geprojecteerd worden op de mal.

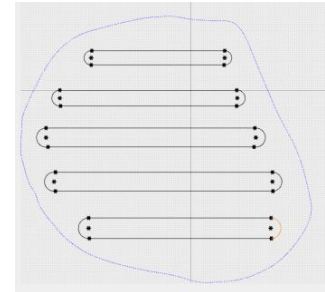
1. Allereerst moeten een sketch openen waarop de cirkels getekend moeten worden
  - a.  Ga naar het tabblad *Sketch*, te vinden in het rood in de tweede horizontale werkbalk
  - b. Klik op het icoon wat hoort bij *New*
    - i. Kies voor *Method de Fit plane*
    - ii. Kies als *Fitting entities* uw object
  - c.  Het is belangrijk dat uw sketch achter uw mal uitkomt. Ga hiervoor naar het tabblad *Align*, en selecteer *Interactive Translate*
    - i. Selecteer als *Main entity* uw sketch
    - ii. Laat voor de rest alle parameters zoals ze zijn
    - iii. Klik op de blauwe pijl die u ziet en beweeg daarmee uw sketch naar achteren (in de negatieve z-richting). Zorg ervoor dat de schets netjes vlak achter uw mal uitkomt
  - d.  Ga nu terug naar het tabblad *Sketch* en selecteer *Import References to Sketch*
    - i. Selecteer als *Selection* uw sketch
    - ii. Selecteer bij *Projection* uw curve die de afscheiding is tussen borst en thoraxwand
    - iii. Selecteer *Apply*. Als u nu op de sketch klikt, naast het tabblad *Word Area*, ziet u uw 2D sketch met uw curve erop getekend

2. U kunt nu beginnen met het tekenen van de gleuven. De grootte en het aantal mag u zelf bepalen, houdt alleen in de gaten dat de mal stevig genoeg moet zijn. Te veel gleuven te dicht bij elkaar kan de mal verzwakken. De onderstaande stap doet u in het tabblad “Uw Sketch naam”, te vinden naast het tabblad *Workplace*. Hier ziet u uw mal niet meer, maar een 2D tekening.


- a.  Ga terug naar het tabblad *Sketch* en selecteer *Create line*
- Zoek met behulp van de projectie op de schets uit welke richting (horizontaal of verticaal) u de gleuven wilt hebben
  - Zorg ervoor dat bij de instellingen de vinkjes aanstaan bij *Enabled*, *Horizontal* of *Vertical*, *Parallel* en *Equal Length*, voor het mooiste resultaat
- b. Teken nu met de lijnen hoe u de gleuven wilt hebben op uw mal. Zorg ervoor dat u niet te dicht bij de projectie komt van uw contour, aangezien er nog halve cirkels aan moeten worden toegevoegd om de gleuven te sluiten

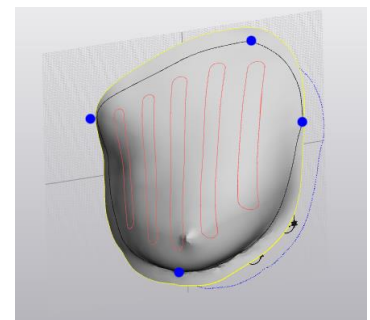
- c.  Klik nu op het drop down menu van *Create cirkel* in het tabblad *Sketch* en selecteer *Create Arc (3 points)*

- Zorg ervoor dat bij de instellingen de vinkjes aanstaan bij *Enabled*, *Snap to point*, *Equal Radius* en *Tangent*, voor het mooiste resultaat
- Selecteer als eerste twee punten de twee uiteindes van twee lijnen die samen één gleuf vormen
- Probeer het derde punt tussen de eerste twee punten te krijgen, zodat er een halve cirkel ontstaat



3. Nu kunt u de getekende gleuven projecteren op uw mal. Ga hiervoor terug naar de *Work Area*, waar u uw mal weer ziet

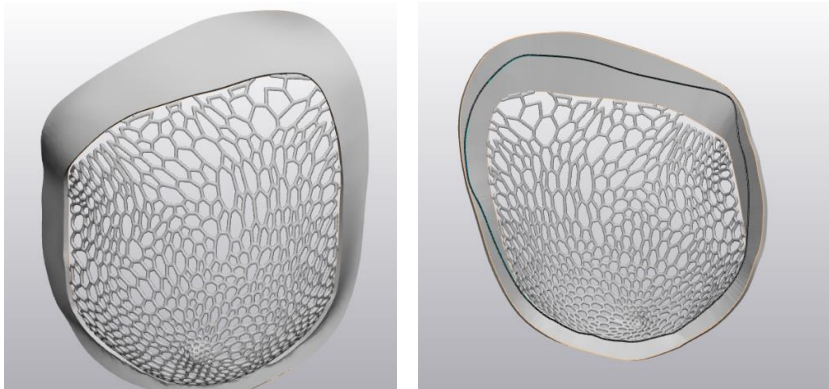
- a.  Ga naar het tabblad *Curve* en selecteer de optie *Project curve*
- Selecteer als *Entities* uw schets en selecteer als *Target entities* uw mal
  - Als *Direction* wilt u dezelfde richting als de schets. Selecteer hiervoor *Direction* en vouw in uw *Object Tree* uw schets uit. Klik dan op het plusje naast de *Object Coordinate System* en selecteer de *Z-axis*. Het gele



Voorbeeld van de geprojecteerde cirkels op de mal

- pijlte in het midden van uw schets zal nu loodrecht op de schets moeten staan, wijzend naar de mal
- iii. Zorg dat de vinkjes bij *Project through*, *Attach curve* en *Split surfaces* aan staan
  - iv. Selecteer *Apply*. U moet nu de gleuven op de mal terugzien
4. Nu moeten de gleuven nog van de mal afgehaald worden. U kunt ondertussen uw schets verbergen, aangezien u deze niet meer nodig zult hebben
- a. Zorg ervoor dat in de *Object Tree* uw mal uitgevouwen is, door op het plusje naar de naam van de mal te klikken. Vouw dan de bijbehorende *Surface List* uit
  - b. U ziet nu dat elke geprojecteerde gleuf een nieuwe surface heeft gemaakt. Als u op één van de surfaces klikt kunt u op uw mal in het groen zien welke gedeelte daarbij hoort. Vind nu de surfaces die bij de gleuven horen
  - c. Selecteer al deze surfaces tegelijk en verplaats ze naar een nieuw object. Dit doet u door met uw rechtermuisknop erop te klikken → *Seperate* → *Move to Part* → *Create New*. Onderin de *Object Tree* ziet u nu een nieuw object, wat uit alle gleuven bestaat
  - d. Klik met uw rechtermuisknop op dit object en verberg het door op *Hide* te klikken. U heeft nu een mal met gleuven
5. Volg nu alle stappen van *Mal 1: Basis mal* op de mal verder af te maken

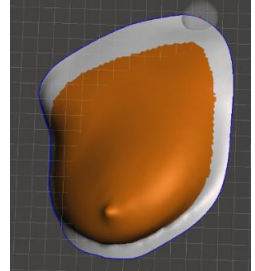
Mal 4: Mal met Voronoi patroon



Resultaat na het doorlopen van alle stappen van mal 4, de mal met Voronoi patroon. Links ziet u de voorkant, rechts ziet u de achterkant, inclusief opstaand randje

Om het Voronoi patroon te maken is het programma Meshmixer nodig. Om deze mal te maken moet u bij sommige stappen meerdere dingen proberen om tot een goed resultaat te komen, een goed resultaat is dus ook afhankelijk van een eigen goede beoordeling. **Let op:** Bij het maken van het Voronoi patroon komt het geraamte iets naar de binnenkant van de mal. Dit betekent dat het volume van de borstmal iets veranderd, wat zeer onwenselijk is. Daarom wordt het voor nu afgeraden om dit patroon te gebruiken voor een borstmal

1. Allereerst moet u uw mal exporten als STL-file, om het te kunnen gebruiken in Meshmixer
  - a. Klik op *File* in de eerste horizontale werkbalk
  - b. Klik dan op *Export* → *STL*
  - c. Selecteer als *Entities* uw mal. U kunt eventueel in de *Object Tree* uw mal de naam geven waarmee u hem wilt opslaan
  - d. Zorg dat de *Output Directory* een plek is waar u uw mal makkelijk in kan terugvinden
  - e. Klik op *Apply*. Uw mal is nu geëxporteerd als STL-bestand



2. Open nu Meshmixer. Hierin gaat u het Voronoi patroon maken. Als eerste wilt u uw mal in tweeën verdelen, een deel wat de rand is (de thoraxwand) en een deel wat de borst is

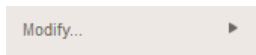
- a. Selecteer *New* en open uw zojuist gemaakte STL-bestand



- b. Selecteer *Select*. U kunt nu met de brush het gedeelte selecteren wat bij de borst hoort. Zorg dat u het helemaal inkleurt

Voorbeeld van een geselecteerde borst in Meshmixer

- i. De instellingen zouden direct goed moeten staan. Gebruik de *Sphere Brush* en kies een *Size* die u zelf prettig vindt werken
- ii. Let goed op dat u niks selecteert wat bij de thoraxwand hoort. Als u dit wel doet, kan uiteindelijk de mal niet gemaakt worden. Gebruik uw mal in 3-matic eventueel als guideline. Het geeft niet als u iets te weinig van uw borst selecteert



- c. Als u tevreden bent over uw selectie kunt u de begrenzing gladder maken. Dit doet u door bovenin *Modify* → *Smooth Boundry* te selecteren

- i. Kies paramters waar u zelf tevreden over bent. In principe zijn de standaard waarden al goed
- ii. Zorg dat er vinkjes aanstaan bij *Preserve Mesh Boundary*, *Preserve Group Borders* en *Create New Groups*
- iii. Selecteer *Accept* als u tevreden bent





- d. Nu kunt u de borst van de rand losmaken door bovenin op *Edit* → *Seperate* te klikken

- i. Er verschijnt nu een klein pop-up venster *Object Browser*. Zorg ervoor dat u het object hebt geselecteerd dat hoort bij de borst


3. Nu kan het Voronoi patroon gemaakt worden. Op het moment heeft het object nog te veel driehoeken, waardoor er geen mooi patroon uitkomt. Daarom moet u deze eerst verminderen. In

dit protocol wordt uitgegaan van een beginhoeveelheid van 10.000 driehoeken. Dit kunt u voor uw eigen object terugvinden in 3-Matic, bij *Properties* als u uw mal hebt geselecteerd

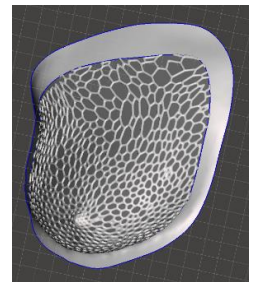
a.  Selecteer weer *Select*. Klik op control + a om de gehele borst te selecteren. De rand is dus niet geselecteerd

b.  Klik op *Edit* → *Reduce*. De parameters staan in principe hier ook goed

- i. Zorg ervoor dat de vinkjes aan staan bij *Preserve Boundaries* en *Preserve Group Boundaries*
- ii. Klik op *Accept*. In principe ziet u weinig veranderen
- iii. Herhaal dit nog een keer, voor extra reductie van de driehoeken

c.  Selecteer nu *Edit* in de verticale werkbalk. Kies *Make Pattern*

- i. Kies als *Pattern Type* de optie *Dual Edges*
- ii. Met de *Element Dimens* kunt u de dikte van het geraamte bepalen
- iii. Het is niet nodig om iets te doen met de overige parameters
- iv. U moet nu zelf beslissen of u tevreden bent. Er zijn verschillende opties:








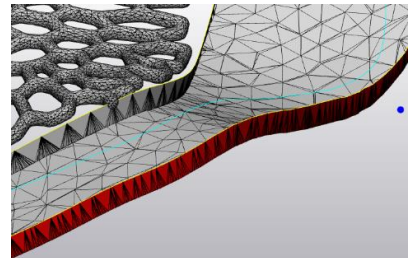
1. Na het klikken op *Dual Edges* loopt het programma vast. U hebt dan nog te veel driehoeken. Ga terug naar het begin van stap 3 en herhaal dit tot u wel een Voronoi patroon krijgt waar u tevreden over bent
2. Het Voronoi patroon dat is ontstaan is te dicht. U moet dan nog een keer het aantal driehoeken verminderen en het dan opnieuw proberen. Herhaal dit tot u tevreden bent
3. Het Voronoi patroon is te grof, de gaten zijn te groot. Het aantal driehoeken is dan te laag. U moet dan uw laatste *Reduce* ongedaan maken. Eventueel kunt u het percentage bij *Reduce* aanpassen om een kleiner aantal driehoeken te verwijderen
4. U bent tevreden over het Voronoi patroon. Klik dan op *Accept*

Voorbeeld van een goed Voronoi patroon in Meshmixer

4. U bent nu klaar is Meshmixer. U moet nu uw mal weer exporten en openen in 3-Matic

a. Selecteer allereerst het object dat bij het Voronoi patroon hoort en het object wat de rand is in de *Object Browser*. Er is een derde object, wat het originele borstobject was. Deze hoeft u niet te selecteren


- b.  Selecteer *Export* in de verticale werkbalk. Sla het bestand op waar u hem weer makkelijk kan terugvinden
- c.  Open nu weer 3-Matic. Als het goed is heeft u de gesegmenteerde mal nog open staan. Klik op *Import Part* in de verticale werkbalk. Selecteer hier uw mal met Voronoi patroon. Ze worden nu beide laten zien
5. Allereerst moet u controleren of uw Voronoi patroon niet over de grens tussen borst en thoraxwand komt. Hiervoor hebben we de curve die deze grens aangeeft nodig
- a. Ga naar het tabblad *Curve*, te vinden in het rood in de tweede horizontale werkbalk
- b.  Klik op het icoon wat hoort bij de optie *Convert to Curve*
- i. Selecteer als *Entities* nu de curve op de gesegmenteerde borst die de grens tussen borst en thoraxwand aangeeft
- ii. Zorg dat het vinkje bij *Create New Part* aanstaat
- iii. U hoeft niks te veranderen aan de *Accuracy*
- iv. Selecteer *Apply*. U heeft nu een nieuw object in uw *Object Tree* wat bij de curve hoort
- c. U kunt nu het object wat bij de gesegmenteerde borst hoort verbergen. Dit doet u door op dit object, in de *Object Tree*, met uw rechtmuisknop te klikken en op *Hide* te klikken. U houdt nu een mal over met Voronoi patroon en de curve
- d. Controleer nu of het Voronoi patroon niet over de curve komt. Als dit wel zo is moet u opnieuw in Meshmixer beginnen
6. Als alles er netjes uitziet kunt u verder gaan. De rand van de mal moet nog een dikte krijgen om het te kunnen printen
- a. Ga naar het tabblad *Fix*, te vinden in het blauw in de tweede horizontale werkbalk
- b.  Zorg ervoor dat u het oppervlak van de rand geselecteerd hebt en selecteer *Invert normal*. De buitenkant van de rand moet nu rood zijn
- c. Ga naar het tabblad *Design*, te vinden in het rood in de tweede horizontale werkbalk
- d.  Klik op het icoon wat hoort bij *Uniform offset*
- i. Selecteer als *Entities* alleen de oppervlakte van de rand van de mal
- ii. Kies *Internal Uniform Offset*






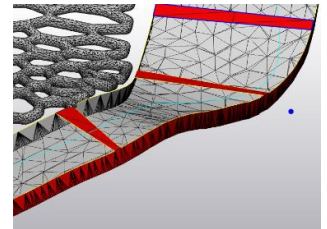
- iii. Kies een distance van 3 mm
- iv. *Preserve Sharp features* mag uit staan, zorg dat *Solid* Resultaat van Internal Uniform Offset bij het Voronoi patroon, aanstaat
- v. Houdt hierbij goed de binnenkant in de gaten. Als het goed gaat ziet de rand er aan de binnenkant uit zoals hiernaast

e. Ga naar het tabblad *Fix*, te vinden in het blauw in de tweede horizontale werkbalk


f.  Klik op het icoon wat hoort bij *Reduce*. Selecteer weer alleen het oppervlak van de buitenrand als *Entities*

- i. De overige instellingen hoeven niet veranderd te worden. U kunt op *Apply* klikken

g.  De wand heeft nu nog geen dikte. Dit kunnen we verhelpen met het maken van verschillende bruggen. Klik op *Create bridges*, te vinden in het *Fix* tabblad



- i. Maak nu een klein aantal bruggen tussen de twee uitstekende randjes aan de binnenkant. Een stuk of 5 zou al genoeg moeten zijn





h.  Klik nu op de *Fix Wizard*, te vinden bij het tabblad *Fix*. Er verschijnt een pop-up venter

Een voorbeeld van het gebruik van *Create Bridges* bij het Voronoi patroon, gekeken

- i. Selecteer als *Part* het hele object wat bij uw Voronoi patroon hoort
- ii. Zorg ervoor dat het vinkje *Full analysis* aanstaat
- iii. In het geel kunt u het advies vinden, hoe u het object het beste kan verbeteren. Door op het knopje *Follow Advice* te klikken, volgt hij automatisch zijn eigen advies op. U moet meerdere malen op dit knopje klikken, ideaal gezien tot alle getallen groen zijn
- iv. Blijf tijdens het doorklikken goed uw mal in de gaten houden. In principe moet het goed gaan, maar soms lost het programma fouten op de verkeerde manier op
- v. Waarschijnlijk zullen er altijd wat *Overlapping triangles* of andere fouten blijven. Zolang dit er niet heel veel zijn is dit geen probleem

7. Als het goed is, is de binnenrand nu helemaal dicht. Uw mal is nu bijna klaar, het moet alleen nog een opstaand randje krijgen waar de grens tussen borst en thoraxwand is, zodat die ook na het printen nog zichtbaar is. Hiervoor gaan we de curve gebruiken die u in stap 5 als nieuw object hebt gecreëerd. U zult nu ook zien dat de curve deels verdwijnt in de mal zelf. Dit bevestigt dat deze manier van het maken van een mal het volume van de borst beïnvloed.

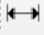
- a. Ga naar het tabblad *Design*, te vinden in het rood in de tweede horizontale werkbalk

- b.  Klik op het icoon wat hoort bij *Extrude*
- c. Klik hier op *Entities* en selecteer het contour dat u op de achterkant van uw mal ziet als grens tussen borst en thoraxwand. De naam van deze contour is nu zichtbaar bij *Entities*
- d. Zorg voor de volgende instellingen:
- Solid* staat uit
  - Kies voor de *Direction* een richting die voor elk punt gunstig is. Dit is een uitdaging omdat het een soort cirkel is, dus probeer verschillende dingen. Begin als uitgangspunt met een richting alleen in de negatieve z-richting (0,0,-1). Evalueer aan het contour of er nog veel rood te zien is. Rode stukken geven aan dat hier geen randje gevormd gaat worden. Probeer dan de z-richting iets te verminderen en ook een beetje de y-richting op te gaan. Voor het mooiste resultaat moet u een richting vinden waarbij het hele contour geel gekleurd is
  - Kies voor *Depth* 2 mm
  - Draft angle* en *Draft outwards* mogen op nul / uit
- e. Klik op *Apply*. Er is nu een nieuw object ontstaan, wat het opstaand randje is. Dit randje heeft nu nog geen dikte
- f.  Geef het randje een dikte door weer op *Uniform offset* te klikken
- g. Selecteer als *Entities* het nieuw gevormde object, wat je randje is
- h. Gebruik dezelfde instellingen als bij het verdikken van de mal, alleen gebruik nu al *Distance* van 0.5 mm
8. Voeg nu het gemaakte randje toe aan uw mal, zodat het één geheel wordt
- Ga naar het tabblad *Design*, te vinden in het rood in de tweede horizontale werkbalk
  -  Klik op het icoon wat hoort bij *Boolean Union*
  - Selecteer als *Entities* het object wat uw mal is en het object wat uw zelfgemaakte opstaande randje is. Beide verschijnen nu bij *Entities*
  - Klik op *Apply*. Er kan eventueel een waarschuwing komen die waarschuwt over 'bad edges', maar dat kan u negeren. U heeft nu een nieuw object, waarbij uw mal compleet is
9. Nu moet u nog een laatste controle doen om eventuele fouten uit uw mal te halen.
-  Ga weer terug naar de *Fix Wizard*, te vinden onder het tabblad *Fix*
  - Ga alle stappen opnieuw door om de laatste fouten uit uw mal te halen
10. Uw mal is nu klaar. U kunt door naar het volgende hoofdstuk Afronden voor de laatste stappen voor het printen

## Hoofdstuk 5: Afronden


Uw mal is nu klaar. Voor de afronding kunt u nog labels aan de mal toevoegen voor meer informatie. Denk hierbij aan afmetingen van de mal, het patiëntnummer en landmarks. Als u afmetingen wilt toevoegen, moet u eerst weten wat de afmetingen zijn.

### Afmetingen vinden van de mal

1. Ga naar het tabblad *Measure*, te vinden in het geel in de tweede horizontale werkbalk
2.  Klik op het icoon wat hoort bij *Distance*
3. Neem voor de hoogte van de borst als eerste punt de eerder gemaakte *Upper Breast Point (UBP)* en als tweede punt de *Lower Breast Points (LBP)*. U ziet nu een blauwe lijn verschijnen met in het midden een geel blokje met een getal erin. Dat is de afstand in millimeters
4. Doe hetzelfde voor de breedte van de borst. Neem hiervoor als eerste punt het *Sternum Point (SP)* en als tweede punt het *Axilair Point (AP)*. U heeft nu de twee afmetingen

Nu kunt u deze afmetingen en andere gegevens op de mal zetten. Als u een landmark op de mal wilt zetten, gebruik dan een 'o' om het punt te markeren. Voorbeeld tekst: 'o Axilair point'. Als u de 'o' dan precies plaatst waar diezelfde landmark op uw mal zit, zal die landmark na het printen nog duidelijk zichtbaar zijn.


### Label toevoegen

1. Ga naar het tabblad *Finish*, te vinden in het rood in de tweede horizontale werkbalk
2.  Klik op het icoon wat hoort bij *Quick label*
  - a. Selecteer als *Method* de optie *Tekst*
  - b. Zorg dat de *Direction* op *Globally perpendicular to surface* staat
  - c. Noteer in het vakje *Text* de tekst die u wil opschrijven
  - d. Kies dan eventuele overige instellingen zoals lettertype en tekstgrootte. Zorg ervoor dat de tekst niet te klein wordt, anders is het mogelijk niet goed leesbaar na het printen
  - e. Als u tevreden bent over de instellingen, selecteert u *Apply*
3. Als u nu met uw muis over de *Work Area* beweegt, ziet u uw tekst in het rood rond bewegen. Kies de plek waar u uw tekst wilt hebben en bevestig dat dan met een linker muisklik
  - a. Let erop dat het label aan de voorkant komt, zodat het volume aan de achterkant niet veranderd

- b. Als u control vasthoudt bij het klikken, dan wordt de tekst in de mal gedrukt, in plaats van erop geplaatst. Dit geeft vaak een mooier resultaat en voorkomt scherpe uitsteeksels

Uw mal is nu helemaal klaar. U hoeft het nu alleen nog maar te exporteren om te printen. Doe eventueel nog een laatste controle met *Fix Wizard* en controleer dat de mal nu uit één object bestaat

Mal exporteren als STL-bestand

1.  Selecteer in de eerste horizontale werkbalk *File* → *Export* → *STL*
2. Selecteer als *Entities* het object waar uw mal uit bestaat. Bij *Output directory* ziet u in welke map het bestand wordt opgeslagen
3. Klik op *Apply*. U heeft nu uw mal opgeslagen als STL-bestand. Deze kunt u nu importeren in de software die hoort bij uw 3D printer



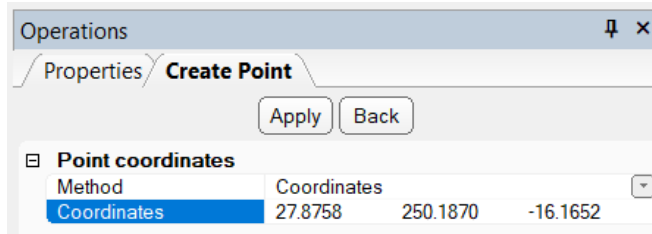
## PROTOCOL 3:

# BEPALING VAN DE ROI IN 3-MATIC AHV 3D FOTO'S

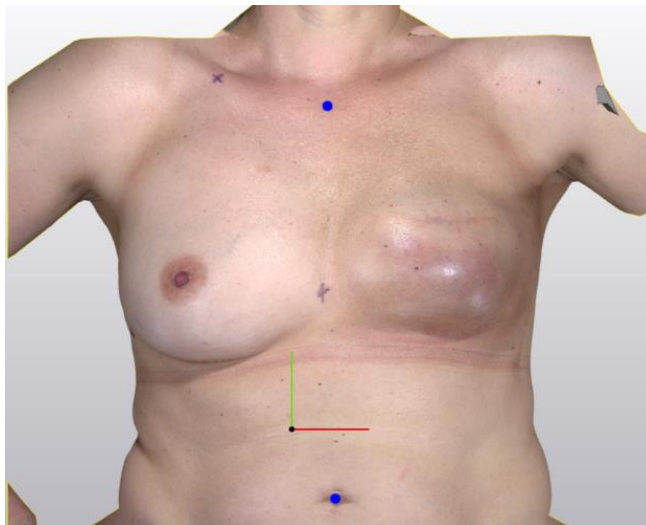
Kuipers, T. van

## Stappen bepaling Region of interest (ROI)

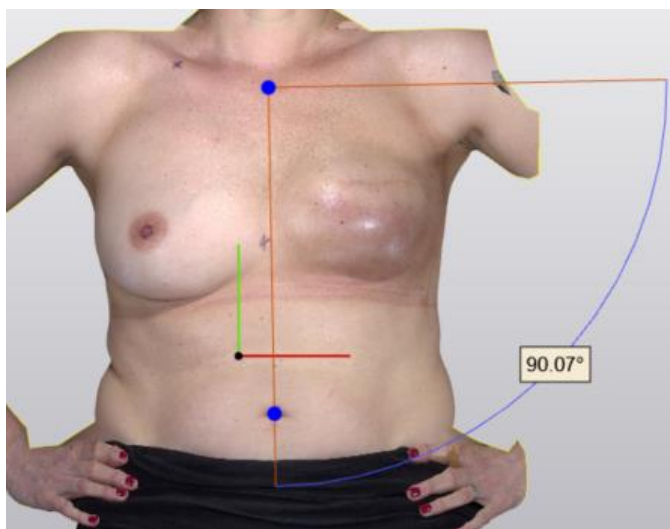
1. Zet een punt op de *Jugular notch* en het midden van de *navel*. Door de gaan naar het menu *Design* → *Create Analytical Primitive* → *Create Point*. Selecteer als *Method Coordinates* en klik daarna onder het vakje *Method* op het vakje *Coordinates*.



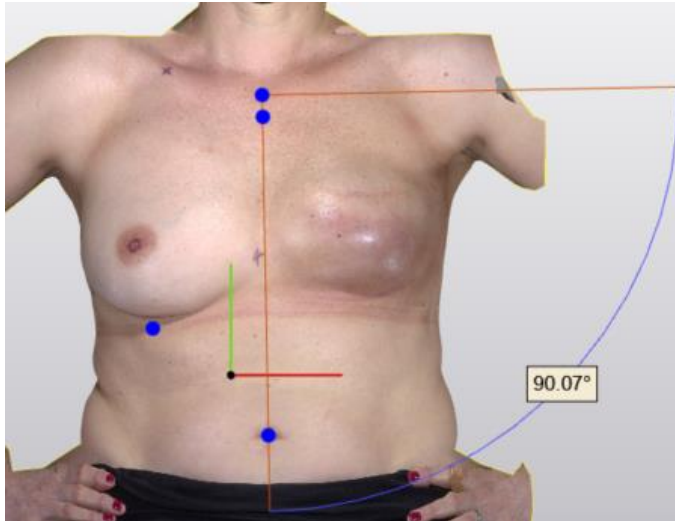
2. Klik op de *Jugular Notch* en selecteer *Triangle Node*. Klik daarna links rechts in het *Operations* menu op *Apply*. Ga hetzelfde te werk voor de *navel*. *Cancel* nu de *Operation*, als het goed is zijn er nu twee blauwe stippen zoals in onderstaande figuur.



3. Meet nu een hoek van 90 graden uit met *Measure* → *Angle*. De eerste klik zet je op het punt vanuit waar je wil meten, de tweede wordt het draaipunt van de hoek. Meet *90 graden* uit. De lijn van navel naar *Jugular Notch* zal de *Midline* van het lichaam zijn.

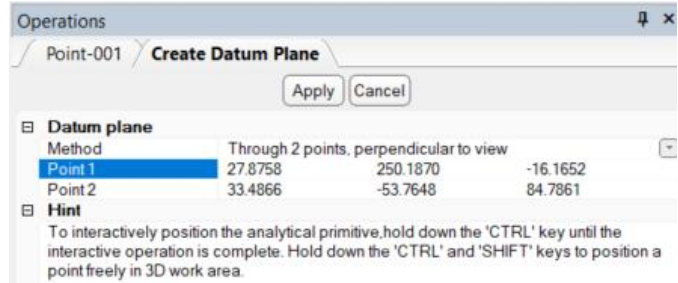


4. Zet 2 centimeter onder de *Jugular Notch* nog een punt zoals in stap 1 op de *Midline*. Zet daarna 1 centimeter onder het laagste punt van de borst een punt. Neem hiervoor de borst die het laagst hangt.

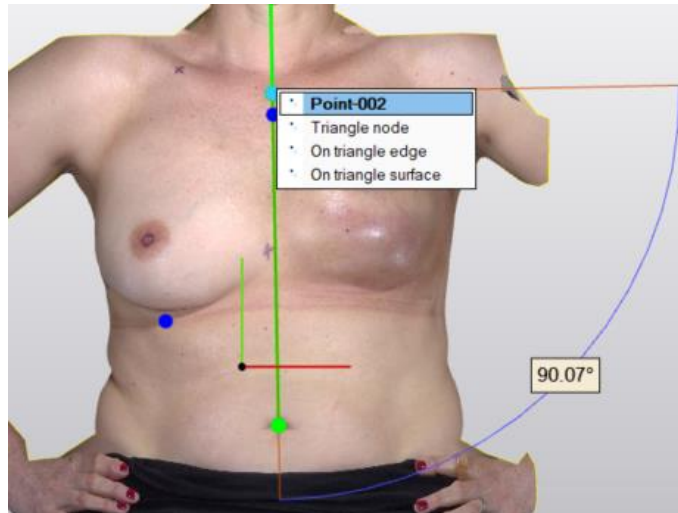


5. Met behulp van zogenoemde Datumplanes gaat de ROI links en rechts bepaald worden. Ga naar *Design* → *Create Analytical Primitive* → *Create Datum Plane*. Selecteer rechtsonder als *Method* → *Through 2 points, perpendicular to view*.  
Selecteer voor point 1 het *jugular notch punt*. Dit doe je door in het operations menu rechtsonder point 1 te selecteren (afbeelding 1) en daarna precies op de punt te gaan staan op het object (afbeelding 2).  
Voor point 2, het punt van de *navel*, herhaal je bovenstaande stappen, alleen selecteer je nu de navel.  
De *Datumplane* over de *Midline* is nu gevormd (afbeelding 3). Doe hetzelfde voor point 2. Druk op *Apply*, de *Midline Plane* is gevormd.

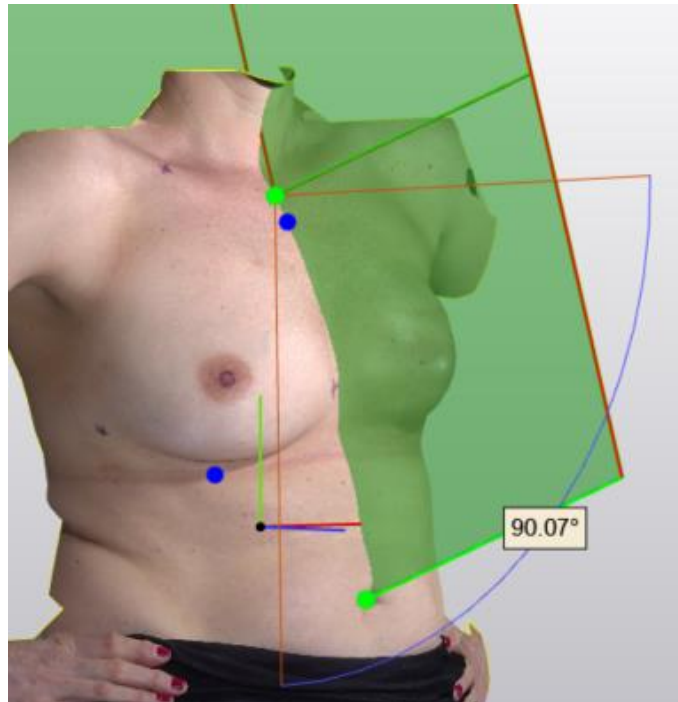
Afbeelding 1: Operation menu



Afbeelding 2: Selecteren van het punt.


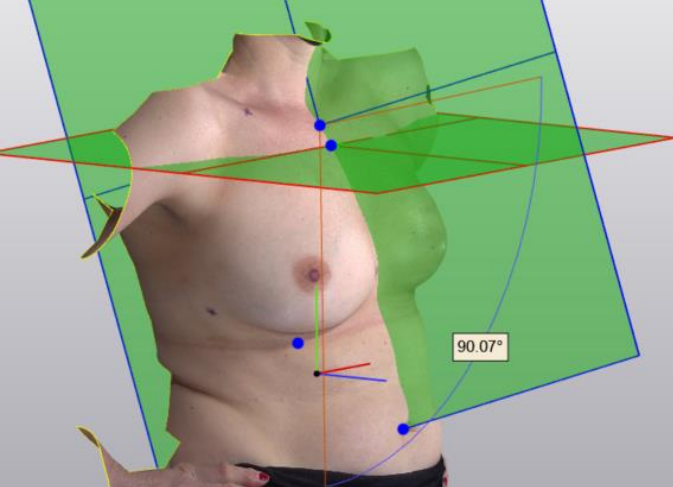
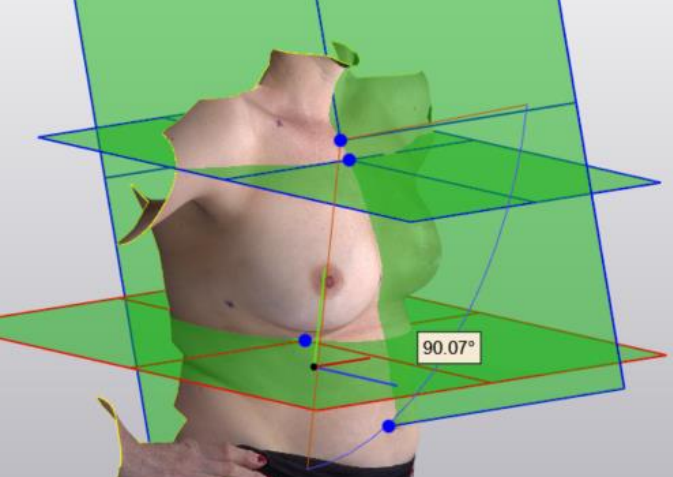


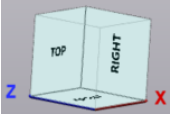
Afbeelding 3: Datumplane ingevoegd


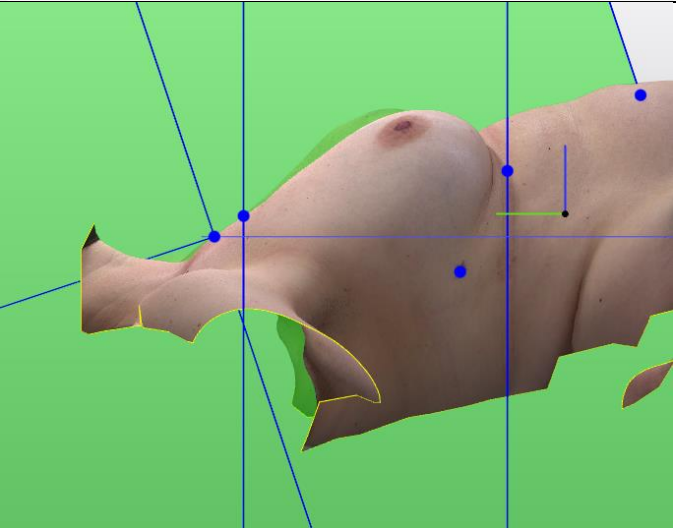
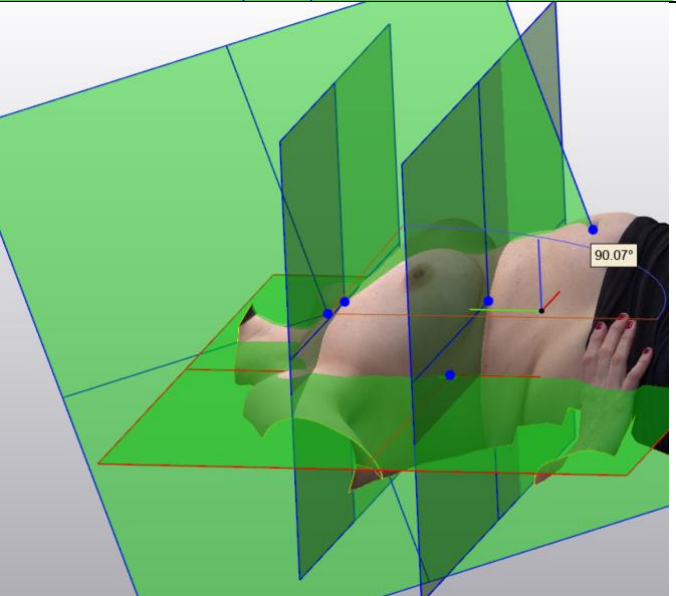




6. Nu gaan we een *Datumplane* maken loodrecht op die van de *Midline* op het punt onder de *jugular notch* en die van het *laagste borstpunt*. Ga naar *Design* → *Create Analytical Primitive* → *Create Datum Plane*. Selecteer rechtsonder als *Method* → *Normal and origin*. Selecteer voor *Normal* 0 – 1 – 0 (normaal in de y-richting). Voor *Origin* kun je het punt 2 cm onder de *jugular notch* selecteren. Druk op *Apply*. Eventueel kan het vlak groter gemaakt worden door het *Datumplane* te selecteren en in het *Operation menu* de delta x en delta y aan te passen.

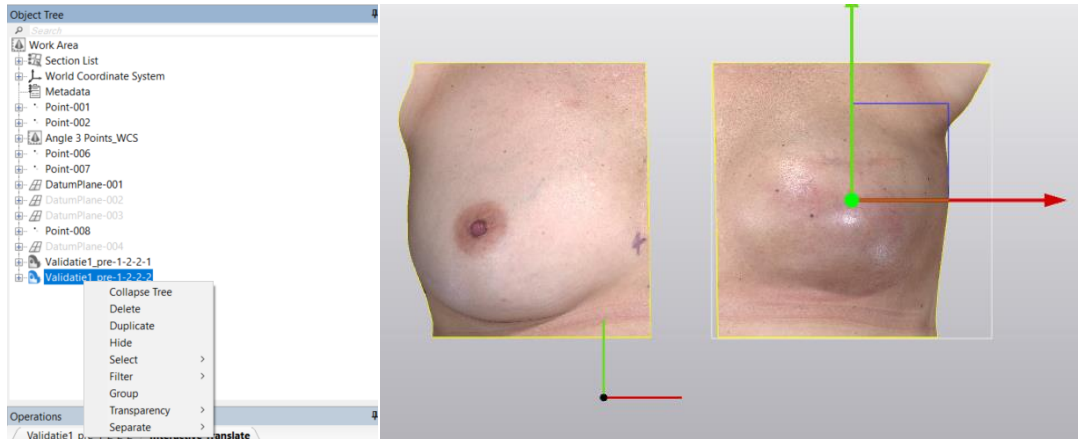
<p>Selecteer in dit menu 0 – 1 – 0</p>	
	
<p>Hoe je plaatje er nu uit moet zien met alle <i>Datumplanes</i> erin.</p>	

7. Op dezelfde manier kun je het vlak maken voor het *laagste borstpunt*. Selecteer daarvoor dat punt in plaats van het punt onder de *jugular notch*.
8. Het laatste *Datumplane* dat we gaan maken zal gemaakt worden op basis van het *laterale borstpunt*. Selecteer in het vakje rechtsonder *left of right*. 
9. Maak een punt (*Design – Create Analytical Primitive – Create Point*) aan op het *laterale borstpunt*. Open weer het *Create Datum Plane* menu en de *method Origin and Normal*. Selecteer voor *Normal* 0 – 0 – 1. Voor *Origin* het *laterale borstpunt*.

<p>Selecteer in dit menu 0 – 0 – 1</p>	
<p>Selecteer het laterale borstpunt.</p>	
<p>Hoe je plaatje er nu uit moet zien met alle <i>Datumplanes</i> erin.</p>	

10. Nu gaan we de *Datumplanes* het object laten snijden zodat de ROI's links en rechts ontstaan. Ga naar *Design* → *Cut*. Selecteer voor *Entities* de *surface* en voor *Cutting entity* de *Datumplanes*. Er zullen door het snijden extra *surfaces* ontstaan in de *object tree*, het is het handigst om de nieuwe *surfaces* direct te verwijderen. Dit doe je door met de rechter muisknop op de *surface* te gaan staan en op *delete* te klikken. Uiteindelijk zou je onderstaande twee vlakken moeten hebben.

Tip: Je kunt de *Datumplanes* en *punten* verstoppen (*hide*) zodat je *work area* overzichtelijker wordt.



11. Je kunt de linker en rechterhelft nu exporteren als een *STL* --> *File* --> *Export* en inladen in het Matlab script.
12. Extra stap: Eventueel kun je de linker- of rechterhelft nog spiegelen. Dit kan in de toekomst nodig zijn voor een ander soort analyse waarbij je de twee *surfaces* over elkaar heen legt. Spiegelen doe je via *Align* → *Mirror*. Selecteer voor *Entities* de linker- of rechterkant. Als *Mirror plane* selecteer je de eerst aangemaakte *Datumplane* (Midline plane). *Copy* hoeft niet aangevinkt te zijn. Druk op *Apply*.

